STUDIES OF BILE ACID-LIKE SIGNALING PATHWAYS

IN MAMMALS AND NEMATODES

APPROVED BY SUPERVISORY COMMITTEE

_____

David J. Mangelsdorf, Ph.D., Thesis Adviser

_____

David W. Russell, Ph.D., Chair

_____

Steven A. Kliewer, Ph.D.

_____

Carole R. Mendelson, Ph.D.

_____

Xiaodong Wang, Ph.D.

To all the people who helped me

STUDIES OF BILE ACID-LIKE SIGNALING PATHWAYS IN MAMMALS AND NEMATODES

by

XIAOYONG ZHI

DISSERTATION

Presented to the Faculty of the Medical School

The University of Texas Southwestern Medical Center at Dallas

In Partial Fulfillment of the Requirements

For the Degree of

DOCTOR OF PHILOSOPHY

The University of Texas Southwestern Medical Center at Dallas

Dallas, Texas

August, 2009

ACKNOWLEDGEMENTS

This moment of writing acknowledgements is one of the most emotional moments in my lifetime. It reminds me of so much help I have received from my friends and colleagues in the past seven years and how lucky I am to have met these great people. Without their strong support, I would not be able to finish my PhD training.

First and foremost, I thank my mentor, Davo Mango from the deep bottom of my heart. Davo is one of the best person I have met in my life. In some sense, he is more than a mentor to me. He gives me fatherly care when I am in a difficult situation. He gives friendly suggestions when I am lost of directions. He also teaches me a lot of life experience as a big brother. I improved a lot under his kind training and patient guidance through the past six years and four months. No matter what I am in the future, I will always be his disciple and follower.

I give my thanks to Steven Kliewer. He is a great scholar and gives me a lot of suggestions in my study. He also has set a good example of hard working, discipline, and courtesy to me. I am fortunate to have him as my director and share his wisdom and ambition.

I am very grateful to Eric Xu. He hosted me for ten months in his laboratory at the Van Andel Institute, during which time I finished one important part of my thesis research. He is knowledgeable, friendly, and ready to help. I am lucky that I will continue my study of the SHP project as his postdoc. I believe I will have a fruitful future under his leadership.

I give my sincere gratitude to my committee members for their help, encouragement, and guidance. They are Chair, Dr. David Russell, Dr. Carole Mendelson,

and Dr. Xiaodong Wang. My committee members are great scientists and also good teachers. They take care of me and bear the burden that I should bear when I am developing my maturity.

I am indebted to my friends and colleagues. I thank Maojun Yang for his wisdom and help on the SHP project. I thank Christian Gocke for his selfless support in my study and friendship. I thank Zhu Wang for his timely aid and reagents.

I can not skip a name, Dr. Antonio Moschetta. He is a smart, warm, interesting, and popular person. I did my rotation with him and learned a lot from him. I always feel confident and active in his company, and miss the good times with him.

I thank Tingwan Sun. We are like a “Band of Brothers”. He charged in front and covered me against the pain of life. He taught me many things in life and work. I am thankful to Dan Motola, Yang Sik Jeong, Tingting Li, Angie Bookout, Yuan Zhang, Michi Umetani, Mingui Fu, Vicky Lin, Dan Schmidt, Makoto Shimizu, and other colleagues for their support and help. Their company gives me confidence for life.

I also thank Edwards Zhou and Kelly Powell at the Van Andel Institute for their assistance in my research. They are great friends and I can not wait to see them again. I appreciate the support from Wenhua Gao, Qing Zhong, Lin Li, Gelin Wang, and Lai Wang in the Wang laboratory, and from Xinle Wu and Shanhai Xie in the McKnight laboratory. They taught me that the fun of life is out of friendship.

Finally, I give my deep thanks to my parents Yong Zhi and Lanzhi Zhang. I know they are my stronghold for ever, even when I am abandoned by the world. Therefore, I can charge forward for my dreams fearlessly. I love them.

STUDIES OF BILE ACID-LIKE SIGNALING PATHWAYS

IN MAMMALS AND NEMATODES

Publication No. _____

XIAOYONG ZHI

The University of Texas Southwestern Medical Center at Dallas, 2009

Supervising Professor: David J. Mangelsdorf, Ph.D.

Bile acids are not only detergents for lipid solubilization and absorption, but also important signaling molecules. They regulate biological events in mammals by acting on nuclear receptors and membrane-bound receptors. Bile acid homeostasis is maintained in part through a FXR-SHP signaling circuit, in which SHP functions as a transcriptional corepressor. The mechanism whereby SHP represses was one focus of my thesis research. I used a number of biochemical strategies including tandem affinity purification to identify SHP interacting proteins. I also successfully solubilized SHP recombinant protein, which was used to generate crystals that diffracted to 3.2 Angstroms.

Bile acid-like molecules function in nematodes to control a variety of life history traits such as dauer and infective L3 formation through the nuclear receptor DAF-12. Although DAF-12 homologues from different nematode species are functionally and structurally conserved, they show differential pharmacological responses to ligands. To that end, I solved the X-ray crystal structure of the hookworm *Ancylostoma ceylanicum*

DAF-12 ligand binding domain and revealed the molecular basis underlying species specific-ligand binding for DAF-12. Furthermore, DAF-12 was shown to be structurally similar to the bile acid sensor FXR, suggesting bile acid-like signaling pathways have been conserved across evolution.

In conclusion, my studies provide new insights into how bile acids are sensed and regulated in mammals and nematodes.

TABLE OF CONTENTS

LIST OF FIGURES AND TABLES

CHAPTER ONE

CHAPTER TWO

CHAPTER THREE

CHAPTER FOUR

CHAPTER FIVE

LIST OF ABBREVIATIONS

3β-HSD	3-beta-hydroxysteroid dehydrogenase
6ECDCA	6α-ethyl-CDCA
acDAF-12	*Ancylostoma caninum* DAF-12
aceDAF-12	*Ancylostoma ceylanicum* DAF-12
AF2	activation function 2
ASBT	ileal apical sodium-dependent bile acid transporter
BSEP	bile salt export pump
C	carbon
C	carboxy
CA	cholic Acid
CBP	CREB binding protein
CARM1	coactivator associated arginine methyltransferase 1
CDCA	chenodeoxycholic Acid
ceDAF-12	*C. elegans* DAF-12
cGMP	cyclic guanosine monophosphate
daf	abnormal dauer formation
DA	dafachronic acid
Dafachronic acid	(25S), 26-3-keto-cholestenoic acid
Daf-c	dauer formation constitutive
Daf-d	dauer formation defective

DAX-1 congenital diseases dosage-sensitive sex reversal and adrenal hypoplasia congenital-1

DBD DNA binding domain

DCA deoxycholic acid

DIN-1 DAF-12 interacting-1

DR direct repeat

EID1 EP300 interacting inhibitor of differentiation

ER estrogen receptor

ER everted repeat

FGF15 fibroblast growth factor 15

FXR farnesoid X receptor

GFP green fluorescent protein

GPS2 G protein pathway suppressor 2

GR glucocorticoid receptor

GRIP1 glucocorticoid receptor interacting protein 1 (i.e., SRC2)

HDAC histone deacetylase

HNF4 hepatic nuclear receptor 4

HRE hormone response element

HSP heat shock protein

IBABP ileal bile acid binding protein

IBAT ileal bile acid transporter (i.e., ASBT)

IR inverted repeat

LBD ligand binding domain

LCA	lithocholic acid
LRH-1	liver related homolog-1
LSD1	lysine specific demethylase 1
LXR	liver X receptor
MDR2	multi-drug resistance 2
MRP2	multi-drug resistance associated protein 2
m/z	mass/charge
N	amino
naDAF-12	*Necator americanus* DAF-12
NcoR	nuclear receptor corepressor
NTCP	Na^+-taurocholate cotransporting polypeptide
OATPs	organic anion transporting polypeptides
PI3K	phosphatidylinositol-3-OH-kinase
PPARs	peroxisome proliferator activated receptors
PR	progesterone receptor
PRMT1	protein arginine methyltransferase 1
PXR	pregnane X receptor
RAR	retinoic acid receptor
RLU	relative light unit
RMSD	root mean square deviation
RNAi	RNA interference
RXR	retinoid X receptor
SHP	small heterodimer partner

SMAD	Sma and Mad related protein
SMILE	SHP-interacting leucine zipper protein
SMRT	silencing mediator of retinoic acid and thyroid hormone receptor
SRC1	steroid receptor coactivator 1
SRC2	steroid receptor coactivator 2 (i.e., GRIP1)
ssDAF-12	*Strongyloides stercoralis* DAF-12
TGFβ	transforming growth factor beta
TRα,β	thyroid receptor alpha, beta
VDR	vitamin D receptor
WT	wildtype
Δ4-DA	(25S), 26-3-keto-4-cholestenoic acid
Δ7-DA	(25S), 26-3-keto-7(5α)-cholestenoic acid

CHAPTER ONE

This thesis is composed of six chapters. A general introduction about nuclear receptors is presented in Chapter One. Nuclear receptors involved in mammalian bile acid signaling pathway are discussed in Chapter Two. At the end of Chapter Two, description of the first focus of my thesis research is given and the related experiments are reported in Chapter Three, which is about biochemical and structural characterization of SHP repression. In Chapter Four, an introduction to bile acid-like hormone signaling pathways in nematodes is discussed. At the end of Chapter Four, scientific questions with respect to the second focus of my thesis research are put forward. My work detailed in Chapter Five addresses these questions experimentally and reveals the structural conservation of bile acid-like nuclear receptor signaling pathways in nematodes. Studies are concluded in Chapter Six and perspectives are also given.

Introduction to Nuclear Receptors

1.1 CLASSIFICATION OF NUCLEAR RECEPTORS

Nuclear receptors are a large group of ligand regulated transcription factors that control a diversity of cellular activities including proliferation, differentiation, metabolism, homeostasis, and detoxification, and so on throughout metazoans.

First nuclear receptors to be cloned in the mid-1980s were glucocorticoid receptor (GR) and estrogen receptor (ER), marking the beginning of the molecular nuclear receptor era (Hollenberg et al., 1985; Walter et al., 1985). The following 20 years have witnessed active and extensive research on this family, driven by discoveries of more members spanning from vertebrates to invertebrates, and an increased understanding of

their roles in animal endocrinology, developmental biology, and pathology.

Thanks to the genome sequencing projects accomplished in the recent years, today the nuclear receptor superfamily includes 48 members in *Homo sapiens*, 49 in *Mus musculus*, 21 in *Drosophila melanogaster*, and 284 in *Caenorhabditis elegans* (Enmark, 2001).

With the expansion of the nuclear receptor superfamily several groups have proposed ways to organize nuclear receptors into distinct classes based on their intrinsic properties.

In 1995, the known nuclear receptors were grouped into four families according to their ligand binding, DNA binding, and dimerization modes. The four families are: steroid receptors, RXR heterodimers, dimeric orphan receptors, and monomeric orphan receptors (Mangelsdorf et al., 1995). In 1997, a method based on sequence alignment and phylogenetic tree construction was used to assign nuclear receptors into six subfamilies (Laudet, 1997). Interestingly, the results mirrored the previous classification, since there is a close correlation between a nuclear receptor's phylogeny and its DNA binding and dimerization properties. Later, this methodology was adopted by the Nuclear Receptor Nomenclature Committee in 1999 and a unified naming/coding system for NHR superfamily was set up (1999). Accordingly, every nuclear receptor has one specific ID number. For example, NR0B2 represents the nuclear receptor in subfamily 0 (numeric) and group B (letter) that contains more than one related gene.

From an endocrinological perspective, the nuclear receptors have been divided into three groups based on the source and binding affinity of their ligands (Chawla et al., 2001). As shown in the Fig. 1.1, the first group of endocrine receptors include

	Nuclear Receptor	Ligands
Endocrine	GR	Glucocorticoid
	MR	Mineralocorticoid
	PR	Progesterone
	AR	Androgen
	ERα,β	Estrogen
	RARα,β	All Trans Retinoic Acid
	TRα,β	Thyroid Hormone
	VDR	Vitamin D, LCA
Adopted Orphan	RXRα,β,γ	9-cis Retinoic Acid
	PPARα,β,γ	Prostanoid, Fatty Acids
	LXRα,β	Oxysterols
	FXR	Bile Acids
	PXR/SXR	Xenobiotics
	CAR	Xenobiotics
Orphan	ERRα,β,γ	Synthetic Steroids?
	HNF4α,γ	Fatty Acids?
	RORα,β,γ	Fatty Acids, Sterols?
	SF-1	Phospholipids?
	LRH-1	Phospholipids?
	DAX-1	?
	SHP	?
	TLX	?
	PNR	?
	GCNF	?
	TR2,4	?
	NGFI-Bα,β,γ	?
	RVRα,β,γ	?
	COUP-TFα,β,γ	?

Figure 1.1 Classification of Vertebrate Nuclear Receptors
Depending on the source and type of circulating ligands, nuclear receptors are classified into three groups. This figure is modified from Chawla, et al., 2001.

glucocorticoid receptor (GR), estrogen receptors (ERs), mineralocorticoid receptor (MR), androgen receptor (AR), progesterone receptor (PR), that bind to endogenous ligands with high affinity (K_d=0.01-10 nM). Vitamin D receptor (VDR), retinoic acid receptors (RARs) and thyroid receptors (TRs) are also in this group. They are intermediary between groups of endocrine receptors and adopted orphan receptors because their ligands require exogenous precursors. The adopted orphan receptor group includes retinoid X receptors (RXRs), liver X receptors (LXRs), farnesoid X receptor (FXR), peroxisome proliferator-activated receptors (PPARs), pregnane X receptor (PXR) and constitutive androstane receptor (CAR), which bind to dietary derived lipids with relatively low affinity (K_d >1 to 10 μM). The third group consists of orphan receptors that await either identification of their ligands or confirmation of the physiological relevance of the lipids found in their ligand binding pockets during protein crystallization (Krylova et al., 2005).

A newer classification has been reported recently, in which, the tissue expression of the 49 mouse nuclear receptors was recorded by quantitative PCR and the following clustering analysis aligned the nuclear receptors around a circular dendrogram separated into distinct physiological zones. In this manner, the nuclear receptors are categorized on a functional basis (Bookout et al., 2006).

1.2 FUNCTIONAL MODULES AND MECHANISMS OF ACTION

The nuclear receptors share a common architectural scheme (Aranda and Pascual, 2001; Chawla et al., 2001; Germain et al., 2006). Typically, a nuclear receptor can be dissected into six regions (A-F) (Fig. 1.2A). The N-terminal A/B region is the most variable in terms of sequence or size and contains the ligand-independent AF1

transactivation domain (activation function 1). This is followed by a highly conserved C region, also termed the DNA binding domain (DBD), which uses two zinc finger motifs to recognize specific DNA sequences within the promoter or enhancer of target genes. Region D functions as a flexible linker or hinge between C and E. Region E is another conserved region that in most nuclear receptors harbor the ligand binding domain (LBD). It also contains the ligand-dependent AF2 transactivation domain (activation function 2), constituting the binding surface for coactivators or corepressors. Notably, the AF2 motif is only a part of the larger domain, which contains a consensus sequence located at the C-terminus of region E (helix H12). Some nuclear receptors have an additional variable F region with unclear functions.

As mentioned above, DNA binding and dimerization are two important properties for nuclear receptors. The specific DNA sequences to which nuclear receptors bind are called hormone response elements (HREs). For non-endocrine receptors, they are composed of one or two half sites specified by the consensus sequence AGGTCA (Fig. 1.2B). One half-site-containing HRE is bound by monomers, while two half-site-containing HREs are occupied by homo- or heterodimers. The affinity and selectivity of the binding (especially for the dimers) are further defined by the orientation and spacing of the half sites, which can be arranged as DR (direct Repeats), IR (inverted Repeats) and ER (everted Repeats) spaced by a specific number of nucleotides. In addition, subtle differences in the consensus sequence and specific flanking sequence also impact the final binding by nuclear receptors. As such, the specific configuration and context of the half-sites in HREs permit each nuclear receptor to regulate its own set of specific target genes (Aranda and Pascual, 2001). On the other hand, the usage of the

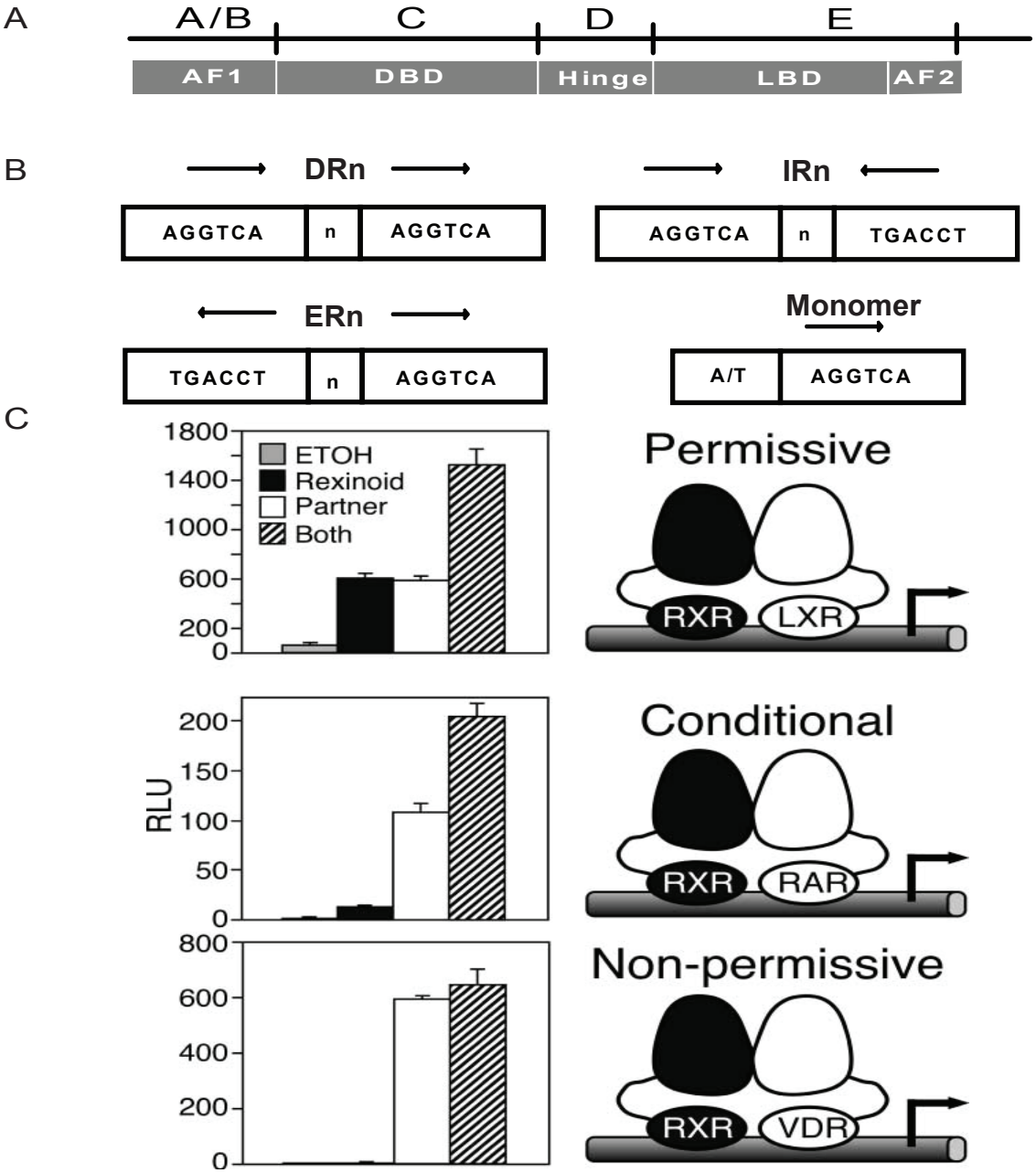

Figure 1.2 Nuclear Receptor Architecture, Response Element, and RXR Heterodimerization Paradigm

(A) Schematic representation of a typical nuclear receptor. (B) Nuclear receptor binding sites. DR, direct repeat; IR, inverted repeat; ER, everted repeat. AGGTCA represents the half site for non-endocrine receptors. *n* represents the number of nucleotides between the half sites. Monomers prefer to bind a half site preceded by an A/T rich sequence. (C) RXR heterodimerization paradigms. Both rexinoid and the partner ligand can activate permissive heterodimers independently or together with a synergistic effect. Rexinoid alone can not activate conditional heterodimers, but has an additive effect in the presence of the partner ligand. Rexinoid can not activate non-permissive partner alone or in combination with the partner ligand. Fig. C is adapted from Shulman, et al., 2004.

similar consensus sequence also allows for the nuclear receptors to crosstalk at the level of DNA binding.

Dimerization (homo- or hetero-) is mediated by interfaces contributed from the DBD, hinge, and LBD (Shulman, 2004). Members of the endocrine receptor group almost exclusively bind as homodimers except for VDR, TR, and RAR, which bind as RXR heterodimers. In comparison, members of adopted orphan receptor group uniformly bind as heterodimers with RXR except for RXR itself, which also functions as a homodimer. Further, the RXR heterodimers can be classified into three paradigms, based on the response to the ligands targeting different RXR's partners (Fig. 1.2C) (Shulman, 2004; Aranda and Pascual, 2001). Permissive heterodimers such as LXRs/RXR respond both to their own cognate ligands and to RXR ligands independently or together synergistically. Non-permissive heterodimers such as VDR/RXR only respond to the non-RXR cognate ligands. RAR/RXR represents the conditional heterodimer and responds to RXR ligands on the condition that RAR ligands are also present. The members in the orphan receptor group use a more diverse DNA binding strategy (Aranda, 2001).

Adopted orphan receptors occupy their target gene promoters in the absence of ligand and interact with corepressors to silence gene expression. The binding of ligand changes the nuclear receptor's conformation, which decreases its association with corepressors and increases the recruitment of coactivators that promote gene expression (Fig. 1.3). In contrast, some endocrine receptors (e.g., AR, MR, GR, and PR) are sequestered in the cytosol by heat shock proteins in the absence of ligand. After binding to the ligands, they dissociate from the heat shock proteins, translocate into the nucleus,

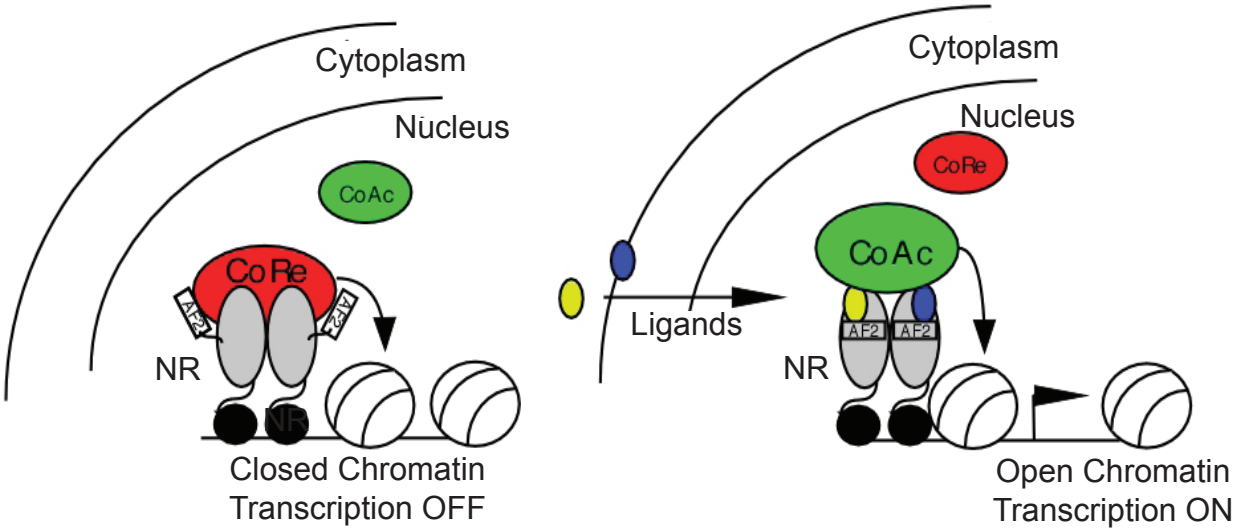

Figure 1.3 Nuclear Receptor working Mode
Adopted orphan receptors sit on the target promoters in the absence of ligand and bind corepressors to inhibit gene expression. Ligand binding causes a change in nuclear receptor conformation, leading to dissociation of corepressors and association of coactivators. The working mode for endocrine receptors is not shown here. NR, nuclear receptors; CoAc, coactivators; CoRe, corepressors. This figure is adapted from Andy Shulman, PhD thesis at UTSW, 2004.

and recruit coactivators for gene activation (Gronemeyer et al., 2004).

1.3 MECHANISTIC REGULATION BY COACTIVATORS AND COREPRESSORS

Since the cloning of the first nuclear receptor coactivator, SRC-1 (steroid receptor coactivator 1 (Onate et al., 1995), and the first nuclear receptor corepressors, SMRT (silencing mediator of retinoic acid and thyroid hormone receptor) and NcoR (nuclear receptor corepressor) (Chen and Evans, 1995; Horlein et al., 1995), around 300 coactivators or corepressors have been reported to mediate a wide array of nuclear receptor functions to date (Lonard and O'Malley, 2007).

Coactivators bind to nuclear receptors via a specific LXXLL motif (L, leucine; X, any amino acid). They can be categorized into three groups based on their mechanisms of action in directing nuclear receptor mediated transcription (Table 1.1).

The first group is related to histone modifications including histone acetylation and methylation. Some coactivators contain intrinsic histone acetyltransferase (HAT) activity. After being recruited to the nuclear receptor target gene promoter, they acetylate local histones to induces the chromatin structure into an “open” state and promote accessibility of the transcriptional machinery (Thakur and Paramanik, 2009). Some coactivators are histone arginine methyltransferases such as PRMT1 (protein arginine methyltransferase 1) and CARM1 (coactivator associated arginine methyltransferase 1). They methylate specific arginines in histone 3 (H3) and histone 4 (H4) to promote gene expression (Klinge et al., 2004; Chen et al., 2000; Baek et al., 2006). It is suggested that methylated histones may induce histone acetylation or create docking sites for other

Coactivators	Mechanisms of Action
SRC1/RIP160	histone acetylation
SRC2/TIF2/GRIP1	ditto
SRC3/pCIP	ditto
CBP/p300	ditto
TIP60	ditto
p/CAF	ditto
GCN5	ditto
PRMT1	histone arginine methylation
CARM1/PRMT4	ditto
Jumonji C containing demethylase	histone lysine demethylation
SWI/SNF	chromatin remodeling
TRAP/ Mediator	docking site for transcriptional machinery
PGC1α	ditto
SNURF	ditto
Corepressors	
SMRT	histone deacetylation
NcoR	ditto
RIP140	coactivator competition and recruitment of HDACs and CtBP
LcoR	ditto
PRAME	coactivator competition and recruitment of HDACs and EZH2
Hairless	coactivator competiton and recruitment of HDACs
REA	ditto
MTA1	ditto

Table 1.1 Mechanisms of Action by Nuclear Receptor Coactivators and Corepressors

Please refer to Thakur and Paramanik, 2009, Augereau, et al., 2006, and Gurevich et al., 2007 for details on nomenclature and primary reference sources.

coactivators (Lunyak et al., 2004).

Histone demethylases can work as nuclear receptor coactivators. Reportedly, JHDM2A, which is a Jumonji C domain containing histone lysine demethylase, facilitates transactivation by androgen receptor (Yamane et al., 2006). LSD1 (lysine specific demethylase 1), another histone demethylase, can also promote androgen receptor target gene expression (Wissmann et al., 2007).

The second group is related to chromatin remodeling. The SWI/SNF complex uses the energy generated by ATP hydrolysis to move histone octamers in a bidirectional and positional manner. This results in a chromatin conformation more accessible to transcriptional factors and basal transcriptional machinery (Schnitzler et al., 1998; Shundrovsky et al., 2006).

Coactivators in the third group work as docking sites and scaffolds to facilitate the recruitment of other coactivators and/or basal transcriptional machinery. For example, PGC1α recruits coactivators SRC-1 and CBP to stimulate gene activation by PPARγ (Puigserver et al., 1999).

Compared to coactivators, less knowledge has been gained for corepressors. SMRT and NcoR are the two best studied. They bind to nuclear receptors RAR, TR, and PPARγ in the absence of ligand, and recruit histone deacetylases (HDACs) to quench gene expression (Thakur and Paramanik, 2009; Karagianni and Wong, 2007). By removing acetyl groups from histones, HDACs transform the chromatin into a “closed” state. The activity of HDACs can be suppressed by a group of structurally distinct chemicals, collectively termed HDAC inhibitors, such as TSA (hydroxamic acid), sodium butyrate (keytone), and trapoxin B (cyclic tetrapeptide) (Mehnert and Kelly, 2007;

Glozak and Seto, 2007; Cress and Seto, 2000).

Recently a new group of nuclear receptor corepressors were reported (Gurevich et al., 2007; Augereau et al., 2006). They are recruited by ligand bound nuclear receptors. These corepressors contain LXXLL motifs and thereby can compete with coactivators for the same binding site on nuclear receptors. They also recruit HDACs, CtBP (C-terminal binding protein), or other corepressors to actively silence gene expression.

1.4 STRUCTURAL BIOLOGY OF NUCLEAR RECEPTORS

The X-ray crystallization techniques have contributed a lot to our molecular understanding of nuclear receptor functions. Historically, the DBD or LBD of a nuclear receptor has been isolated for crystallization in order to study DNA binding property or ligand regulated activity, respectively. The first nuclear receptor DBD structure was solved in 1991 for GR (Luisi et al., 1991), and the first LBDs were accomplished in 1995 for TRα and RXRα (Wagner et al., 1995; Bourguet et al., 1995). Because of the high flexibility and mobility in some structural modules, such as region A/B and D, structure determination of a full length nuclear receptor was quite a challenge. The complex structure of the full length PPARγ and RXRα sitting on a DNA fragment is the first of its kind and was reported in 2008, illustrating a comprehensive structural picture of nuclear receptor action (Chandra et al., 2008).

In terms of pharmacology, the nuclear receptor LBD is most interesting. Hence, crystallization of nuclear receptor LBDs has been the subject of intense study for years and as a result, most of the LBDs have been solved, leaving very few unfinished in the orphan receptor group. In general, all of the LBD structures known so far adopt a similar

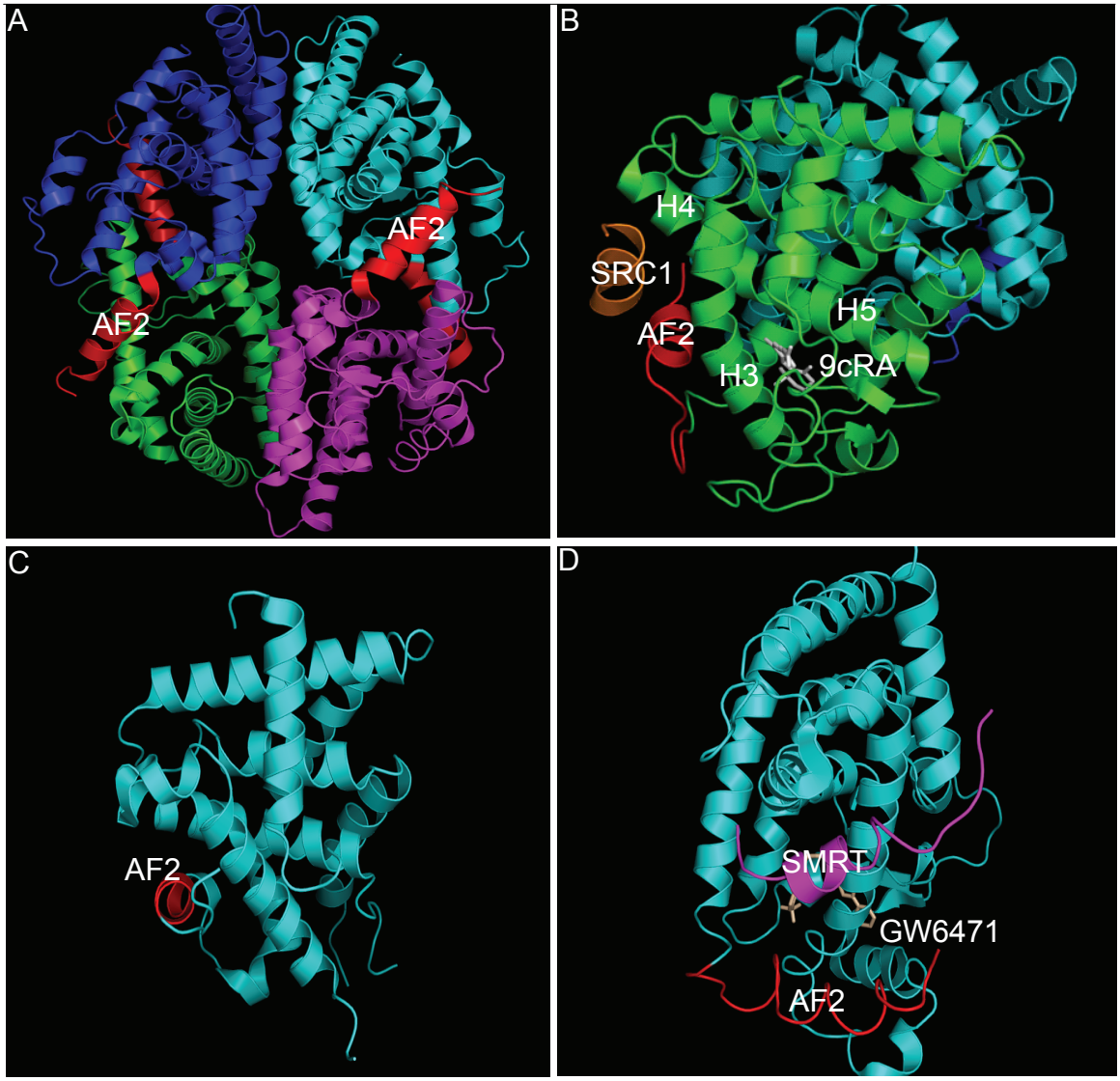

Figure 1.4 Ribbon Structure Representation of Nuclear Receptors in Different Conformations

(A) RXR heterotetramer in the absence of ligand. The AF2 helix (red) is protruded into the coactivator binding groove of the nearby monomer. **(**B**)** RXR-PPARγ heterodimer **i**n the presence of 9-cis retinoic acid (9cRA, RXR ligand) and Gi262570 (not shown**,** PPARγ ligand). The AF2 helix (red) of RXR (green) is in active state and interacts with the coactivator peptide (orange). (C) COUP-TF2. The AF2 helix (red) fits into its own coactivator binding groove, indicating an auto-inhibitory conformation. (D) PPARα in the presence of antagonist, GW6471 (white). The corepressor peptide (magenta) prevents the AF2 helix (red) of PPARα into the active position. SRC1, steroid receptor coactivator 1; SMRT, silencing mediator of retinoic acid and thyroid hormone receptor; AF2, activation function 2.

3-D architecture, appearing as a well wrapped three-layer α-helical sandwich made of 10-13 α-helices (H1-H13) and 2-4 β-strands. Nevertheless, there are some structural variations in specific nuclear receptors. For example, NR5A group members such as LRH-1 and SF1 have a large protruding helix H2, which forms an additional layer (Krylova et al., 2005). In FXR the β-strands are replaced by a long helix H6 (Mi et al., 2003).

The presence (or absence) of ligands also has a profound influence on the global conformation of nuclear receptors. For instance, in the absence of ligands, RXRα exists as a disc-shaped tetramer consisting of two dimers symmetrically packed along helices H3 and H11 (Fig. 1.4A). The AF2 helix (H12) of every monomer extends away from the core body and occupies the coactivator binding groove (AF2 domain) of its proximate monomer belonging to a different dimer, indicating an auto-repressive conformation (Gampe et al., 2000b). However, in the presence of ligands, for example 9-cis retinoic acid, the AF2 helix of RXRα folds back and packs against the core body. Together with other structural elements from helices H3-H5, it forms a groove to accept the LXXLL-containing motif from coactivators (Gampe et al., 2000a) (Fig. 1.4B). This represents an active conformation for activated nuclear receptors to interact with coactivators. Inside the groove, the LXXLL motif adopts a two-turn α-helix. Three leucines from this motif are pointing inward and stabilized via hydrophobic interaction with nearby non-polar amino acids. The two ends of the LXXLL motif are locked by hydrogen bonding with one positive amino acid from the C-terminus of RXR helix H3 and one negative amino acid from the center of helix H12, which are collectively termed charge clamp residues. It is speculated that in this way, coactivators are recruited and

bound to liganded nuclear receptors for downstream effects.

In comparison to the auto-inhibitory conformation exemplified by RXRα, some nuclear receptors such as COUP-TFII or PPARs take another conformation for self repression in the absence of ligands (Fig. 1.4C) (Kruse et al., 2008; Nolte et al., 1998; Uppenberg et al., 1998; Xu et al., 1999). They fold the AF2 helix against the core body. But instead of into the active position described above, the folding extends the helix very close to the coactivator binding groove and blocks the entry site for coactivators. This conformation is also seen in some nuclear receptors bound by antagonists, for example, ERα complexed with OHT (4-hydrooxytamoxifen) (Shiau et al., 1998).

Usually, the binding of antagonists promotes and stabilizes the nuclear receptor interacting with corepressors. As demonstrated in the structure of PPARα complexed with its antagonist GW6471 (Xu et al., 2002) (Fig. 1.4D), the AF2 helix packs against the core body but with a specific distance to the coregulator binding groove. This distance is suitable for the binding of a longer motif specified by LXXXIXXXL/I in corepressors such as SMRT and NcoR but not for the LXXLL motif found in coactivators. The corepressor motif adopts a three-turn α-helix and interacts with the nuclear receptor via similar hydrophobic and hydrogen bonding interactions. This model provides the molecular basis for gene repression mediated by unliganded or antagonist-bound nuclear receptors.

In summary, the conformation of a nuclear receptor determines its ability to recruit coactivators or corepressors, which is precipitated by the binding of ligands (agonists or antagonists). The conformation can be functionally boiled down to the coregulator binding surface or AF2 domain with the AF2 helix as the most dynamic and

definitive element. When the AF2 helix is set at an active position, an active conformation is formed and the coactivator binding is preferred. In contrast, when the AF2 helix is orientated away from the active position, the resultant conformation does not favor the coactivator binding and/or it favors the corepressor binding. Notably, these events, such as ligand binding, conformation switch, and coregulator recruitment are mutually influential. For example, the binding of coactivators may be instrumental to the ligand's stabilization in the ligand binding pocket.

Besides improving our understanding of coregulator function, structure studies of the nuclear receptor LBD also provide us molecular information about the ligand binding pocket, allowing for development of pharmaceutical intervention of nuclear receptor functions.

Clearly, structure biology has proven its power in advancing nuclear receptor research. While most of the nuclear receptor structures have been determined, some important questions are still remaining in this field. For example, so far we have only determined the fully intact structure of a nuclear receptor complexed with a coregulator peptide, instead of the intact coregulator protein. One of the goals of my research was to address this issue (see Chapter Three).

CHAPTER TWO

Nuclear Receptors in Mammalian Bile Acid Signaling Pathways

2.1 BILE ACID HOMEOSTASIS

Bile acids are traditionally regarded as detergents that solubilize cholesterol and help absorption of dietary lipids, cholesterol and fat-soluble vitamins in the intestine. Current studies show they also work as important signaling molecules by acting on a number of nuclear and membrane bound receptors to regulate a variety of biological events (Hylemon et al., 2009) (Fig. 2.1).

2.1.1 Bile Acid Biosynthesis

Bile acids are produced in the liver from cholesterol and contributes to 90% of cholesterol elimination from the body (Russell, 2003; Russell, 2009). The whole reaction involves a number of cytochrome P450 enzymes for catalysis and can be reduced to two pathways: the classic pathway and the alternative pathway (Fig. 2.2). In the classic pathway, CYP7A1 (cholesterol 7α-hydroxylase) is the first and also rate-limiting step enzyme, subject to tight transcriptional and enzymatic regulation. Its products then undergo several steps of ring structure modification, one of which is mediated by CYP8B1 that adds the hydroxyl group to the C12 (12α-hydroxylase). CYP27A1 carries on the reaction by adding hydroxyl groups consecutively to C27, leading to the formation of a carboxylate group. The following cleavage reaction shortens the side acyl chain by three carbons and produces the bile acids that are in an active form ready for conjugation. In humans and rats, these bile acids are cholic acid (CA) and chenodeoxycholic acid

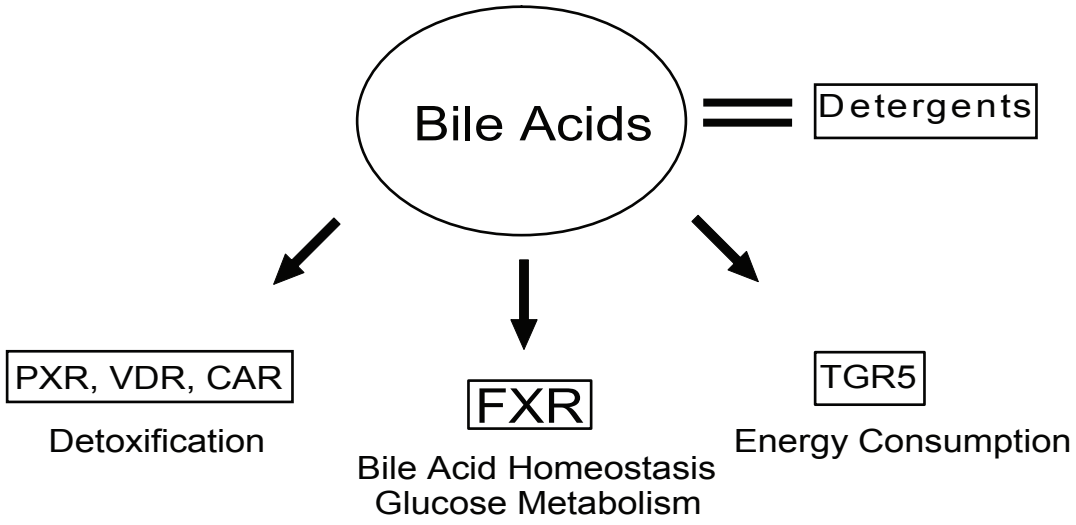

Figure 2.1 Bile Acid Signaling Pathways
Bile acids work as detergents to solubilize cholesterol in the gallbladder and help absorption of fat-soluble dietary components. They regulate a diversity of biological events by acting on nuclear receptors and membrane-bound receptors.

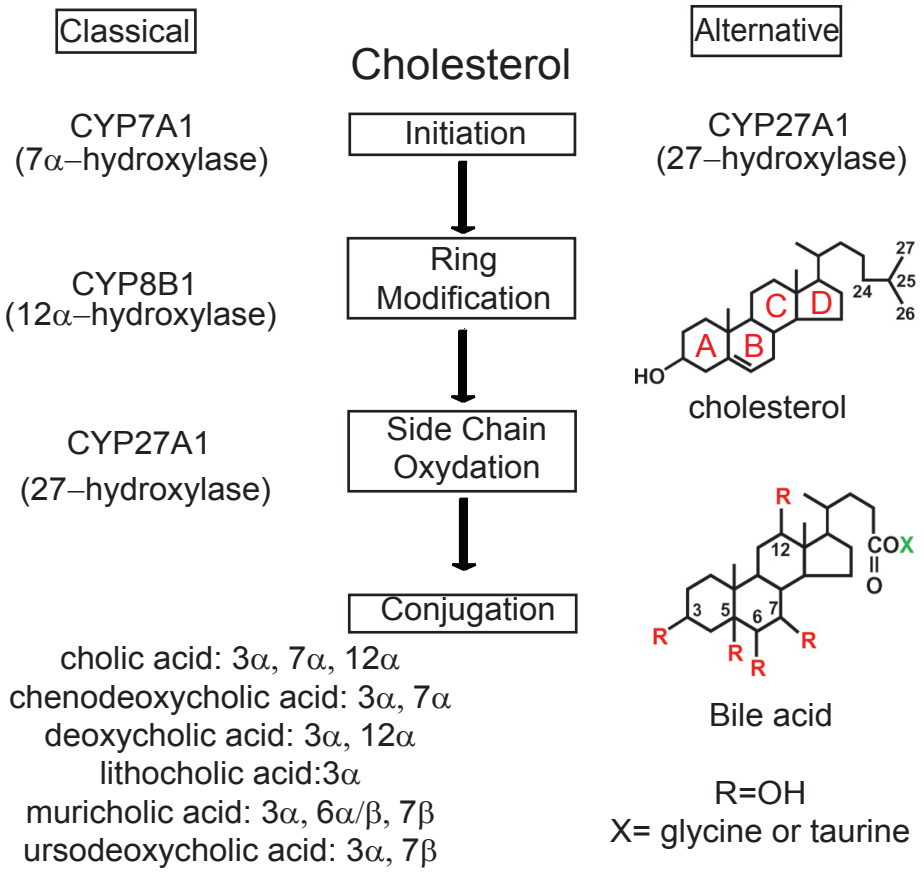

Figure 2.2 Bile Acid Biosynthesis
Two biochemical pathways are represented for bile acid biosynthesis. The classical pathway only happens in liver, with CYP7A1 as the first and rate-limiting step enzyme. CYP27A1 is the major initiating enzyme in the alternative pathway. In different species, the composition of bile acids is different. Rings A-D in the steroid skeleton of cholesterol are marked in red. Chemical structures of cholesterol and bile acid are adapted with permission from Russell, 2009.

(CDCA), whereas CDCA is converted to muricholic acids (3α, 6α/β, 7β) in mice and ursodeoxycholic acid (3α. 7β) in bear. They are termed primary bile acids. CA and CDCA are conjugated to taurine or glycine in the liver to become more hydrophilic for transport.

The alternative pathway begins with oxysterol synthesis catalyzed by a number of hydroxylases, with CYP27A1 being the most predominant one. The major output of this pathway is CDCA.

2.1.2 Bile Acid Enterohepatic Circulation

The conjugated bile acids are actively transported out of the liver and into the bile duct system together with cholesterol and phospholipids by membrane bound transporters such as BSEP (bile salt export pump), MDR2 (multi-drug resistance 2), and MRP2 (multidrug resistance associated Protein 2). The biliary liquids are stored in the gallbladder during the interval between meals and released into the small intestine in response to feeding signals (Hofmann, 2009).

Bile acids are re-absorbed in the intestine with ileum as the major absorption site, where bile acids are actively taken up by the salt-dependent transporter IBAT (ileal bile acid transporter, also called ASBT). Once inside the enterocytes, the bile acids are buffered by IBABP (ileal bile acid binding protein) and escorted to the basolateral membrane where they are pumped out by the heterodimeric organic solute transporter OSTα/β into the portal veinous system that feeds back to liver. Bile acids flow in the vein plasma, bound to albumin or lipoproteins and are re-absorbed by hepatocytes through the basolateral membrane via NTCP (Na^+-taurocholate cotransporting polypeptide,

Na^+-dependent bile acid uptake) and OATPs (organic anion transporting polypeptides, Na^+-independent bile acid uptake). In this way, 95% of the circulating bile acids are recycled (Fig. 2.3). The remaining 5% escapes the absorption in the small intestine and reach the colon where they are subject to bio-transformations mediated by intestinal bacteria including deconjugation and 7α-dehydroxylation. 7α-dehydroxylation converts cholic acid to deoxycholic acid (DCA) and chenodeoxycholic acid to lithocholic acid (LCA), which collectively are named secondary bile acids. Part of these bile acids are passively extracted by the colon, return to the liver via the portal system and become re-conjugated, while the rest are secreted in feces, accounting for 1-3% of the total circulating bile acids. Accordingly, around 600mg of bile acids are lost on a daily basis and compensated by bile acid biosynthesis from cholesterol. The enterohepatic circulation and biosynthesis of bile acids constitute the key components of bile acid homeostasis (Houten et al., 2006; Kullak-Ublick et al., 2004; Martinez-Augustin and Sanchez de Medina, 2008).

2.2 NUCLEAR RECEPTOR REGULATION OF BILE ACID HOMEOSTASIS

Regulation of bile acid synthesis involves LXRα, RXR, LRH-1, HNF4α, FXR, and SHP (Lu et al., 2000; Goodwin et al., 2000) (Figure 2.4). In rodents, CYP7A1 is the target gene of LXRα, which is activated by oxysterols. By sensing cholesterol/oxysterol levels in the liver, LXRα feedforward controls bile acid conversion. Disruption of LXRα in mice abolished the CYP7A1 induction by high cholesterol diet (Peet et al., 1998). However, in cultured cells, RXR/LXR alone is not sufficient to induce the CYP7A1 promoter activity (Lu et al., 2000). Expression of CYP7A1 requires the involvement of

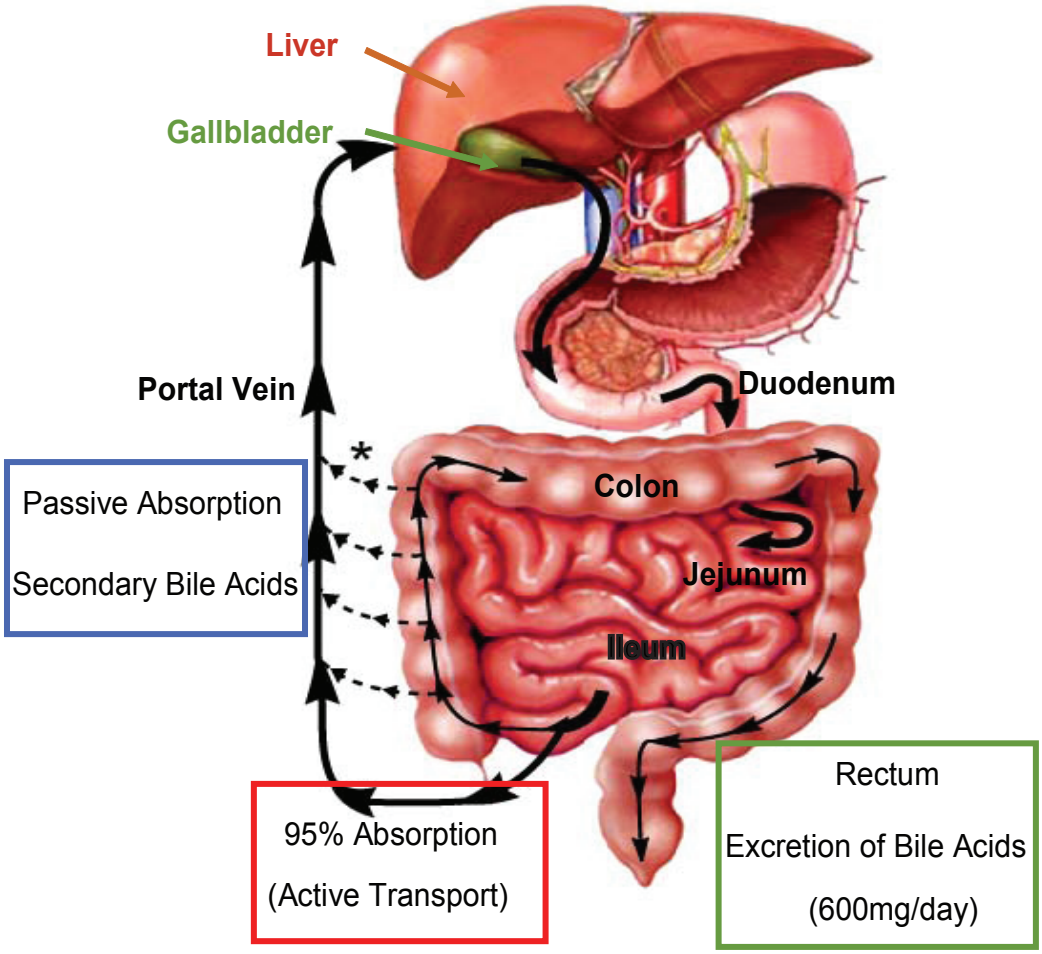

Figure 2.3 Bile Acid Enterohepatic Circulation
Bile acids circulates between liver and intestine. 95% of bile acids are re-absorbed in ileum by transporter-mediated active absorption. The unabsorbed 5% goes to colon, where a portion of them are taken up by passive transport. 1-3% of total bile acids (600mg) escape the recycling everyday and are excreted in the feces. They are compensated by hepatic bile acid biosynthesis. This figure is adapted with permission from Hylemon, et al., 2009.

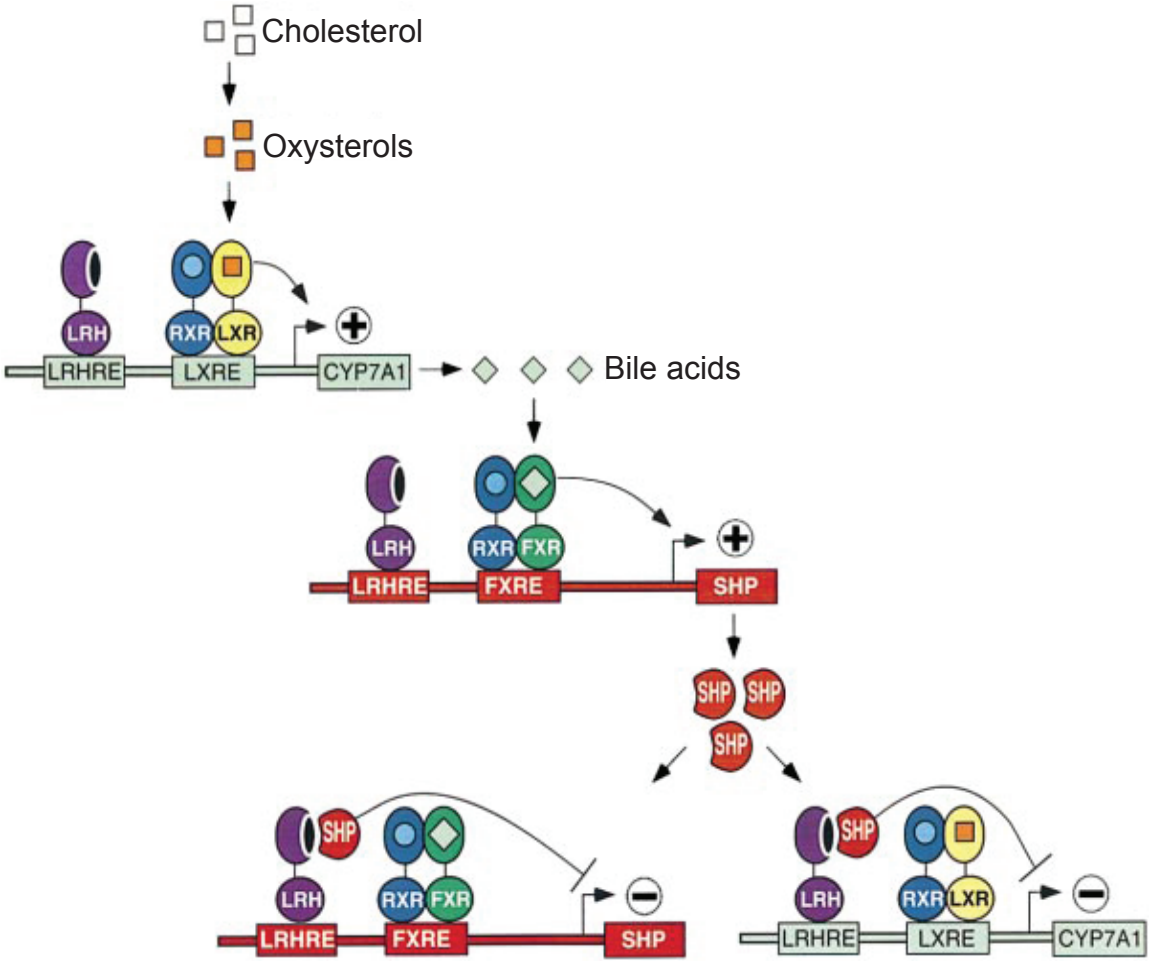

Figure 2.4 Feedback Regulation of Bile Acid Homeostasis by Nuclear Receptors
The level of oxysterols is increased when cholesterol is accumulated in liver. Oxysterols activate LXR to produce more CYP7A1, which is the rate-limiting step enzyme in conversion of cholesterol to bile acids. In this way, cholesterol catabolism is facilitated. Bile acids are ligands for FXR and stimulate the expression of FXR target genes including SHP. SHP moves to the promoters of its own and CYP7A1, inhibiting the promoter activity via LRH-1 (or HNF4α, which is not shown in the figure). FXR and SHP form the feedback regulatory loop to control the bile acid level. This figure is adpated from Lu, et al., 2000.

two other nuclear receptors, LRH-1 and HNF4α. Both are believed to be transcriptional competence factors by their potential chromatin remodeling functions. Specific disruption of LRH-1 in the mouse liver does not change the CYP7A1 expression level, whereas specific disruption of HNF4α in the mouse liver reduces the CYP7A1 expression level, suggesting they have different functions on the promoter of CYP7A1 (Lee et al., 2008); (Hayhurst et al., 2001). It is believed that on the promoter of CYP7A1, HNF4α works both as a transcriptional competence factor and activator, while LRH-1 functions as a competence factor. LRH-1 can also serve as a transcriptional activator on the promoter of some genes such as CYP8B1 and SHP. The mRNA levels of these two genes are decreased in the LRH-1 liver specific knockout mice (Lee et al., 2008).

The feedback regulation of bile acid synthesis is mediated by nuclear receptors FXR, SHP, LRH-1, and HNF4α (Fig. 2.4). FXR is activated by bile acids to induce a number of target genes including SHP and FGF15 (fibroblast growth factor 15) (Lu et al., 2000; Goodwin et al., 2000; Inagaki et al., 2005). SHP works as a transcriptional corepressor, binding to LRH-1 or HNF4α on the promoter of CYP7A1 and thereby inhibiting the gene transcription. FGF15 functions as an enterohepatic signal, binding to the liver receptor FGFR4 and igniting an intracellular cascade that synergizes with SHP to repress the CYP7A1 expression (Fig 2.5). Both FGF15 and SHP are required for effective repression of the CYP7A1 expression in mouse liver. SHP also attenuates its own expression by interacting with LRH-1 or HNF4α on its own promoter. In this way, FXR–SHP and FXR-FGF15 form two signaling circuits to control bile acid biosynthesis.

Enterohepatic circulation is regulated by FXR and SHP (Martinez-Augustin and Sanchez de Medina, 2008; Houten et al., 2006). Inside the hepatocytes, FXR facilitates

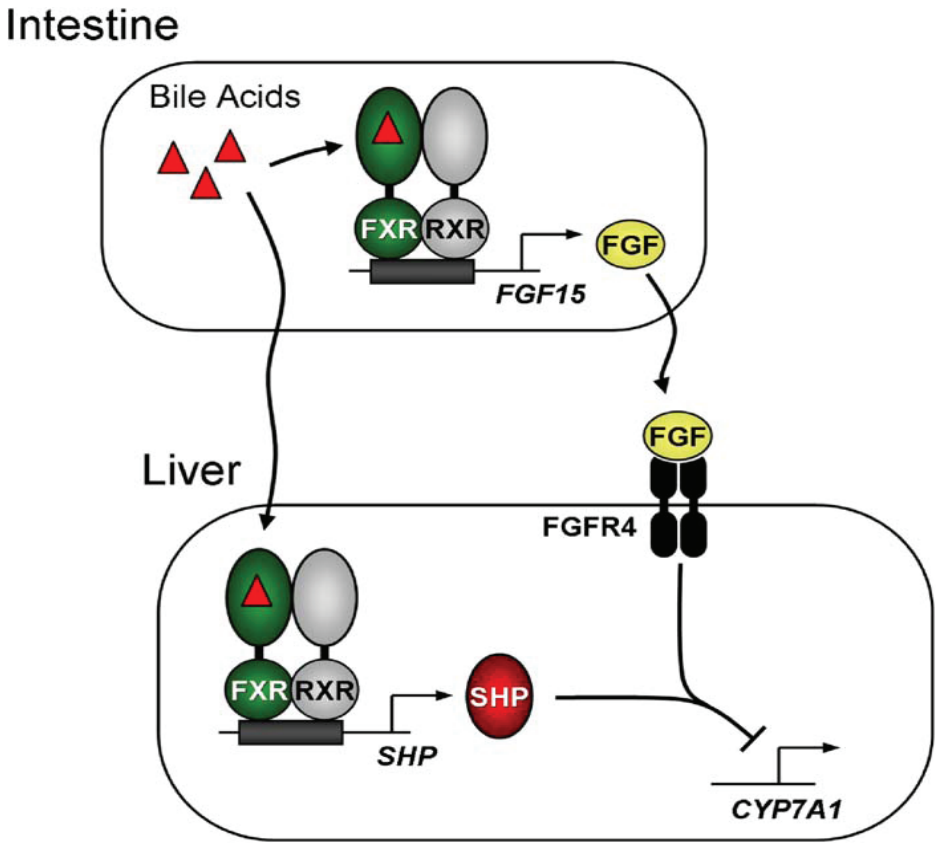

Figure 2.5 Coordinate Repression of CYP7A1 by SHP and FGF15 Signaling Pathway

Bile acids activate FXR to produce FGF15 in intestine. FGF15 functions as an endocrine hormone and acts on the liver receptor FGFR4 to ignite an intracellular cascade, which synergizes with SHP to repress CYP7A1. This figure is adapted from Inagaki, et al., 2005.

the translocation of bile acids out of the liver by inducing the gene expression of BSEP and MRP2. FXR prevents bile acids from flowing back to the liver by inhibiting the gene expression of NTCP through SHP. Thus FXR controls the “in” and “out” transport of bile acids.

Inside the enterocytes, FXR represses the gene expression of IBAT through SHP, thereby limiting the transport of bile acids into the ileum. FXR increases the expression of OSTα/β to promote the removal of bile acids. FXR also up-regulates the expression of IBABP, which buffers and escorts the bile acids during their intracellular transport. In this fashion, FXR precludes bile acids from accumulating in the intestine.

2.3 FXR BILE ACID SIGNALING PATHWAY

2.3.1 FXR

FXR was first isolated from a rodent liver cDNA library and named for its activation by farnesol metabolites (Forman et al., 1995; Seol et al., 1995). Later, bile acids were found to be its physiological ligands (Wang et al., 1999; Parks et al., 1999; Makishima et al., 1999). There are two FXRs in mouse and one in human. Mouse FXRβ is a lanosterol sensor (Otte et al., 2003). In this thesis, FXR is referred to as FXRα.

Upon ligand stimulation, FXR up-regulates a cohort of target genes, which, in most cases, contain an IR-1 consensus element in their promoter or enhancer regions (Pellicciari et al., 2005). FXR also regulates certain genes in a negative way. This is achieved through FXR-SHP signaling cascade and/or FGF15 signaling cascade. Activated FXR increases the expression of SHP, thereby promoting its occupation of a number of FXR target promoters. Upon binding, SHP functions as a potent transcriptional

corepressor to silence the gene expression. Activated FXR also increases the expression of FGF15 in mouse intestine, which works as an enterohepatic endocrine hormone to down-regulate gene expression in a SHP dependent or independent manner (Inagaki et al., 2005).

FXR can be activated by bile acids and synthetic agonists such as GW4064 (EC_{50}=70 nM) (Pellicciari et al., 2005). Among bile acids, CDCA was shown to be most potent based on cell reporter assays (EC_{50}=10 μM) (Makishima et al., 1999; Parks et al., 1999). The structure of FXR complexed with a CDCA derivative (6ECDCA, 6α-ethyl-CDCA) was determined in 2003 (Mi et al., 2003). It revealed a unique ligand orientation in the known nuclear receptor structures. The ligand's D ring (Please refer to cholesterol structure in Fig. 2.2) in the steroid skeleton and side acyl chain face the helix 1, whereas other steroid ligands are arranged in the opposite direction in their cognate nuclear receptors.

FXR plays a key role in maintaining bile acid homeostasis. This is evidenced by FXR null mice, which have decreased bile acid pools, reduced bile acid fecal excretion, and elevated plasma bile acids. FXR null mice have poorer tolerance to 1% cholic acid diet compared to their wildtype littermates (Sinal et al., 2000).

FXR also plays a significant role in regulating glucose metabolism. FXR null mice exhibit increased serum glucose level and insulin resistance (Ma et al., 2006). Activation of FXR by GW4064 lowered the serum glucose level in db/db mice (a mouse model for type II diabetes) and improved insulin sensitivity (Zhang et al., 2006).

In summary, FXR bile acid signaling pathway contributes to the bile acid and carbohydrate homeostasis. This is achieved through FXR target genes and downstream

effectors, among which SHP and FGF15 represent two important signaling circuits.

2.3.2 FXR-SHP Signaling Circuit

SHP (small heterodimer partner) was isolated in a yeast two hybrid assay (Seol et al., 1996). It contains only a putative LBD compared to a typical nuclear receptor. SHP can heterodimerize with other nuclear receptors and repress their transactivation (Lee et al., 2007).

The heterodimerization is believed to be mediated by the N-terminal LXXLL motifs in SHP (Johansson et al., 2000; Borgius et al., 2002). For full interaction with some nuclear receptors, the C-terminal region in SHP is also required (Lee et al., 2000). It is proposed that SHP uses its AF2 domain to recruit corepressors for active repression (Lee et al., 2000; Borgius et al., 2002). Accordingly, a model of two step repression by SHP is shown in Fig. 2.6. LRH-1 activates its target genes by recruiting coactivators via the AF2 domain. In the first step of SHP repression, SHP uses its LXXLL motifs to bind to the same surface occupied by coactivators in LRH-1. As a result, coactivators are dissociated from LRH-1 and transactivation is attenuated. In the next step, SHP recruits transcriptional corepressors via its AF2 domain to actively silence the gene expression.

The importance of FXR-SHP signaling circuit in FXR bile acid signaling pathway is evidenced by SHP null mice (Wang et al., 2002; Kerr et al., 2002). SHP null mice have increased bile acid pool size, consistent with increased expression level of CYP7A1 and CYP8B1 in liver. However, CYP7A1 and CYP8B1 could still be repressed by bile acids (but not GW4064), suggesting the presence of SHP-independent pathways in the feedback regulation of bile acid biosynthesis. In comparison to SHP null mice, SHP liver

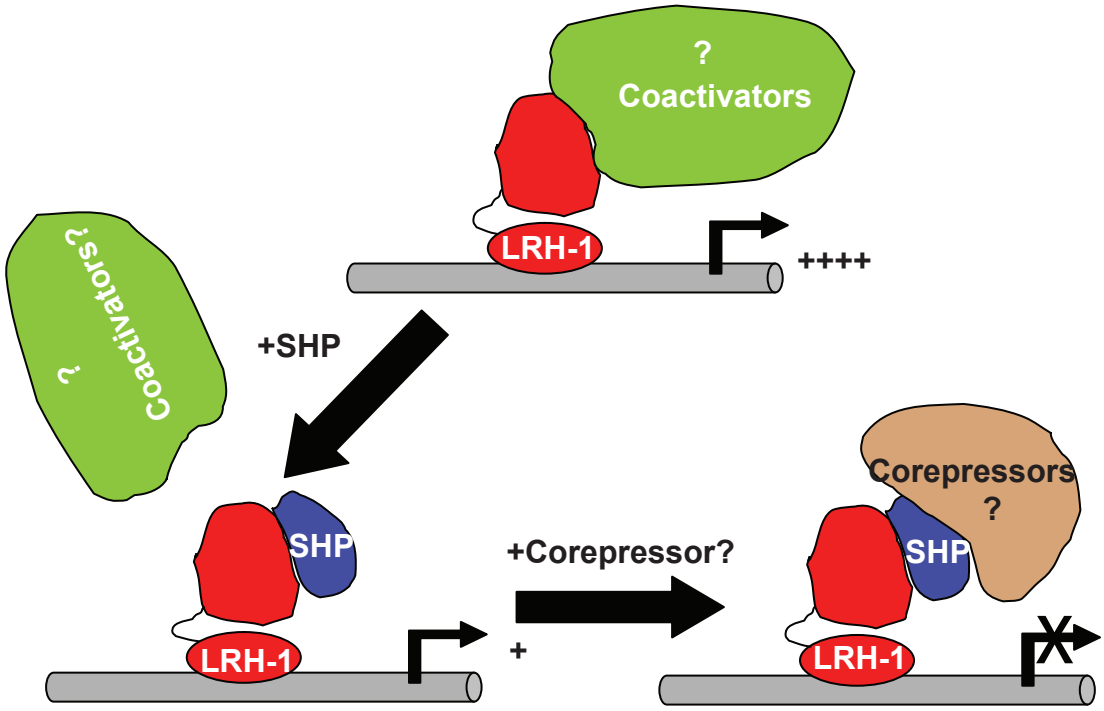

Figure 2.6 A Model of SHP Two Step Repression
SHP represses LRH-1 transactivation in two steps. First, SHP binds to the AF2 domain of LRH-1 and competes for the same binding site with coactivators, leading to attenuation of transcription. Second, SHP recruits corepressors to actively silence the gene expression. AF2, activation function 2.

specific transgenic mice exhibit depleted bile acid pool (Boulias et al., 2005).

2.3.3 FXR-FGF15 Signaling Circuit

FXR-FGF15 signaling circuit represents a recently discovered pathway in maintaining bile acid homeostasis (Inagaki et al., 2005). FGF15 is expressed in small intestine and induced by FXR activation. FGF15 functions as an enterohepatic endocrine hormone by acting on the liver receptor FGFR4 and initiating an intracellular cascade that culminates in CYP7A1 repression. FGF15 and FGFR4 are required for GW4064 and cholic acid repression of CYP7A1, suggesting SHP repression of CYP7A1 is dependent on FGF15 signaling pathway in liver. For effective repression of CYP7A1, the FXR-FGF15 signaling circuit also requires the presence of SHP. In this manner, a liver corepressor (SHP) and an intestinal hormone (FGF15) synergize with each other to achieve the feedback regulation of bile acid biosynthesis.

2.4 OTHER BILE ACID SIGNALING PATHWAYS

2.4.1 PXR, CAR, and VDR Bile Acid Signaling Pathways

PXR, CAR, and VDR are also capable of mediating bile acid signaling pathways by eliminating toxic accumulation of bile acids (Kullak-Ublick et al., 2004; Modica et al., 2009). They are activated by LCA and its derivative 3-keto LCA (Xie et al., 2001; Staudinger et al., 2001; Zhang et al., 2004). As a result, metabolizing enzymes (e.g., CYP3A and CYP2B) and membrane transporters are up-regulated to remove toxic species of bile acids from cells (Modica et al., 2009; Hofmann, 2009). In this manner, these nuclear receptors function as auxiliary pathways to assist FXR in maintaining bile

acid homeostasis.

2.4.2 TGR5 Bile Acid Signaling Pathway

TGR5 is a Gα protein coupled receptor (Maruyama et al., 2002). It can be activated by free and conjugated bile acids (Kawamata et al., 2003). As a result, an intracellular kinase cascade is activated, which leads to activation of enzymes and factors involved in energy consumption (Houten et al., 2006). Therefore, TGR5 represents another physiological bile acid signaling pathway, through which bile acids control energy metabolism.

2.5 RESEARCH DESCRIPTION

One focus of my thesis research was to understand the molecular mechanism whereby SHP controls the bile acid feedback regulatory loop. One aspect of this work included identification of SHP interacting proteins. The endpoint of study was to provide answers to these questions: (1) How does SHP achieve it repressive activity? (2) How does SHP respond to FGF15 signaling pathway? Some factors may mediate the connection between SHP repressive activity and FGF15 signaling cascade. Upon FGF15 activation, these mediators may enhance the recruitment of the inhibitory activity of SHP to the target promoters. Post-translational modification events may also play a role in this process by occurring on SHP or SHP interacting corepressors, as a result of which, their interactions are increased. (3) How is the SHP protein itself regulated in cells? Protein stability and intracellular localization are interesting issues. Discoveries of the interacting proteins that belong to know enzymatic machineries may suggest possible modifications

of SHP protein, directing the way to future functional investigation.

Because SHP repression requires binding to the partner, it was of interest to understand the molecular basis for how SHP interacts with its nuclear receptor partners. The structural determination of SHP complexed with its partner (e.g., LRH-1) will provide us this information. To that end, I initiated the following studies: (1) Elucidation of the 3-D structure of SHP, which represents one of a few structures in the nuclear receptor superfamily remaining to be solved. Analysis of the ligand binding pocket will help us evaluate the possibility of whether SHP is bound by ligands. (2) Elucidation of the binding surface between SHP and its partner. It is speculated that SHP uses a second LXXLL motif to bind to the AF2 domain of its partner. This hypothesis can be validated by solving SHP structure in complex with a partner. Moreover, this would allow determination of other parts of SHP structure that might be important in protein-protein interaction. Importantly, this structure would represent the first of a nuclear receptor (LRH-1) complexed with a complete LXXLL motif-containing coregulator (SHP) in the field of nuclear receptor research.

Toward the first aim, I planned to use a number of biochemical strategies, including co-immunoprecipitation. The key to the second aim is achieving enough SHP recombinant protein for crystallization. Since SHP was known to be an insoluble protein based on the data of former work in our laboratory and others, different solubilization methods were tested. In parallel, the structure-function relationship studies would be done based on SHP sequence homology to other nuclear receptors with available structure information. The first part of my thesis research focuses on biochemical and structural analysis of SHP repression.

CHAPTER THREE

Biochemical and Structural Analysis of SHP Repression

3.1 INTRODUCTION

Isolation of SHP interacting proteins will provide insights into the mechanisms whereby SHP represses transcription. A number of SHP interacting proteins have been reported in recent years, including EID1 (EP300 interacting inhibitor of differentiation 1), GPS2 (G protein pathway suppressor 2), and SIMILE (SHP-interacting leucine zipper protein), which were isolated based on the yeast two hybrid system (Bavner et al., 2002; Sanyal et al., 2007; Xie et al., 2008). A newer one, pmsd1 (a component of the 26S proteasomal complex), was isolated in co-immunoprecipitation assays (Miao et al., 2009). GST pull down and tandem affinity purification are two powerful tools in dissecting protein interactions and represent different methods to isolate SHP binding partners.

SHP repression requires its binding to the partner nuclear receptor. It is of interest to understand the underlying molecular basis of this interaction. X-ray crystallography is an effective technique in analyzing nuclear receptor structures. Recently, the crystal structure of DAX-1 (the closest vertebrate relative to SHP) was reported (Sablin et al., 2008). Two DAX-1 ligand binding domains (LBD) interact with one LRH-1 LBD at the C-terminus (Figure 3.1). The DAX-1 LBDs use the same interface to interact with LRH-1, specified by a PCFXXLP motif (X, any amino acid), while the LRH-1 LBD uses two different interfaces to bind DAX-1. One of these sites is the major binding site, reminiscent of the coactivator binding site, and the other is a minor site, contributed by elements from helices H7 and H11. The extremely narrow hydrophobic pocket in the DAX-1 LBD excludes the possibility of harboring ligands. Helix H12 is folded back into

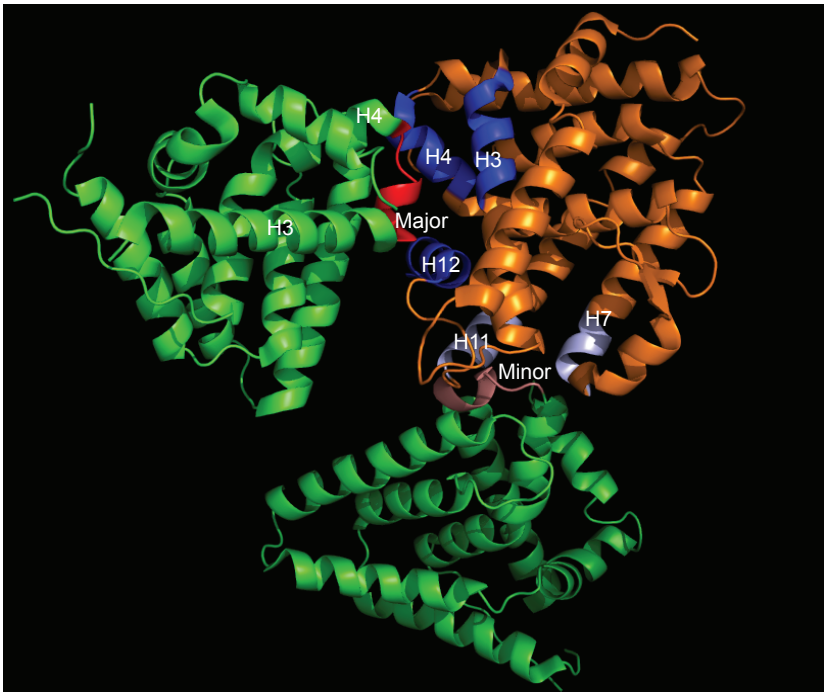

Figure 3.1 3-D Structure of the DAX-1/LRH-1 Complex in Ribbon Representation
LRH-1 is shown in orange. Two DAX-1 molecules are shown in green. The major binding site (Major) between LRH-1 and DAX-1 involves structural elements from DAX-1 (in red) and LRH-1 (in blue, AF2 domain). The minor binding site (Minor) involves structural elements from DAX-1 (in salmon) and LRH-1 (in light blue, H7 and H11). This figure is adapted with permission from Sablin, et al., 2008.

its own coregulator binding groove, representing an auto-inhibitory conformation. The determination of SHP structure is impeded by obtaining soluble recombinant protein.

Structure modeling is one way to predict the structural details when the crystal structure is not available. A number of SHP structure models have been proposed based on the crystal structures of HNF4α, ERRγ, and USP (the insect homolog of RXR) (Park et al., 2004; Macchiarulo et al., 2006). Recently, the COUP-TF2 LBD crystal structure was solved by our collaborator (Dr. Eric Xu, Lab of Structure Science, Van Andel Institute) (Kruse et al., 2008). Since COUP-TF2 shares relatively high sequence similarity to SHP (45%), its structural information is helpful for understanding SHP repression.

In this chapter, experiments regarding biochemical analysis of SHP repression are first presented, including TSA (HDAC inhibitor) treatment assay and tandem affinity purification. A new SHP model based on the COUP-TF2 structure is proposed, followed by validating assays. Last, the first successful strategy to solubilize SHP protein (in bacteria) is reported. The work for SHP crystallization is presented. To that end, SHP crystals are obtained that diffract to 3.2 Angstroms.

3.2 MATERIALS AND METHODS

3.2.1 Plasmids

FLAG-HA-SHP was constructed based on the vector N-terminal p3xFLAG-CMV (Sigma). A short polypeptide containing three linkers (GSAGG), HA (YPYDVPDYA), and one linker was introduced between FLAG and SHP by PCR in order to improve the immunoprecipitation efficiency. The SHP mutants used for transfection or crystallization

assays were created by site-directed mutagenesis (Stratagene) and verified by sequencing. In order to improve the solubility of recombinant SHP protein, mouse SHP10CS (mutation of the last ten cysteines to serines) cDNA and mouse LRH-1 LBD (residues 318-560) or human LRH-1 LBD (residues 299-541) cDNA were cloned into the multiple cloning sites of the engineered SUMO pETDuet vector (Novagen), respectively for coexpression. The expressed SHP/LRH-1 complex was purified and applied for crystallization. Because the N-terminal protein sequence (~20 amino acids) of SHP was predicted to be unstructured, in order to reduce its adverse influence on SHP crystallization, a SHP mutant with the N-terminal 17 amino acids removed was constructed and named SHP10CSx2. Mouse SHP10CS and human LRH-1 LBD cDNAs were cloned into the multiple cloning sites of the engineered GST pETDuet vector, respectively for expression of GST-SHP/LRH-1, which was used in AlphaScreen assays.

Tilapia DAX-1 (tDAX-1, mentioned in discussion section) was cloned by RT-PCR. Fishes were sacrificed and testis mRNA was prepared as described (Bookout et al., 2006). PCR primers were designed based on tDAX-1 cDNA sequence (GenBank accession number AY135397). The 5' primer sequence is TGGATCCCGCCATGGACAGCGCGTGTCGTTG and the 3' primer sequence is TGCTAGCTATCTGCAGAAGAGCATGTC. The annealing temperature is 52 ℃. PCR products were verified by sequencing.

3.2.2 Reagents

SHP antibodies were produced in collaboration with the laboratory of Dr. David Russell, the antibody core facility at UTSW, or National Institute of Biological Sciences at Beijing, China.

3.2.3 Cell Culture and Cotransfection Assays

All immortal cell lines were maintained as described elsewhere (Lu et al., 2000; Shulman et al., 2004). Mouse primary hepatocytes were prepared as documented (Chen et al., 2004). HEK293 cells (8000 cells/well in a 96-well plate) were transfected by lipofectamine 2000 (Invitrogen) or calcium phosphate. COS7 cells (2000 cells/well in a 96-well plate) were transfected by Fugene 6 (Roche). HepG2 cells (5000 cells/well in a 96-well plate) and mouse primary hepatocytes were transfected by lipofectamine 2000. Cotransfection assays were conducted in 96-well plates as reported (Shulman et al., 2004). Vehicle or indicated compounds were added to each well 6 hours post-transfection and then incubated for 18 hours. Cells were harvested for luciferase and β-galactosidase activities as described (Shulman et al., 2004; Lu et al., 2000). Data represent the mean ± s.d. from triplicate assays.

3.2.4 Stable Cell Line Establishment

In order to perform tandem affinity purification to isolate SHP interacting proteins, Flag-HA-SHP stable cells were established (Yang et al., 2002). First, HEK293 cells were transiently transfected with the plasmid Flag-HA-SHP using lipofectamine 2000. Two days after transfection, the cells were dislodged and transferred to 15 cm plates. One day after transfer, G418 (1 mg/ml) was applied for selection. The resistant clones appeared in 2-3 weeks and were picked up for expansion. The resistant clones were also pooled for expansion.

3.2.5 Nuclear Extract Preparation

Nuclear extracts from cultured cells were prepared as described elsewhere (Wang et al., 1993; Yang et al., 2002; Chen et al., 2005). The cells were collected and washed

once by 1x PBS. Then the cells were resuspended in buffer A (10 mM HEPES, pH 8.0, 10 mM KCl, 0.1 mM EDTA, 1 mM DTT, 0.5 mM PMSF) and swelled on ice for 15 minutes. 10% NP40 was added to a final concentration of 0.5%. Subsequently the cells were vortexed on a table vortex for 1 minute and centrifuged at 13,000 rpm for 10 minutes at 4 ℃. The supernatant was used as cytosolic extracts and transferred to a new tube. The pellet was resuspended in pre-chilled buffer C (20 mM HEPES, pH 8.0, 0.4 M NaCl, 1mM EDTA, 1mM DTT, 1 mM PMSF) by pipetting up and down and then subjected to sonication for 3 times (amplitude 20-30) at 20 seconds each by using the micro ultrasonic cell disrupter (Contes) in the cold room. The nuclear lysates were rocked for 45 minutes at 4 ℃ and centrifuged at 13, 000 rpm for 30 minutes. The supernatant was used as nuclear extracts and transferred to a new tube. The protein concentration of cytosolic and nuclear extracts was determined in the Bradford protein assay (Biorad) and diluted to 1 mg/ml by using pre-chilled buffer D (20 mM HEPES, pH 8.0, 1 mM EDTA, 0.2% NP40). The cytosolic and nuclear extracts were ready for immunoprecipitation assays. Protein inhibitors (Roche) were included in buffer A and C.

Mouse liver nuclear extracts were obtained as described (Sheng et al., 1995). Around 100-150 mg frozen mouse liver was cut, transferred to a 15 ml round bottom falcon tube and mixed with 1.2 ml homogenization buffer (20 mM Tris HCl, pH 7.4, 2 mM MgCl2, 0.25 M Sucrose, 10 mM EDTA, 10 mM EGTA, 5 mM DTT, 0.1 mM leupepetin, protease inhibitors). The samples were homogenized for 3 times (amplitude 5-6) at 20 seconds each by using a homogenizer (Power Gen 125) and then centrifuged at 4000 rpm for 5 minutes at 4 ℃. The supernatant was decanted. The pellet was resuspended with 1.8 ml homogenization buffer and transferred to a 2 ml microfuge tube.

The liver nuclei were spun down at 2000 rpm for 5 minutes at 4 ℃. The supernatant was decanted. The pellet nuclei pellet was resuspended in 300 µl of buffer C (20 mM HEPES, pH 7.6, 2.5% glycerol, 0.42 M NaCl, 1.5 mM MgCl2, 1 mM EDTA, 1 mM EGTA, protease inhibitors). The samples were rocked for 45 minutes at 4 ℃ and then centrifuged at 100,000 rpm for 30 minutes. The supernatant was used as nuclear extracts and transferred to a new tube.

3.2.6 Tandem Affinity Purification and Co-immunoprecipitation

Co-immunoprecipitation assays were conducted as reported (Boulias and Talianidis, 2004). The cellular lysates were mixed with the appropriate antibodies and protein A sepharose beads and rocked for 1 hour at 4 ℃. Then the lysates were spun down at 2000 rpm for 5 minutes and washed for 3 times with co-immunoprecipitation buffer (50 mM Tris HCl, pH 7.5, 15 mM EGTA, 100 mM NaCl, 0.1% Triton X-100). Finally, the samples were spun down and 4x SDS loading buffer was applied for the SDS-PAGE and western blot analysis.

Tandem affinity purification was performed and detailed (Chen et al., 2005). The cellular lystates were mixed with anti Flag M2 affinity gel (Sigma) and incubated overnight at 4 ℃. The next day, the samples were washed for 3 times with TBS buffer (50 mM Tris HCl, pH 7.4, 150 mM NaCl) plus 0.2% NP40. The samples were spun down and incubated with 3 gel volumes of 3x Flag peptides (200 ng/µl in TBS, Sigma) for 4 hours. Then the samples were spun down and the supernatant was transferred to a new tube. The elution step was repeated once. The supernatants were pooled, mixed with anit HA affinity gel (Sigma), and incubated overnight at 4 ℃. The next day, the samples were washed 3 times with TBS buffer plus 0.2% NP40. Finally, the samples were spun down

and incubated with 3 gel volumes of HA peptides (200 ng/ul in TBS, Sigma) for 4 hours. Then the samples were spun down and the supernatant was transferred to a new tube. The elution step was repeated once with the overnight incubation. The supernatants were pooled, concentrated by appropriate centrifugal filters (Amicon Ultra), and subjected to SDS-PAGE and silver stain analysis.

3.2.7 SHP modeling

This work was done by our collaborator at the laboratory of Dr. Eric Xu. The alignment of the human small heterodimer partner (SHP, Entrez code: NP_068804) and human COUP-TF2 (pdb code 3CJW) were performed using ICM program (version 3.4.8b, 2006, Molsoft LLC, San Diego, CA) (Schapira et al., 2001). The homology module was used to create a model and the molecular mechanics module was used for optimization.

3.2.8 Protein Purification, SHP Crystallization and Data Collection

Mouse SHP (10CS or 10CSx2) and the LRH-1 LBD (human or mouse) were coexpressed in BL21 DE3 cells. Cells were harvested and lysed as documented (Li et al., 2005b). Protein was purified in two steps including HIS purification and gel filtration, punctuated by Ulp1 (SUMO protease) overnight cleavage to remove the SUMO tag immediately in front of SHP. GST-SHP was purified as described (Li et al., 2005b).

Protein complex mouse SHP10CSx2 and human LRH-1 LBD yielded crystals. The crystals were grown at 20 ℃ in hanging drops containing 3.0 μl of the protein solution (3.0 mg/ml) and 2.0 μl of well solution containing 0.95-1.0 M imidazole (pH 7.0-7.1). The crystals were flash-frozen and stored in liquid nitrogen before X-ray diffraction.

The diffraction data were collected with a MAR225 CCD detector at 21-ID

beamline at the Advanced Photon Source at Argonne National Laboratory (Argonne, Illinois, United States). The observed reflections were reduced, merged, and scaled with DENZO and SCALEPACK in the HKL2000 software package (Otwinowski Z, 1997).

3.2.9 AlphaScreen Assays

I performed the work at the laboratory of our collaborator, Dr. Eric Xu, at the Van Andel Institute. The assays were conducted using the AlphaScreen assay kit as described (Li et al., 2005b) (Perkin-Elmer). 100 nM of GST-LRH-1 (human LBD) or 100 nM of GST-SHP complexed with human LRH-1 LBD was applied. 20 nM, 60 nM and 100 nM of biotinylated EID1 peptides were used.

3.3 RESULTS

3.3.1 SHP Repression is TSA Resistant in liver cells

Classical nuclear receptor corepressors such as SMRT recruit HDACs for gene repression (Yu et al., 2003). It was interesting to test if SHP also recruits HDACs for gene repression. Therefore, the HDAC inhibitor TSA was added in cotransfection assays to dissect SHP repression mechanism. In order to indicate that TSA can derepress HDAC inhibition, SMRT repression of Gal4-RAR transactivation was included as a control. The reporter UAS-luc (the Gal4 response element fused to the luciferase gene) and the transcription factors Gal4-LRH-1 and Gal4-HNF4α were used in experiments. As shown in Fig. 3.2A and B TSA treatment (100 ng/ml) did not reverse SHP repression on LRH-1 or HNF4α transactivation in HepG2 cells, while it did reverse the repression of SMRT on RAR transactivation, suggesting SHP repression is TSA resistant in liver cells. TSA treatment assays were also performed in mouse primary hepatocytes by using the reporter

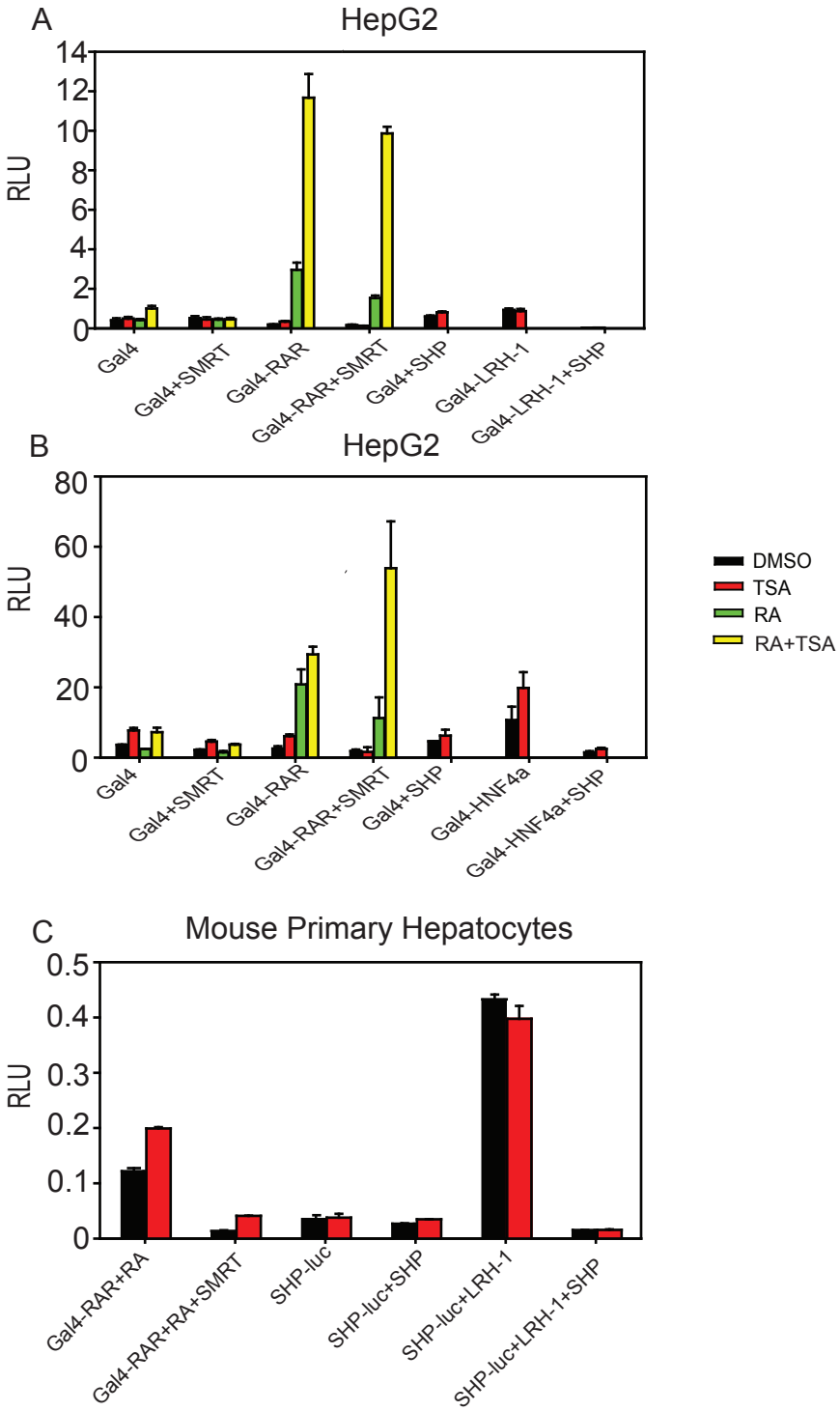

Figure 3.2 SHP Repression is TSA Resistant in Liver Cells
Cotransfection assays are performed in HepG2 (A-B) and mouse primary hepatocytes (C). UAS-luc (A-B) and SHP-luc (C) are used as reporters. TSA, HDAC inhibitor, 100ng/ml; RA, all trans retinoic acid, 1μM. RLU, relative light unit.

SHP-luc (the SHP promoter fused to the luciferase gene). As shown in Fig. 3.2C, TSA did not influence SHP repression on LRH-1 transactivation. These results indicate that HDACs or HDAC-dependent corepressors do not play a global role in SHP regulated events in liver.

3.3.2 Tandem Affinity Purification of SHP Interacting Proteins

Tagging (e.g., FLAG) immediately in front of SHP protein yielded poor immunoprecipitation efficiency in immunoprecipitation assays. Therefore, linkers were introduced between tags and SHP protein. FLAG-HA-SHP was constructed and used for HEK293 stable cell line establishment. Tandem affinity purification was performed to purify SHP associated proteins. The purified SHP complex was visualized by silver staining. The associated SHP proteins were identified by mass spectrometry (protein chemistry technology center, UTSW). They are γ-catenin (~140KD), mitochondrial inner membrane protein (~80KD), HSP70 (~70KD, Heat Shock Protein) and β-actin (~40KD) (Fig. 3.3A). Unfortunately, the interactions of these proteins with SHP could not be validated in subsequent co-immunoprecipitation experiments. Coexpression of HSP70 and SHP did not increase the solubility of SHP in bacteria.

3.3.3 SHP Antibody Test

A SHP antibody would be a key tool to examine SHP's repression mechanism. We have spent considerable effort raising SHP antibody. While we were successful in acquiring a SHP antibody that recognizes SHP protein overexpressed in COS7 cells (Fig. 3.3B), the titers were never of high enough quality to specifically detect SHP protein

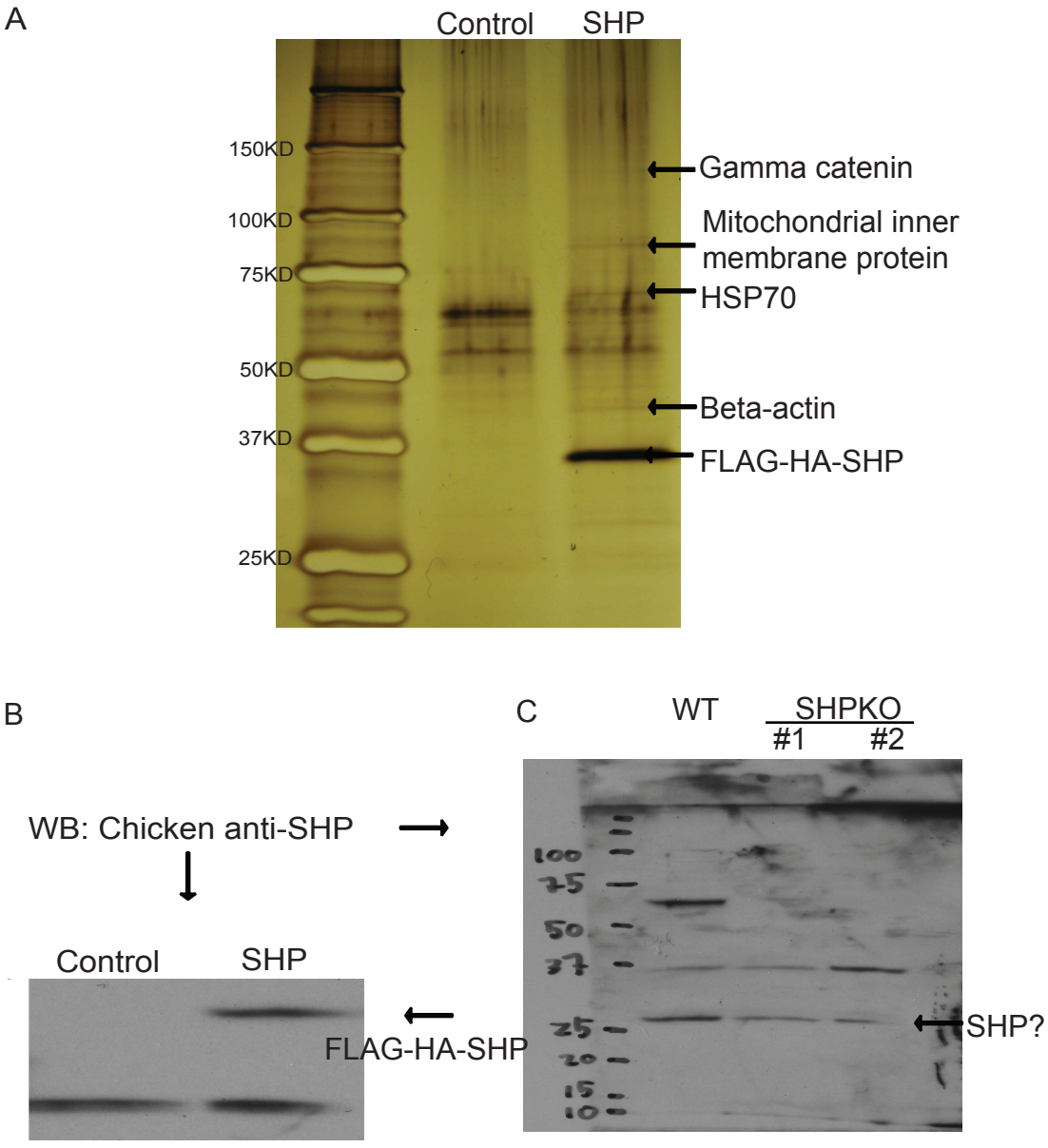

Figure 3.3 Biochemical Characterization of SHP Repression
(A) Tandem affinity purification of SHP interacting proteins from HEK293 cells. (B-C) The prepared chicken SHP antibody specifically recognizes FLAG-HA-SHP overexpressed in COS7 cells (B) but not endogenous SHP (C). As indicated in C, liver nuclear extracts were prepared from wildtype or SHP knockout (KO) mice. Two SHP knockout mice were used and marked as #1 and #2. Chicken SHP antibody detects one band (close to SHP protein size) in all samples.

prepared from mouse nuclear extracts. As shown in Fig. 3.3C, SHP antibody raised in chicken recognized one band (close to the SHP protein size) in both wildtype and SHP knockout samples. We are continuing to pursue making SHP antibodies. However, it is of interest to note that several labs (and companies) have also tried unsuccessfully to generate a reliable SHP antibody, suggesting that a novel approach will be necessary.

3.3.4 SHP Modeling Study

In collaboration with the laboratory of Dr. Eric Xu, we proposed a new SHP structural model based on the X-ray crystal structure of COUP-TF2. According to this model and our understanding of nuclear receptor structures, a number of SHP mutants were suggested (Fig. 3.4A). These mutants were speculated to disrupt certain aspects of SHP function, such as charge clamp, cofactor recruitment, dimerization, and ligand binding.

Cotransfection assays were performed in HEK293, COS7, and HepG2 cells to examine the functional consequence of these mutations (Fig. 3.4B). Of these, L66R (cofactor recruitment) strongly impaired SHP repression (3 fold less repressive), while mutation of amino acids involved in the putative ligand binding pocket, such as T58W, V65W, and F240A, had weaker effects.

Gal4-SHP mutants were constructed in order to examine the effect of these mutations on the intrinsic SHP repressive activity. VP16-SHP mutants were also constructed to examine the effect of these mutations on SHP and LRH-1 interaction. As shown in Fig. 3.5A, there was no significant difference between SHP wildtype and mutants in terms of basal repression of the Gal4 reporter. Fig. 3.5B indicates that R74A

A

FUNCTIONS	MUTATED AMINO ACIDS IN MOUSE SHP
Charge Clamp	(1) R74A, (2) D255A, (3) R74A/D255A
Cofactor Binding	(4) L66R, (5) V70R, (6) L91R
Dimerization	(7) I220A/L221A, (8) L221A/L222A (9) R219A, (10) D181A, (11) D181A/R219A
Ligand Binding	(12) T58W, (13) C59W, (14) E61W (15) A62W, (16) V65W, (17) G96W (18) L100W, (19) E114W, (20) A 115W (21) A148W, (22) D237W, (23) F240A, (24) R241A

B

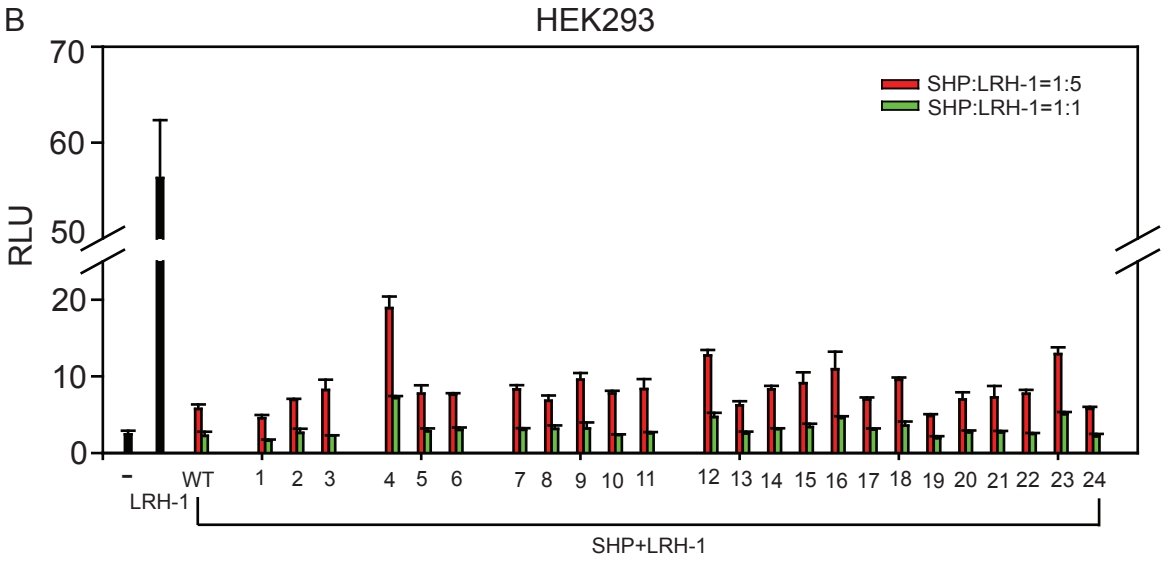

Figure 3.4 SHP Modeling Study- Part 1

(A) Proposed amino acid mutations in mouse SHP based on the new SHP model. (B) Cotransfection assays are performed in HEK293, HepG2, and COS7 cells using SHP-luc as the reporter. A representative result in HEK293 cells is shown here. The numbers (X-axis) in B represent SHP mutants listed in A. Repression of LRH-1 transactivation by SHP mutants are compared to that by SHP wildtype (WT). RLU, relative light unit.

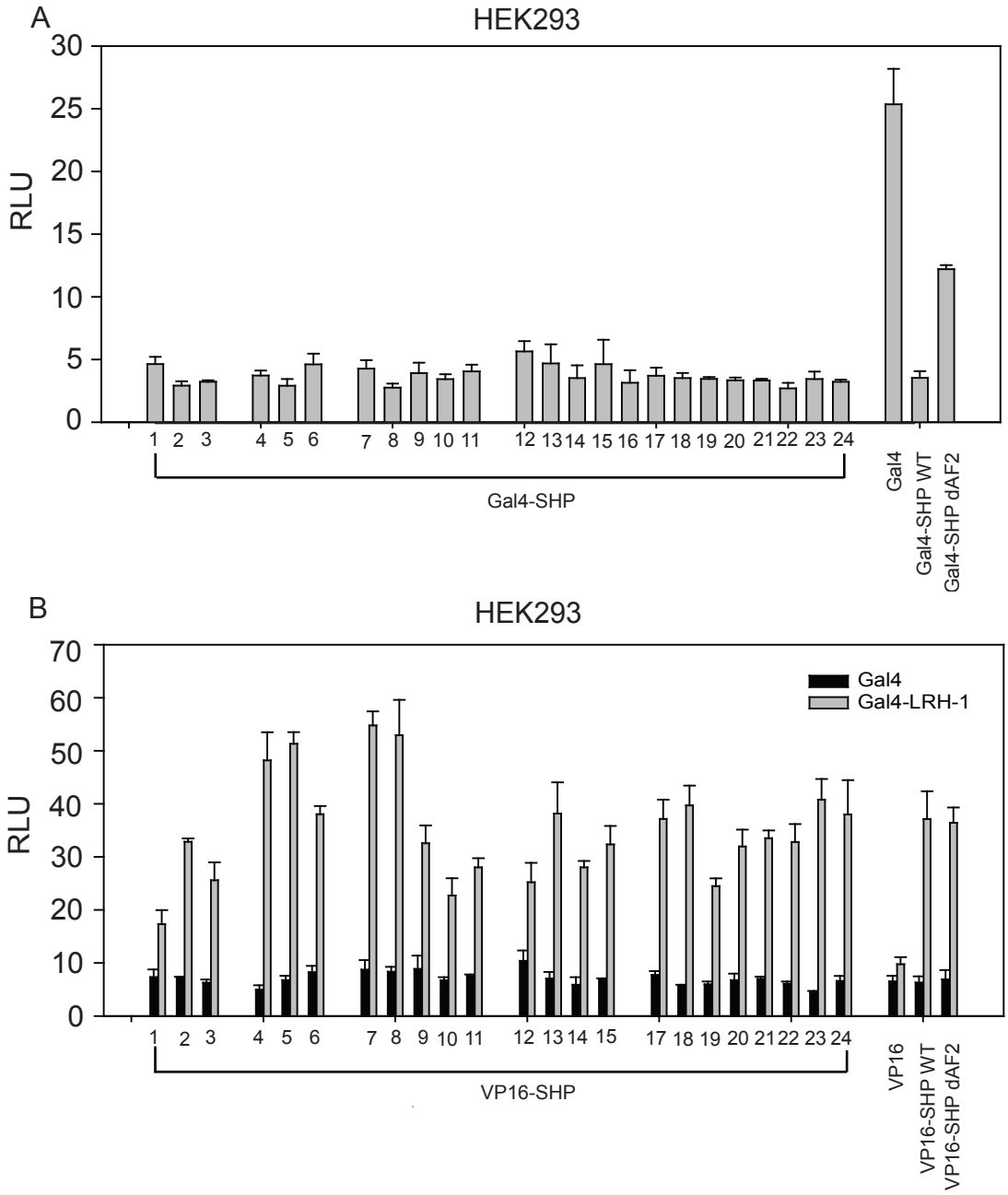

Figure 3.5 SHP Modeling Study-Part 2
(A) Gal4-SHP cotransfection assays are performed using UAS-luc as the reporter to examine the basal repression of Gal4 by SHP. (B) Mammalian two hybrid assays are conducted to examine the interaction between SHP and LRH-1. The numbers (X-axis) represent SHP mutants listed in Fig. 3.4A. The function of mutants are compared to SHP wildtype (WT) and SHP dAF2 (deletion of SHP AF2 helix). RLU, relative light unit.

(charge clamp) decreases SHP and LRH-1 interaction by 50%, while R74A/D255A (charge clamp), D181A, R219A/D181A (dimerization), T58W, E61W, and E114W (ligand binding) decreases SHP and LRH-1 interaction by 30%. The results suggest that the modeling did not appear to accurately predict the functional surfaces of SHP. One interpretation is that SHP may have a different 3-D structure.

3.3.5 Solubilization of SHP Protein

Cysteines, particularly those located on the protein surface, often affect recombinant protein folding by forming random disulfide bonds and hence result in poor protein solubility. It is noted that there are 12 cysteines in mouse SHP, which is an unusually high proportion relative to most proteins. Mutation of cysteines to serines has been shown to stabilize the nuclear receptor SF-1 (Krylova et al., 2005). Therefore, the same strategy may also be able to stabilize the nuclear receptor SHP.

However, the cysteines in SHP are conserved across species, suggesting they may have important roles in SHP function. Consequently, functional assays are needed to direct mutagenesis and find mutants that are not only soluble, but also functional compared to the wildtype.

Therefore, a comprehensive set of SHP mutants with different configurations of cysteines to serines mutations were constructed. Then, they were screened in cotransfection assays (Fig. 3.6A). One of the mutants, SHP10CS (the last 10 cysteines mutated to serines) showed activity similar to wildtype SHP. This mutant also mimicked wildtype SHP in its ability to interact with LRH-1, repress basal transcription, and interact with the methyltransferase, G9a (Fig. 3.7). These results support the notion that

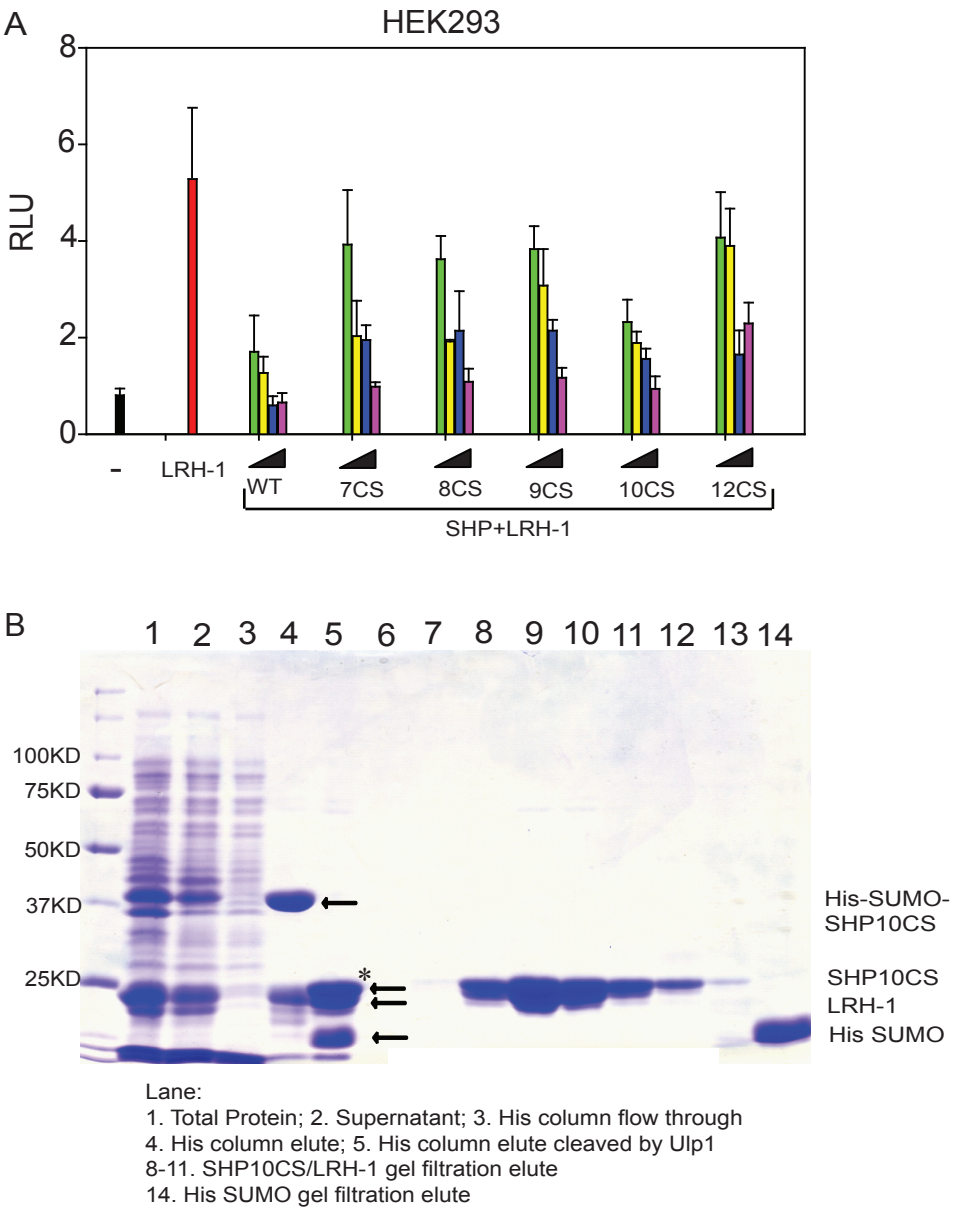

Figure 3.6 Solubilization of SHP Protein

(A) Cotransfection assays are performed to identify functional SHP mutants. 7CS, C42S-C44S-C53S-C59S-C80S-C189S-C203S; 8CS, 7CS plus C155S; 9CS, 7CS plus C93S and C94S; 10CS, 9CS plus C155S; 12CS, all cysteines mutated. SHP10CS behaves similarly to SHP wildtype (WT) in a SHP dose dependent manner. (B) Coomassie blue staining shows purification of SHP10CS in complex with the LRH-1 ligand binding domain. SHP10CS has a molecular weight close to the LRH-1 LBD. Therefore, the bands (asterisk) representing SHP10CS and LRH-1 are narrowly separated on the gel. Identities of the bands pointed by arrows are listed on the right of the gel. RLU, relative light unit.

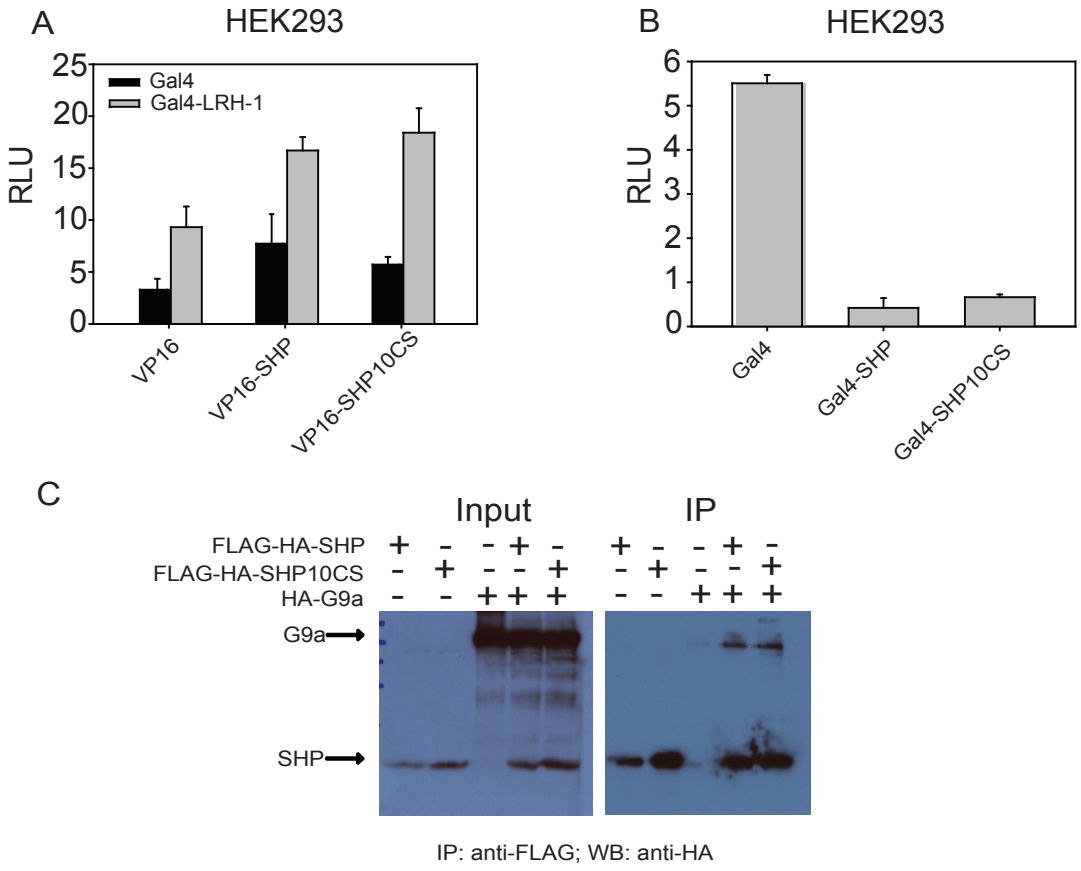

Figure 3.7 Functional Examination of SHP10CS
(A) Mammalian two hybrid assays are performed to examine the interaction between SHP10CS and LRH-1. (B) Gal4-SHP cotransfection assays are performed to examine the basal repression of Gal4 by SHP10CS. (C) Coimmunoprecipitation assays are performed in COS7 cells to examine the interaction between SHP10CS and G9a. G9a is histone methyltransferase and reported to interact with SHP. RLU, relative light unit.

SHP10CS faithfully represents its wildtype counterpart in functionality and very likely maintains the structural integrity related to its function.

Encouragingly, SHP10CS was weakly soluble in bacteria. More importantly, its solubility and stability were greatly improved by coexpression with either mouse or human LRH-1 LBD. We followed the strategy of coexpressing and copurifying SHP10CS and the LRH-1 LBD as a protein complex (Fig. 3.6B). To reduce the potential disordered sequences at the N-terminus of SHP, we also made a SHP mutant with the N-terminal 17 amino acids removed and named it SHP10CSx2. Six liters of BL21 DE3 culture yielded around 100 mg of protein complex after purification, which was subsequently used for crystallization.

3.3.6 SHP Crystallization

Purified SHP/LRH-1 complex was next subjected to crystallization screens with robotic assistance (using PHOENIX). The promising microcrystals were then optimized in 24-well plates by manipulation of different parameters, including buffer pH, salt, precipitant, protein concentration, the volume ratio of protein to buffer, etc. As a result, I obtained needle-shaped crystals in hanging drops by using SHP10CSx2 and human LRH-1 LBD (Fig. 3.8A). These crystals were diffracted to 3.2 Angstroms in one direction but not 90 degree clockwise, suggesting they were not properly packed in one direction and further optimizations were required (Fig. 3.8B)

3.4 DISCUSSION

It is reported that SHP interacts with HDACs for gene repression and SHP

A

B

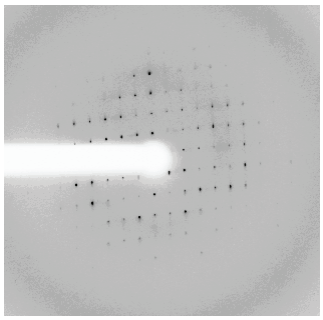

Figure 3.8 SHP Crystallization
(A) SHP crystals were grown at 20℃ in hanging drops containing 3.0 µl of the protein solution (3.0 mg/ml) and 2.0 µl of the well solution containing 0.95-1.0 M imidazole (pH 7.0-7.1). (B) One example of X-ray diffraction pattern for SHP crystals. 3.2 Angstrom resolution is achieved for one facet of these crystals.

repression can be reversed by HDAC inhibitor TSA treatment (Boulias and Talianidis, 2004; Gobinet et al., 2005). However, these experiments were not performed in liver cells, which are physiologically related to SHP repression. My work indicated that SHP repression is TSA resistant in HepG2 cells and mouse primary hepatocytes, suggesting HDACs are not the major repressive force involved in SHP repression in liver and SHP may use histone deacetylation independent mechanism for gene silencing.

I purified SHP associated proteins from HEK293 cells. However, the interactions of these proteins with SHP could not be validated in subsequent co-immunoprecipitation assays. The purified SHP protein from HEK293 cells was also analyzed by mass spectrometry to detect the potential modifications. It was shown that a small portion of SHP protein, at K68 has a 28KD shift (Fig. 3.9A). This suggests that SHP K68 may be modified, possibly by dimethylation (28KD). Mutation of SHP K68 to R68 did not affect SHP repression in cotransfection assays (Fig. 3.9B).

In liver, SHP repression is dependent on the FGF15 signaling pathway (Inagaki et al., 2005). It is speculated that recruitment of SHP interacting corepressors requires activation of FGF15 signaling pathway in cells. FGF15 treatment did not influence SHP repression in HEK293 cells (data not shown). One interpretation is that FGF15 coreceptor is lack in HEK293 cells (Kurosu et al., 2007) . I also used liver cells such as HepG2 and mouse Hepa1-6 to set up FLAG-HA-SHP stable cells. HepG2 cells grew too slowly and mouse Hepa1-6 cells yielded too few FLAG-HA-SHP protein. Therefore, future work in progress is being directed at improving FLAG-HA-SHP yields in these cells.

Co-immunoprecipitation of endogenous SHP complex is an ideal strategy. However, the lack of a good SHP antibody is clearly one of the reasons why it has been

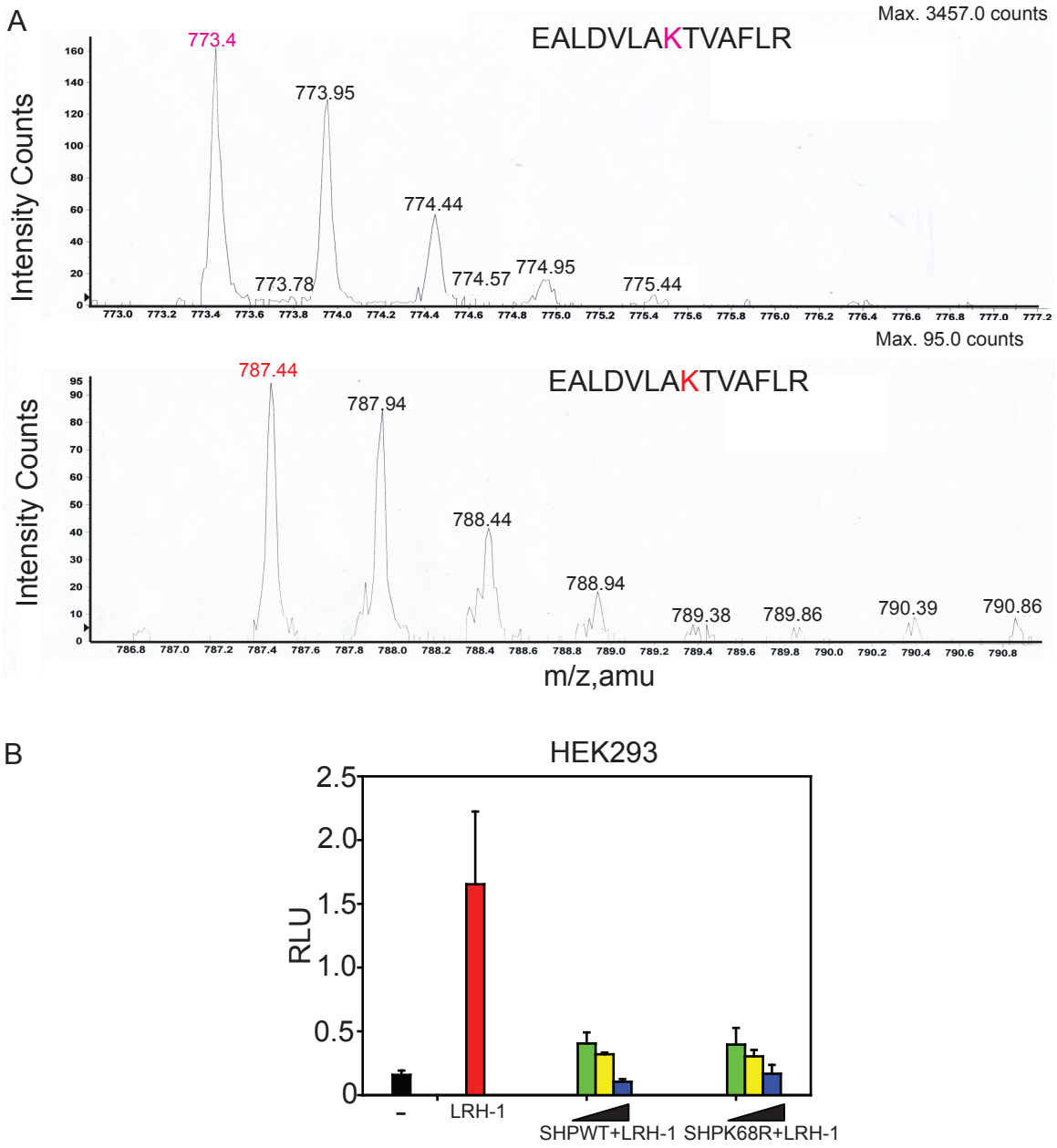

Figure 3.9 Mass Spectrometry Analysis of SHP Modification
(A) Time-of-flight (TOF) mass spectrometry analysis indicates that a small potion of SHP protein has a 28KD shift at K68. The upper panel shows unmodified SHP peptide with a mass to charge ratio of 773.4 (in magenta). The lower panel shows modified SHP peptide with a mass to charge ratio of 787.44 (in red). K68 is the modification site and speculated to be dimethylated. Of note, the positive charge is gone when K68 is modified. (B) Cotransfection assays are performed to test the effect of K68 mutation on SHP repression of LRH-1 transactivation. RLU, relative light unit.

difficult for any one to successfully work out this strategy. Historically, antibodies for nuclear receptors have been difficult to obtain. While there are many reasons, potential modifications of the receptor may be a primary component of this issue. From personal discussions with Dr. Yi Zhang (Professor of University of North Carolina at Chapel Hill), I found that it was also hard to get histone antibodies by using unmodified histones, whereas acetylated histone peptides worked fairly well. This suggests we might need to use modified SHP peptides for immunization.

The determination of the SHP structure represents a challenge in nuclear receptor structural biology. One rate-limiting step is the solubilization of SHP recombinant protein. Here, I report that by using function-directed cysteine mutagenesis and coexpression with its biding partner, a large quantity of SHP recombinant protein was purified for crystallization. These proteins may now also be used for antibody production and biochemical assays. This strategy works for DAX-1 solubilization, too. In my studies on SHP, I expressed a large quantity of full length tilapia DAX-1 protein in bacteria by mutating four cysteines to serines (C77S, C93S, C112S, and C223S) (Figure 3.10B). These mutations do not influence DAX-1 function in cotransfection assays (Figure 3.10A). The DAX-1 LBD was solved recently (Sablin et al., 2008). However, the relevance of this structure has been challenged by many studies, which suggest the N-terminal LXXLL motifs (not included in the DAX-1 LBD) are sufficient and necessary for DAX-1 to interact with other nuclear receptors (Suzuki et al., 2003). Therefore, my preliminary studies developed another method for solubilizing DAX-1 for crystallization work, which will help in better understanding its true structural character.

Reportedly, crystallization of a number of nuclear receptor LBD complexes

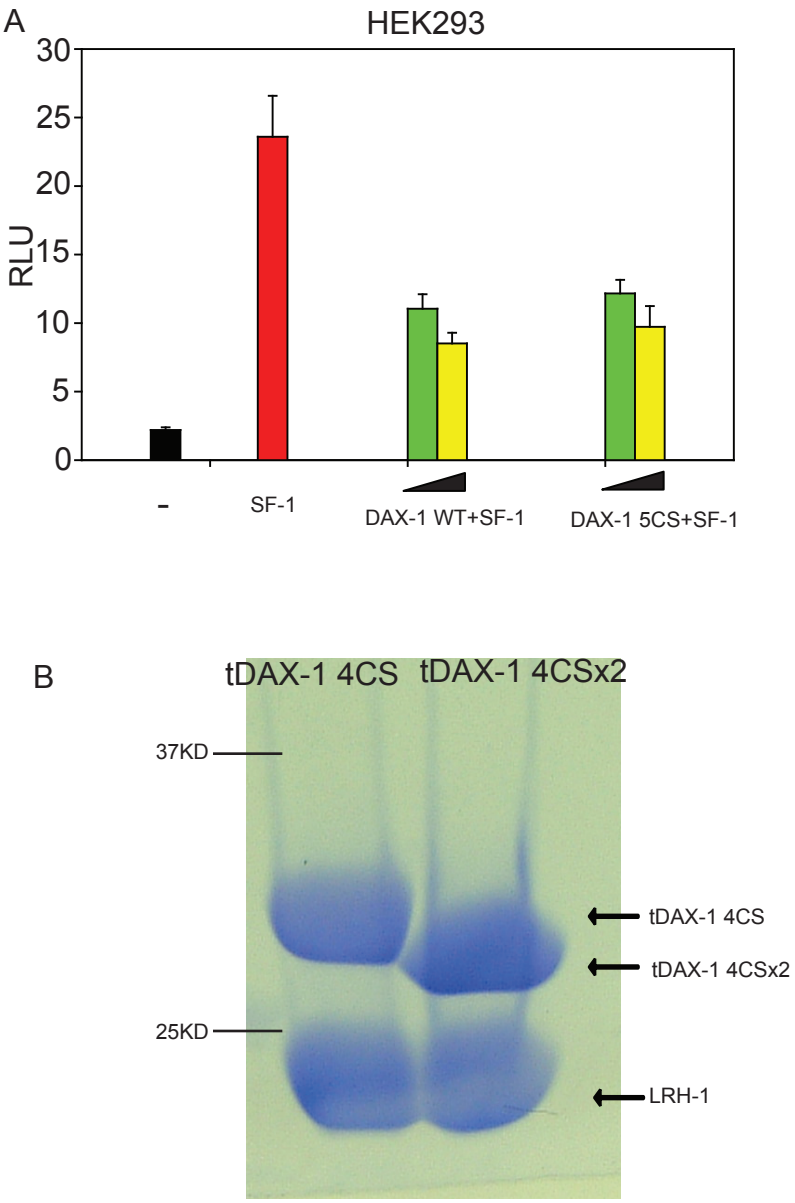

Figure 3.10 Solubilization of DAX-1

(A) Cotransfection assays are performed to screen for functional mouse DAX-1 mutants. Mouse DAX-1 5CS repression of SF-1 transactivation is indicated here. SHP-luc is used as the reporter. 5CS, C204S-C257S-C276S-C292S-C398A (not S); WT, wildtype; RLU, relative light unit. (B) Four cysteines in tilapia DAX-1 (tDAX-1) corresponding to the above mutated mouse DAX-1 cysteines are mutated to serines. Coomassie blue staining indicates the purified tDAX-1 4CS in complex with the human LRH-1 ligand binding domain. tDAX-1 4CSx2 is a tDAX-1 mutant with the N-terminal 24 amino acids removed to reduce the potential disordered sequences at the N-terminus of tDAX-1 (still containing LXXLL motif). tDAX-1 4CS, C77S-C93S-C112S-C223S.

necessitates the inclusion of LXXLL motifs (Wang et al., 2009; Li et al., 2005b; Bledsoe et al., 2002; Li et al., 2005a). LXXLL motifs are thought to stabilize the relatively dynamic AF2 helix (helix 12) in the receptor. Therefore, inclusion of SHP interacting LXXLL motifs or the like may optimize SHP crystal packing. EID1 interacts with SHP in a SHP AF2 helix dependent manner (Bavner et al., 2002). We designed several peptides based on the protein sequence information of EID1's SHP interaction domain and performed AlphaScreen assays to identify the peptides, which can specifically interact with SHP/LRH-1 complex. As shown in Fig. 3.11, peptides M2 and M3 specifically interacted with SHP/LRH-1 complex, but not LRH-1. The interacting peptides contain the amino acid sequence NKVFL, a variable version of LXXLL. This may represent the consensus sequence in corepressors for SHP binding.

In conclusion, the success of making soluble SHP protein and crystals have permitted ongoing structural studies that, while not complete, show great promise for future success. Thus, it is predictable that in the near future, we will solve the SHP/LRH-1 complex structure. This will represent only the second complex structure in the field of nuclear receptor research, in which a nuclear receptor (LRH-1) is bound by its heterodimeric coregulator (SHP). The unveiling of SHP's ligand binding pocket will also direct us to design synthetic chemicals, or hunt for endogenous ligands, promising the pharmacological interference of SHP physiology.

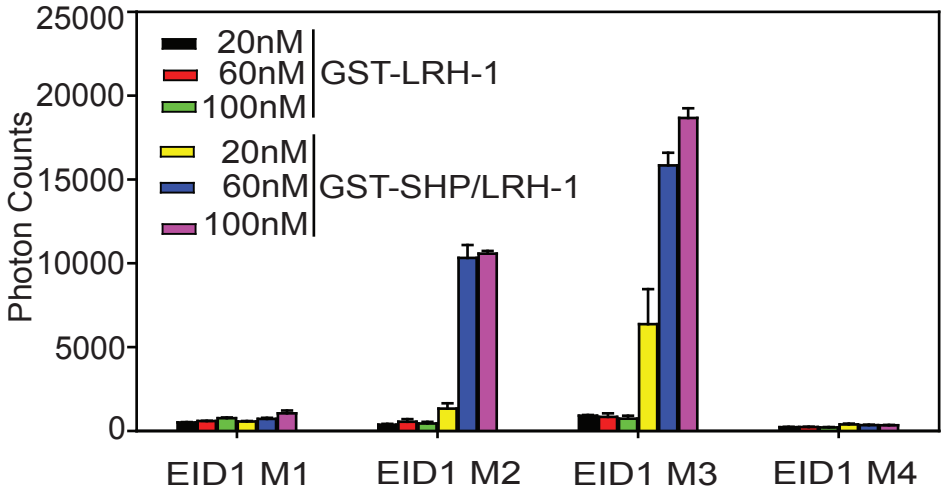

Biotinylated Peptide	Sequence
EID1 M1	RGLFPEAGADLEGDEFDDW EDDYEFPEEERWSG
EID1 M2	AMHRVSAALEEANKVFLTAR AGDALDGGFQARSE
EID1 M3	SGAMHRVSAALEEANKVFL RT
EID1 M4	SGAMHRVSAALEEAN

Figure 3.11 Screen for SHP Interacting Peptides
AlphaScreen assays are performed to screen for SHP interacting peptides that will be included in SHP crystallization optimization. EID1 M1-M4 are peptides derived from EID1. 20nM-60nM represent the concentrations of peptides used in assays. Sequences of peptides used in assays are listed in the lower panel. The motif highlighted in red is proposed to mediate SHP binding. GST-SHP is constructed based on SHP10CS.

CHAPTER FOUR

Introduction to Bile Acid-like Hormone Signaling Pathway in Nematodes

4.1 NUCLEAR RECEPTORS IN NEMATODES

The completion of the *C. elegans* genome sequencing project in 1998 predicted 284 nuclear receptors in this small animal, far outnumbering 48 in human and 21 in fruit fly. Further studies suggested that the abundance of nuclear receptors is not limited to *C. elegans*, but is also shared by other nematode species, supporting the hypothesis that nuclear receptor gene expansion happened as an early event during nematode evolution (Sluder and Maina, 2001). The appearance of so many nuclear receptors was considered, in the case of *C. elegans*, to be the result of an explosive burst of gene duplications of an ancestral HNF4α, which also accounted for the divergence of nuclear receptors (Robinson-Rechavi et al., 2005). The majority of nuclear receptor genes in *C. elegans* were shown to be expressed and functional based on EST (Expressed Sequence Tag) analysis and GFP promoter fusion expression, as were nuclear receptors in other nematode species such as *C. briggsae* and the filarial parasite *Brugia malayi* (Sluder and Maina, 2001).

Nuclear receptors in nematodes are divergent. With *C. elegans* as an example, only 15 out of 284 nuclear receptors are able to be placed into the six previously described vertebrate subfamilies based on sequence identity, while the remaining are fairly divergent and speculated to have a common HNF4α ancestor (Antebi, 2006; Sluder and Maina, 2001) .

The majority of our knowledge about nuclear receptors in *C. elegans* is so far

limited to 14 conserved members as shown in Table 4.1. The functions of these nuclear receptors revealed from tests, such as phenotypical screen, RNAi, and targeted mutation, suggest that nuclear receptors in *C. elegans* regulate a broad spectrum of life functions including dauer formation, sex determination, molting, neural differentiation, metabolism, and xenobiotic defense, and so on. Of note, some functions are conserved in agreement with their sequence similarity to homologs in mammals or flies, while others are involved in worm-specific life events. In the following part of this section, I will briefly discuss dauer formation in *C. elegans*, since it pertains to my studies on the nuclear receptor DAF-12. For more information on the roles of nuclear receptors in nematode physiology, the reader is referred to other reviews (Magner and Antebi, 2008; Antebi, 2006).

Normally, worms develop rapidly from embryos through their four larval stages (L1, L2, L3 and L4) to adults in 2-3 days at 20 ℃. They then reproduce over a 3- to 5-day period and live for another 2-3 weeks (Fig 4.1). If they encounter harsh conditions such as high temperature, lack of food, or crowded population at the end of the L1 stage, they adopt another developmental strategy. They enter a stage termed dauer, which is parallel to the L3 stage, and stay in this stage for up to four months during which time they can recover to adulthood. During dauer, worms undergo significant changes with respect to their morphology, physiology, metabolism, and behavior (Fielenbach and Antebi, 2008). Morphologically speaking, the dauers have a dauer-specific cuticle (lateral ridges on the exterior), constricted pharynxes, darkened intestine, and ceased gonadal migration, which can be detected under a dissecting microscope. What's more, the specific physical structure renders worms resistant to tough environment insults, for example, 1% SDS treatment (Hu, 2007).

C.elegans Nuclear Receptor	Mammalian Nuclear Receptor
DAF-12	PXR, CAR, VDR, LXR, FXR
NHR-8	No relative
NHR-48	No relative
SEX-1	Rev-erb
NHR-23	RORs
NHR-25	SF-1/LRH-1
NHR-49	HNF4α
UNC-55	COUP-TFs
FAX-1	PNR
NHR-91	GCNF
NHR-85	Rev-erb
NHR-67	TLX
NHR-41	TR2/TR4
NHR-6	Nurr1/NGFI-Bs/Nurr77

Table 4.1 Comparison between *C.elegans* and Mammalian Nuclear Receptors
Please refer to Sluder and Maina, 2001 for details on nomenclature and primary reference sources.

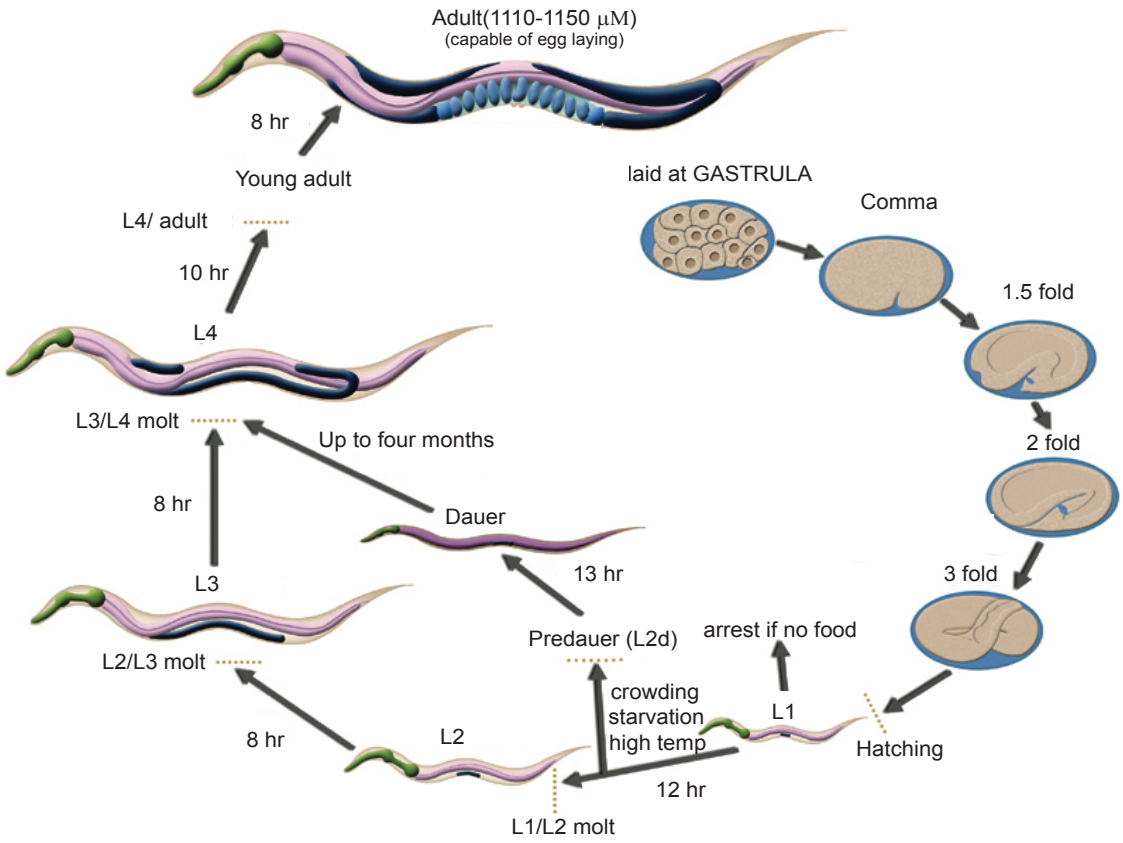

Figure 4.1 *C.elegans* Reproductive Life Cycle
Under favorable conditions, the worm has four larval stages between hatching eggs and adults, punctuated by molts. When harsh conditions are encountered at the end of L1 (Larval stage 1), the worm chooses to enter the predauer and dauer stages, which can last for up to four months before the worm resumes the normal reproductive development. The figure is adapted with permission from www. wormatlas.org. Copyright, wormatlas, 2009.

Recently, a group of genes were identified as being involved in worm dauer formation, and collectively termed DAF (abnormal dauer formation) genes (Hu, 2007). Mutations of these genes caused either a dauer constitutive phenotype (Daf-c) or a dauer deficient phenotype (Daf-d). Interestingly, mutations of the nuclear receptor, DAF-12, produced both phenotypes depending on the mutation positions. In general, mutations in the putative DAF-12 DNA binding domain or disruptions of the whole protein produced a Daf-d phenotype, while mutations in the putative ligand binding domain generated a Daf-c phenotype. This discrepancy is reconciled by the "molecular switch" function of DAF-12 as a nuclear receptor. Simply put, DAF-12 controls both entry into, and exit from, the dauer diapause. In the absence of ligands, DAF-12 works as a repressor to promote the worm development into the dauer stage. Mutations in LBD disrupt DAF-12's ability to sense the ligands and thus favor the dauer formation regardless of the environmental cues (Motola et al., 2006). On the contrary, mutations in DBD abrogate the repressive activity of DAF-12 that is required for dauer formation, resulting in the circumvention of the dauer stage. This molecular scenario finds its counterpart in the heterochronic development mediated by DAF-12, as Daf-c is more penetrant than Daf-d (Antebi et al., 2000). In addition to its role in dauer formation and developmental timing, DAF-12 controls many other worm life history traits such as reproductive growth, longevity, fat storage, and stress management (Antebi et al., 1998; Antebi et al., 2000; Gerisch et al., 2001).

Other genes involved in dauer formation have been placed into different signaling pathways including cGMP, TGFβ and IIS (Insulin/IGF-1 Signaling) and different steps related to hormone/ ligand production, transport, secretion and sensing. To summarize,

the regulation of dauer formation is a sophisticated program composed of commands sent from different pathways and distributed through different signaling networks, ultimately converging onto the DAF-12.

Nuclear receptors in *C. elegans* are an example of how these proteins function in various aspects of nematode life. Some functions are also conserved across nematode species in governing similar developmental events. For example, the infective L3 stage of parasitic nematodes is similar to the dauer diapause in free living relatives. Both are regulated by DAF-12-like molecules in a similarly mechanistic manner, as evidenced by our group (Wang et al., 2009). This is allowing us to translate our knowledge of *C. elegans* into pharmaceutical intervention of nematode parasitism. It was hypothesized that parasitic nematodes evolved from free living nematodes (Dieterich and Sommer, 2009), based on the findings that a considerable proportion of life traits of free living nematodes and their underlying regulatory mechanisms are conserved in their parasitic relatives. Because nuclear receptors govern many of these processes, they may be promising drug targets for dealing with nematode pathology.

4.2 DAUER FORMATION REGULATION IN NEMATODES

C. elegans genetics have played a critical role in our understanding dauer formation. DAF genes were isolated by mutation based phenotypical screens and grouped into different regulatory pathways by way of genetic epistasis and synergy (Fielenbach and Antebi, 2008). The first regulatory pathway is related to the production, detection, and interpretation of outside signals. It is termed chemosensory signaling, and is characterized by the involvement of a group of chemosensory neurons that are located at

two major head sensory organs called amphids. These neurons are classified into specific cell types and govern dauer formation with different readouts. From laser ablation experiments, ASI, ADF, and ASJ neurons produce dauer-inhibiting signals, while ASJ neurons facilitate dauer formation and recovery. Indeed, the hormones that control the dauer formation are partly mapped to these neurons. For example, DAF-7 (TGFβ homolog) is expressed exclusively in ASI cells, and DAF-28 (insulin-like peptide) is expressed in ASI and ASJ cells, indicating that the chemosensory signaling pathways direct the downstream signaling pathways by producing hormonal outputs.

The second regulatory pathway is composed of several signaling pathways including, cGMP, TGFβ, and IIS circuits based on epistatic experiments (Fielenbach and Antebi, 2008; Hu, 2007). The cGMP signaling pathway is upstream to the other two parallel signaling pathways. The gene *daf-11* is one of the best studied in the cGMP pathway, which encodes a trans-membrane guanylyl cyclase (GCY) and is expressed in the sensory cilia. It is likely that cGMP stimulates generation of hormones that activate downstream signaling pathways, leading to inhibition of dauer formation and progression of reproductive growth (Fielenbach and Antebi, 2008).

TGFβ signaling pathway is one of the major hormone signaling pathways responsive to changing cGMP levels (Savage-Dunn, 2005). DAF7, the homolog of TGFβ in *C. elegans*, is only expressed in nematode neurons while the receptors and downstream transcriptional effectors are widely expressed in tissues, including those remodeled during dauer formation, and include intestine, hypodermis, and pharynx. There are two types of membrane bound receptors for DAF-7, type I encoded by daf-1, and type II by daf-4. The binding of DAF-7 induces phosphorylation and activation of DAF-4, which

recruits downstream effector SMAD proteins for phosphorylation. These SMAD proteins include DAF-8 and DAF-14, which are translocated into the nucleus upon phosphorylation to enact cascades leading to reproductive development. Clearly, any mutations of genes along the signaling cascade can cause the Daf-c phenotype. DAF-8 and DAF-14 lack a DNA binding domain and function by antagonizing the transactivation of DAF-3 and DAF-5, which represent a SMAD-like transcriptional activator, and a SNO-SKI transcriptional coactivator, respectively. In accord with this, mutations of daf-3 or daf-5 caused the Daf-d phenotype and suppressed the Daf-c phenotype mentioned immediately above (Thomas et al., 1993).

The IIS signaling pathway is another circuit downstream of cGMP signaling. Indeed, in addition to dauer formation, this pathway controls a lot of other important worm life history traits. A case in point is longevity. DAF-2 is the *C. elegans* homolog of IR (Insulin Receptor). Activation of DAF-2 triggers a kinase signaling pathway leading to phosphorylation of a FOXO-like transcriptional factor, DAF-16, to facilitate its nuclear export. DAF-16 transactivation favors the dauer formation and mutations of DAF-16 cause the Daf-d phenotype. According to the most recent model, activated DAF-2 recruits IST-1 (IRS homolog) and stimulates the PI3 kinase, AGE-1. Activation of the AGE-1 increases the cellular level of PIP3. In the presence of PIP3, the AKT kinase, PDK, phosphorylates and activates a number of downstream effector kinases such as AKT-1, AKT-2, and SGK, which in turn phosphorylate DAF-16. One negative regulator in this pathway is DAF-18, which is the homolog to PTEN and acts as the PIP3 phosphatase. Mutations of DAF-18 promote the dauer formation.

The IIS signaling pathway crosstalks with the TGFβ signaling pathway and both

regulate an overlapping set of target genes through DAF-16 and DAF-3, respectively. It would be easy to think that the two pathways directly control dauer formation by inducing physiological alterations in dauer remodeled tissues. However, some key components in the two pathways are not expressed in remodeled tissues and the phenotype of mutants can be rescued by neural re-expression alone, suggesting the existence of a secondary required hormone signaling pathway.

It is now known that this secondary signaling pathway uses small lipophilic molecules for communication. Nuclear receptor DAF-12 is the core molecular switch in this layer of regulation. It is expressed in a wide range of tissues, including those undergoing dauer remodeling (Snow and Larsen, 2000). Before its physiological ligands were identified by our group, numerous lines of evidence had suggested DAF-12 is regulated by steroid hormones (Antebi et al., 2000; Gerisch et al., 2001). One of the most intriguing findings was that mutations of a CYP450 enzyme, DAF-9, caused the same DAF-c phenotype, as mutations in the DAF-12 LBD. Considering that the expression pattern of DAF-9 was restricted to XXX cells, the epidermis, and spermatheca (revealed by GFP fusion experiments), it was suggested that DAF-9 catalyzed the production of DAF-12 ligands, which would then be transported to the target tissues to activate DAF-12 and thereby generate the physiological response of avoiding dauer formation and supporting reproductive growth. As predicted, a group of bile acid-like molecules named dafachronic acids (DAs) were subsequently isolated in a series of elegant experiments and shown to be the bona fide DAF-12 ligands (Motola et al., 2006). This work elucidated a clear picture of dauer hormone biosynthesis from cholesterol in *C. elegans*, in which DAF-9 works at the last step of DA generation. A recently identified Rieske-like

oxygenase, DAF-36, works at the first step in the pathway to generate the Δ7 sterol (precursor to Δ7-DA, the most potent known DAF-12 ligand) (Rottiers et al., 2006). In addition, this endocrine signaling model was further supported by discovery of two putative cholesterol transport proteins NCR-1 and NCR-2. These are homologous to human Niemen-Pick type C proteins (NPC) and their mutations also lead to the Daf-c phenotype, reminiscent of DAF-9 mutations.

As mentioned previously, coregulators constitute important components for nuclear receptor signaling. Ligand-gated DAF-12 is no exception and its repression was found to be strictly dependent on DIN-1 (DAF-12 Interacting-1), a corepressor for DAF-12 isolated by yeast two hybrid (Ludewig et al., 2004). Mutations of DIN-1 produced the Daf-d phenotype and suppressed the Daf-c phenotype resulting from mutations in DAF-9 or DAF-12, while DAF-9 or DAF-12 is placed downstream to all the signaling pathways discussed above. Interestingly, to date no p160-like coactivators have been discovered in the worm, although mutations in the DAF-12 AF2 domain suggest functional orthologs must exist (Antebi et al., 2000). In summary, DAF12, coregulators, and proteins involved in the ligand biosynthesis pathway form the bottom layer of regulation to effect the dauer biological transformation.

4.3 DAF-12 REGULATES DAUER FORMATION BY SENSING BILE ACID-LIKE MOLECULES

Cholesterol has two important roles in mammals. In one case, it is used as a building block for constructing cell membranes and the other, it is used as the precursor for bile acid and steroid hormone production. Only the latter function is required in

worms. This is evidenced by the limited distribution and small concentration requirement (~20 nM) of cholesterol for worm reproductive growth (Matyash et al., 2001; Merris et al., 2003). *C. elegans* can not biosynthesize cholesterol as mammals do and as such their reproductive growth is strictly dependent on the dietary cholesterol.

Our understanding of cholesterol metabolism in *C. elegans* has been nicely advanced by recent work from our laboratory. Based on these new findings (Fig. 4.2), cholesterol is now known to first be converted to 7-dehydrocholesterol and this step appears to be catalyzed by the Δ7-desaturase DAF-36 (Rottiers et al., 2006). 7-dehydrocholesterol was found to be the most abundant (~56%) sterol in worms (Chitwood, 1999). Next, 4, 7-cholestadiene-3-one is believed to be produced under the action of an as yet undiscovered enzyme reminiscent of the HSD3B7 that functions in the classic bile acid biosynthesis pathway in mammals. Then a putative 5α-reductase (similar to mammalian 5β-reductase, AKR1D1) is believed to catalyze the generation of lanosterone. Finally, DAF-9 works as a C27-oxygenase to produce a carboxylate group at C27, resulting in a synthesis of 3-keto-7, (5α)-cholestenoic acid, also named Δ7-dafachronic acid (DA) for its role in dauer formation and heterochronic development. A similar molecule differing in the position of double bond, Δ4-DA, is also found as an endogenous cholesterol metabolite, and is believed to be generated by DAF-9 from the dietary substrate, 4-cholesten-3-one (Motola et al., 2006).

In this model, lanosterone is proposed to be reversibly converted to lanosterol, an identified sterol in worms accounting for 6% in total sterols. This step is likely catalyzed by an enzyme similar to mammalian dehydrogenase AKR1C4, which handles the interconversion between C3-keto and C3-OH (Russell, 2003). Then the produced

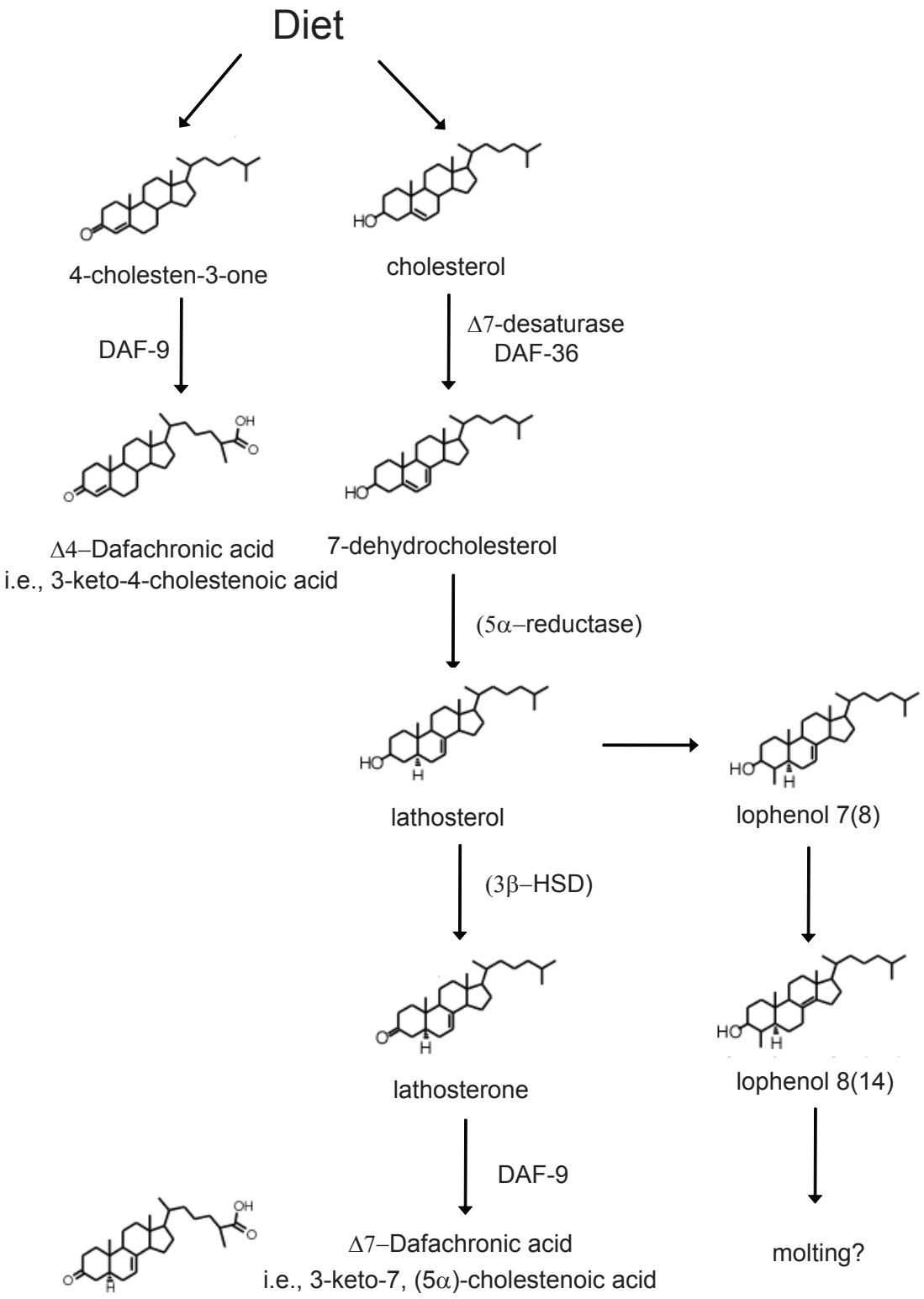

Figure 4.2 A New Model of Cholesterol Metabolism in *C.elegans*
This figure is adapted from Dan Motola, PhD thesis at UTSW, 2006.

lanosterol is methylated at C4 to become lophenol 7(8) (which has a double bond between C7 and C8), which can be further transformed into lophenol 8(14) by isomerization of the double bond. This branch of cholesterol metabolism may be involved in the generation of ligands for molting, while dafachronic acid pathway is involved in the generation of ligands for preventing or exiting from dauer diapause.

As far as the chemical structure is concerned, Δ4- and Δ7-DAs are very similar to bile acids. The biosynthesis of DAs also mirrors that of bile acids. Cholesterol undergoes a similar series of ring and side-chain modifications including isomerization, dehydrogenation, reduction and hydroxylation. Importantly the enzymes catalyzing these reactions also find their counterparts in nematodes and mammals. An example is DAF-9, which is enzymatically and functionally orthologous to mammalian CYP27A1 (Motola et al., 2006). Taken together, this suggests that the bile acid biosynthesis pathway evolutionarily conserved and bile acid-like molecules may have been used as signaling molecules over a long period that can be traced back to before the appearance of vertebrates.

Indeed, DAs are important signaling molecules in worms. They work as nutrient signals through a nuclear receptor to direct decisions regarding the energy conservation (dauer) and energy consumption (reproduction). This is reminiscent of the same function of bile acids in directing energy management via FXR in mammals (see Chapter Two). As mentioned, DAs achieve biological effects through the nuclear receptor DAF-12. DAs activate *C. elegans* DAF-12 in cell cotransfection assays. DAs were shown bound to DAF-12 directly in AlphaScreen assays (Motola et al., 2006). Critically, two different 3-D structures of DAF-12 bound to Δ7-DA have been solved, which are the focus of Chapter

Five. It is worthwhile emphasizing that DAs are *bona fide* ligands for DAF-12 because they were identified in wildtype but not DAF-9-null worms. DAs rescued the Daf-c phenotype caused by mutations in upstream signaling pathways, suggesting that DAF-12 ligand generation is the culminating point of regulation.

Considering the conservation between DAs and bile acids from a ligand perspective, it would be interesting to ask if DAF-12's functions are conserved in structurally similar nuclear receptor homologs. Based on primary sequence (mainly DBD) analysis, DAF-12 is closest to mammalian LXR, VDR, and PXR (Antebi et al., 2000). The relationship to the latter two is intriguing because bile acids are ligands for VDR and PXR, suggesting mammalian VDR and PXR may reserve some DAF-12 functions to control mammalian life history traits such as longevity. However, DAF-12 was also shown to be activated by bile acid precursor (25S)-cholestenoic acids, which are weak ligands for LXR (Held et al., 2006). This suggests that DAF-12 may use a specific structural mechanism to recognize certain related bile acid-like molecules. In this regard, structural analysis of DAF-12 should provide insights into ligand binding and activation. The clarification of structural mechanism for DAF-12 will help identify its closest mammalian relative and provide new research avenues for examining this nuclear receptor's function.

In closing, DAF-12 is regulated by a class of bile acid-like molecules in worms. Their biosynthesis is not limited to a single tissue. For example, the first enzyme DAF-36 is expressed in the worm intestine, while the last enzyme DAF-9 is expressed in neurons and hypodermis. This may represent an ancient form of endocrinology. Indeed, DAs work as endocrine hormones to coordinate organism-wide transformation. This process may

represent an ancient scheme that mimics modern bile acid enterohepatic circulation and signaling.

4.4 CONSERVATION OF BILE ACID-LIKE HORMONE SIGNALING PATHWAYS IN PARASITIC NEMATODES

One developing idea in *C. elegans* biological studies is to translate this knowledge into our understanding of nematode parasitism control. Parasitic nematodes are considerable threats to human quality of life and economic development; they also cause live stock death and crop damage (Jasmer et al., 2003). Many efforts have been invested to design safe and effective pharmaceuticals (Hotez et al., 2006).

Comparative genomics contributes to our molecular understanding of nematode parasitic life (Mitreva et al., 2005). It has been proposed that parasitic nematodes evolved from free living ancestors and the dauer stage was one key step in their evolution (Dieterich and Sommer, 2009; Viney, 2009). Morphologically speaking, the infective L3 stage in parasitic nematodes is very similar to the dauer stage in free living counterparts, which is characterized by thickened body wall cuticle, non-feeding, non-growing behavior, and resistance to harsh conditions. The infective L3 larvae recover to become reproductive adults when they enter the appropriate hosts (usually species-specific), where they produce eggs to begin a new life cycle. While some parasites are strictly dependent on the hosts to finish one life cycle (e.g., hookworm *Ancylostoma ceylanicum*), some parasites have alternative life cycles and can choose between a parasitic or free living form upon access to appropriate host signals (Viney and Lok, 2007). A case in point is *Strongyloides stercoralis*, which causes disseminated strongyloidiasis and infects

millions of people per year. This alternative life cycle may represent a “half-way” mark in the evolution from a free living to a parasitic animal (Ogawa et al., 2009). As hypothesized, this strategy expedites the evolution of parasitism by providing a phenotypic plasticity, which is recapitulated by the free living life-cycle on one hand, and development of a host-specific feeding strategy on the other hand. The obligatory parasites are generated by a specialization of parasitic characteristics concomitant with the loss of free living behavior. This model makes more sense from a symbiotic standpoint, since obligatory parasitic nematodes are usually less pathogenic than alternative counterparts.

Regardless of their different life styles, the parasitic nematodes make the transition from infective L3 stage to reproductive stage in response to host signals, reminiscent of a similar transition in *C. elegans* from dauer diapause to reproductive growth. Interestingly, both processes are regulated in a similar mechanistic manner. A key piece of evidence supporting this conclusion came from the cloning of DAF-12 homologs from parasitic nematodes such as *Strongyloides stercoralis* (human host) and hookworms *Ancylostoma caninum* (dog host), *Ancylostoma ceylanicum* (pan-specific host) and *Necator americanus* (human host) (Wang et al., 2009). These parasitic DAF-12s share high sequence similarity with each other as well as with *C. elegans* DAF-12. Demonstration of the similarity in function between these DAF-12 homologs has come from a number of biochemical assays. All are activated by DAs in cell cotransfection assays and have been shown to bind to DAs directly in AlphaScreen assays (see Chapter Five) (Wang et al., 2009). This suggests that DAF-12 is conserved in parasitic nematodes, both structurally and mechanistically. DA treatment partially recovered iL3 larvae in

hookworms and *S. stercoralis*. Δ7-DA (not Δ4-DA) killed iL3 formation of *S. stercoralis*, by causing them to molt into development-defective larvae. This suggested that bile acid-like molecules also work as important signaling molecules in parasitic nematodes to direct host-specific development and reproductive growth. Such a signaling paradigm may have evolved with nematode speciation. This brings up the interesting idea that bile acids or bile acid-like molecules may play important roles in the parasitic adaptation of nematodes. Bile acid-like molecules are ubiquitously present in animals and have been conserved structurally and functionally across evolution. Access of such host-specific signaling molecules to nematodes would have permitted the parasites to abolish the obligation to regulate their own endogenously similar signaling molecules, thereby facilitating the transition to obligatory parasitism. Therefore, the extent to which nematodes depend on this class of molecules for parasitic evolution would be an intriguing topic.

Pharmacologically speaking, the above studies pointed to a new avenue of therapy for nematode associated diseases. The infective life-cycle of parasitic nematodes can be disrupted by targeting DAF-12 pharmacologically (Wang et al., 2009). This would represent a universal strategy to treat nematode infections that affect one quarter of the people on Earth. To that end, characterizing the 3-D structure of DAF-12 across several species would be a significant step in developing effective drugs.

4.5 RESEARCH QUESTIONS AND STRATEGIES

The first DAF-12 (*S. stercoralis*) LBD structure (also the first worm nuclear receptor structure) was solved by our group (Wang et al., 2009). The structure revealed

the molecular basis for DAF-12 activation. The binding of DAs drives the conformation of DAF-12 into an active state that favors the recruitment of LXXLL motif-containing coactivators. Furthermore, analysis of the ligand binding pocket validated the insights gained from worm genetics. However, mutations in other species directed by this structure demonstrated different pharmacological responses. This motivated us to identify the structural features behind these observations. In addition, sequence alignments revealed that *S. stercoralis* DAF-12 is more divergent from the *C. elegans* homolog than hookworms. Hence, determination of hookworm DAF-12 structure would complement our understanding of the structural mechanism for *C. elegans* DAF-12 activation. Furthermore, it would help us develop drugs that might effectively target hookworms.

In the next chapter, I will discuss my successful effort to solve the hookworm *Ancylostoma ceylanicum* DAF-12 LBD structure and show how this structure has led us to identify an ancient structural mechanism for bile acid-like molecule signaling.

CHAPTER FIVE

Structural Conservation of Bile Acid-like Nuclear Receptor Signaling Pathways in Nematodes

5.1 INTRODUCTION

Nematode parasitism is a threat to human health care and economic development (Jasmer et al., 2003). Parasitic nematodes are hypothesized to have evolved from free living ancestors and their infective larvae 3 stage (iL3) is morphologically similar to the dauer stage in *C. elegans* (Viney, 2009; Viney et al., 2005; Dieterich and Sommer, 2009). The regulation of the iL3 stage in parasitic nematodes was poorly understood until a couple of recent studies revealed that the DAF-12 signaling pathway plays a critical role (Ogawa et al., 2009; Wang et al., 2009). DAF-12 homologs in *Strongyloides stercoralis* (ssDAF-12), human and hamster hookworm *Ancylostoma ceylanicum* (aceDAF-12), dog hookworm *Ancylostoma caninum* (acDAF-12), and hamster hookworm *Necator americanus* (naDAF-12) have been cloned and sequence analysis reveals a significant level of identity with *C. elegans* DAF-12 (ceDAF-12). These parasitic DAF-12s can be activated by DAs in *in vitro* assays (Wang et al., 2009). Moreover, DA treatment partially caused the iL3 larvae from hookworms and *S. stercoralis* to start feeding and Δ7-DA effectively blocked iL3 formation in *S. stercoralis*, by forcing the iL3 larvae to prematurely molt into development-defective larvae (Wang et al., 2009). These findings suggested that DAF-12 is a conserved nuclear receptor across nematode species and that it represents a potential drug target to treat nematode parasitism (Wang et al., 2009).

The ssDAF-12 LBD X-ray crystal structure revealed the general molecular basis for receptor activation in the presence of ligands. However, mutation studies based on

sequence homology indicated species-specific pharmacological responses. In order to further study the structural biology of DAF-12 and to elucidate the structural features for species-specific ligand binding, I solved the hookworm aceDAF-12 LBD structure. By comparing the two parasitic DAF-12 LBD structures, I identified the structural elements responsible for the species-specific ligand responses. I also compared the aceDAF-12 LBD to mammalian nuclear receptor LBDs. Interestingly, DAF-12 shares many structural features specific to only one other receptor FXR, especially with respect to the orientation of the bound ligand. This result suggests that DAF-12 is functionally similar to FXR, and that bile acid-like signaling pathways have been conserved across evolution. Finally, I report that mammalian bile acids and bile acid precursors can activate nematode DAF-12s, indicating that the nematode bile acid-like signaling pathway can crosstalk with the mammalian bile acid signaling pathway.

5.2 MATERIALS AND METHODS

5.2.1 Plasmids and Reagents

The mutants used for crystallization or transfection assays were created by site-directed mutagenesis (Stratagene) and verified by sequencing. Dafachronic acids were synthesized as described elsewhere (Wang et al., 2009).

5.2.2 Protein Preparation and Crystallization

DAF-12s were cloned as described and inserted into the 6x His-GST vector (engineered pET24) (Wang et al., 2009). The proteins were expressed in BL21 (DE3) cells, purified by a GST column and their ligand-binding activity was tested in AlphaScreen assays (Li et al., 2005b). The aceDAF-12 LBD was cloned into a

6x-His-SUMO vector and expressed in BL21 (DE3) cells. The protein was first purified over a histidine column, then the SUMO tag was cleaved using the Ulp1 protease, and the final protein was subjected to gel filtration. The purified protein was mixed with the SRC1-4 or SRC2-3 peptides and Δ7-DA for crystallization. The molar ratio of these components was 1 (DAF-12 protein): 1.5 (SRC peptides): 5 (Δ7-DA). Crystals were grown at 20 ℃ in sitting drops containing 1.0 µl of the protein solution (8.0 mg/ml) and 1.0 µl of well solution containing 0.1 M sodium acetate, pH 5.1, 0.2 M ammonium acetate, 26% PEG2K. Crystals showed up in two days and grew in clusters to 30-40 micron in about one week, at which time they were flash-frozen and stored in liquid nitrogen.

5.2.3 Data Collection, Structure Determination, Refinement, and Superposition

The diffraction data were collected with a MAR225 CCD detector at 21- ID beamline at the Advanced Photon Source at Argonne National Laboratory (Argonne, Illinois, United States). The observed reflections were reduced, merged, and scaled with DENZO and SCALEPACK in the HKL2000 package (Otwinowski Z, 1997). The structure was determined with the PHASER program by molecular replacement using the crystal structure of ssDAF-12 as a model. Manual model building was carried out with O system (Jones et al., 1991) and QUANTA (Accelrys, Inc.), and structure refinement was processed with crystallography NMR software and CCP4 programs refmac5. Protein model superposition was performed using program O. The data collection and structure determination statistics are summarized in Table 5.1.

5.2.4 AlphaScreen Assays

The binding of the cofactor motifs to the DAF-12s was determined by alpha

Data collection	
APS beam line	21-ID
Space group	$P2_1$
Resolution, Å	50-1.53
Cell parameters a, b, c, Å	48.0, 85.1, 66.1
β, °	107.1
Unique reflections	76415 (7633)
Rsym	0.095 (0.886)
I/σ	28.8 (2.4)
Completeness, %	100 (99.8)
Redundancy	7.5 (7.2)
Structure determination	
Resolution, Å	30-1.53
NO. of reflections	70848
NO. of residues	513
NO. of solvent molecules	411
NO. of non-H atoms	9725
Rwork	18.60%
Rfree	21.80%
rmsd bonds, Å	0.05
rmsd angles, °	3.04
Average B factor, $Å^2$	16.1

Table 5.1 Data Collection and Structure Determination Statistics

screen assays as described (Li et al., 2005b; Motola et al., 2006). The assays were conducted by using AlphaScreen assay kit (Perkin-Elmer). Reaction mixtures consisted of 50 nM 6x His-GST fusion proteins, 20 nM biotinylated peptides, 1 μM Δ4- or Δ7-DA or no ligand, 5 μg/ml nickel chelate coated acceptor beads and 5 μg/ml strepavidin coated donor beads in a buffer containing 50 mM MOPS (pH7.4), 50 mM NaF, 50 mM CHAPS, and 0.1 mg/ml bovine serum albumin. The peptides used in our studies were listed in Table 5.2.

5.2.5 Cotransfection Assays

HEK293 and COS7 cells were cultured and transfected in 96-well plates as reported (Shulman et al., 2004; Wang et al., 2009). 15 ng of the coactivator SRC2 (GRIP1) was coexpressed with ssDAF-12 in Fig. 5.5D and 5.7B to increase the transfection signal. The same amount of SRC2 was coexpressed with aceDAF-12 and ceDAF-12 in Fig. 5.7C.

5.3 RESULTS

5.3.1 Crystallization of the Hookworm aceDAF-12 LBD

Primary structure analysis revealed hookworm DAF-12 LBDs are identical except for one amino acid (A449 in acDAF-12 and naDAF-12, and V449 in acDAF-12). The hookworm DAF-12 LBDs share 46% sequence identity to the ssDAF-12 LBD (Fig. 5.1A). In this study, we chose the aceDAF-12 LBD for crystallization, since *Ancylostoma ceylanicum* is a pan-specific hookworm. Reportedly, crystallization of a number of nuclear receptor LBD complexes necessitates the inclusion of LXXLL motifs (Wang et al., 2009; Li et al., 2005b; Bledsoe et al., 2002; Li et al., 2005a). Since the

Peptide	Sequence
SRC1-2	SPSSHSSLTERHKILHRLLQEGSP
SRC1-4	QKPTSGPQTPQAQQKSLLQQLLTE
PGC1α-1	QEAEEPSLLKKLLLAPANTQ
TRAP-1	GHGEDFSKVSQNPILTSLLQITGN
CBP-1	SGNLVPDAASKHKQLSELLRGGSG
NcoR-2	GHSFADPASNLGLEDIIRKALMGSF
SHP-1	PCQGSASHPTILYTLLSPGP
SHP-2	VAEAPVPSILKKILLEEPNS
SMRT-2	ASTNMGLEAIIRKALMGKYDQ
SRC2-3	QEPVSPKKKENALLRYLLDKDDTKD
SRC3-1	AENQRGPLESKGHKKLLQLLTSS
SRC3-2	TSNMHGSLLQEKHRILHKLLQNG

Table 5.2 Sequence of Peptides Used in AlphaScreen Assays

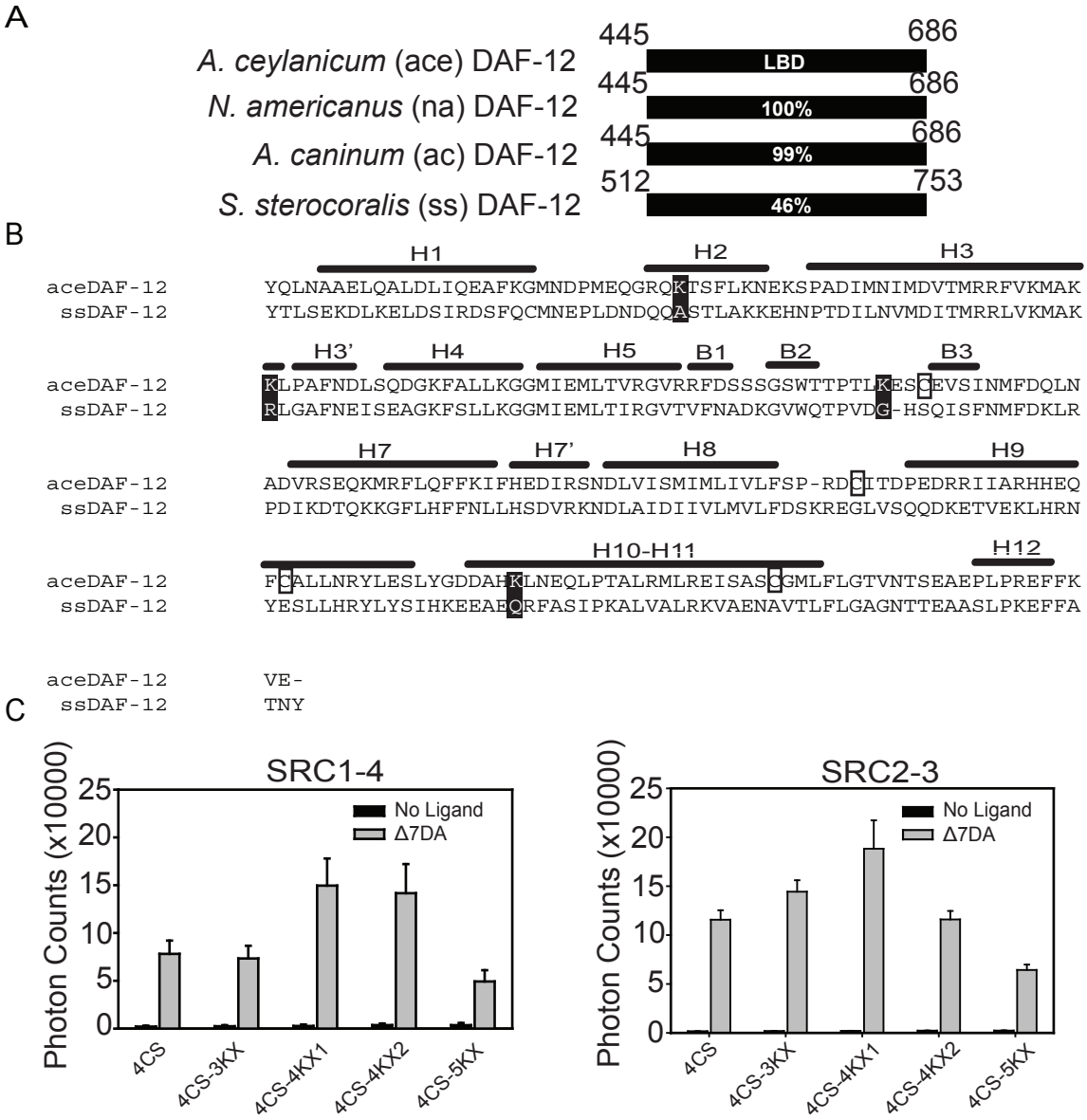

Figure 5.1 Strategy for Crystallization of the aceDAF-12 LBD

(A) Sequence identity of DAF-12 homologues from parasitic nematodes. Numbers refer to the amino acid position in the ligand binding domain of each receptor. (B) The alignment of secondary structural elements of the aceDAF-12 LBD is based on the crystal structure of the ssDAF-12 LBD. H, α-helix; B, β–strand. Cysteines in aceDAF-12 that were mutated to serines are boxed. Lysines in aceDAF-12 that were mutated to the corresponding amino acids in ssDAF-12 are highlighted in black. This mutant is named aceDAF-12 4CS-4KX1 and was used for subsequent crystallization. (C) Ligand binding functions of aceDAF-12 mutants for crystallization are examined in AlphaScreen assays. SRC1-4 and SRC2-3 are LXXLL motif containing peptides and interact with aceDAF-12 as shown in Fig. 5.2. 4CS, C176S-C230S-C248S-C284S; 4CS-3KX, K98A-K128R-K173G plus 4CS; 4CS-4KX1, K98A-K128R-K173G-K265Q plus 4CS; 4CS-4KX2, K98A-K128R-K173G-K86Q plus 4CS; 4CS-5KX, K98A-K128R-K173G-K265Q-K203N plus 4CS. 1μM of DA is used.

LXXLL-containing cofactors in *C. elegans* remain elusive, we performed AlphaScreen assays to search through our mammalian LXXLL-containing peptide library for aceDAF-12 LBD interacting peptides. As shown in Fig. 5.2A, aceDAF-12 showed strong binding to SRC1-4 and SRC2-3, in comparison to weaker binding to SRC1-2, PGC1α-1, and SHP-2 in the presence of DAs. ac, na, and ss DAF-12s had similar binding patterns in the assays (Fig. 5.2B-D). Accordingly, SRC1-4 and SRC2-3 peptides were included in our crystallization trials along with the DA ligands.

Initial attempts to express aceDAF-12 LBD yielded low amount of soluble protein. Since cysteine mutation is a widely used strategy to solubilize recombinant proteins by preventing the random formation of disulfide bonds and precipitation, we mutated the four cysteines in the aceDAF-12 LBD to serines (CS) (Krylova et al., 2005).Evaluation of the predicted positions of these cysteine residues based on the ssDAF-12 LBD X-ray crystal structure suggested these cysteines are distributed in loops or kinks, away from the functional cores (Fig. 5.1B). Mutation of cysteines markedly increased aceDAF-12 LBD solubility and yielded 3-4mg of protein from six liters of culture, making crystallization possible. To facilitate crystallization, we also mutated a number of non-conserved lysines in aceDAF-12 corresponding to surface amino acids in ssDAF-12 that might affect crystal packing due to the flexibility of the lysine side chain (KX) (Fig. 5.1B). As a result, several aceDAF-12 LBD mutants were made and used for crystallization. one of these, named aceDAF-12 LBD 4CS-4KX1, yielded primo crystals for structure determination. Interestingly, these crystals could only be grown by using the sitting drop but not hanging drop technique under our precipitation conditions. Notably, as predicted from the ssDAF-12 LBD structure, CS and KX mutations did not affect the

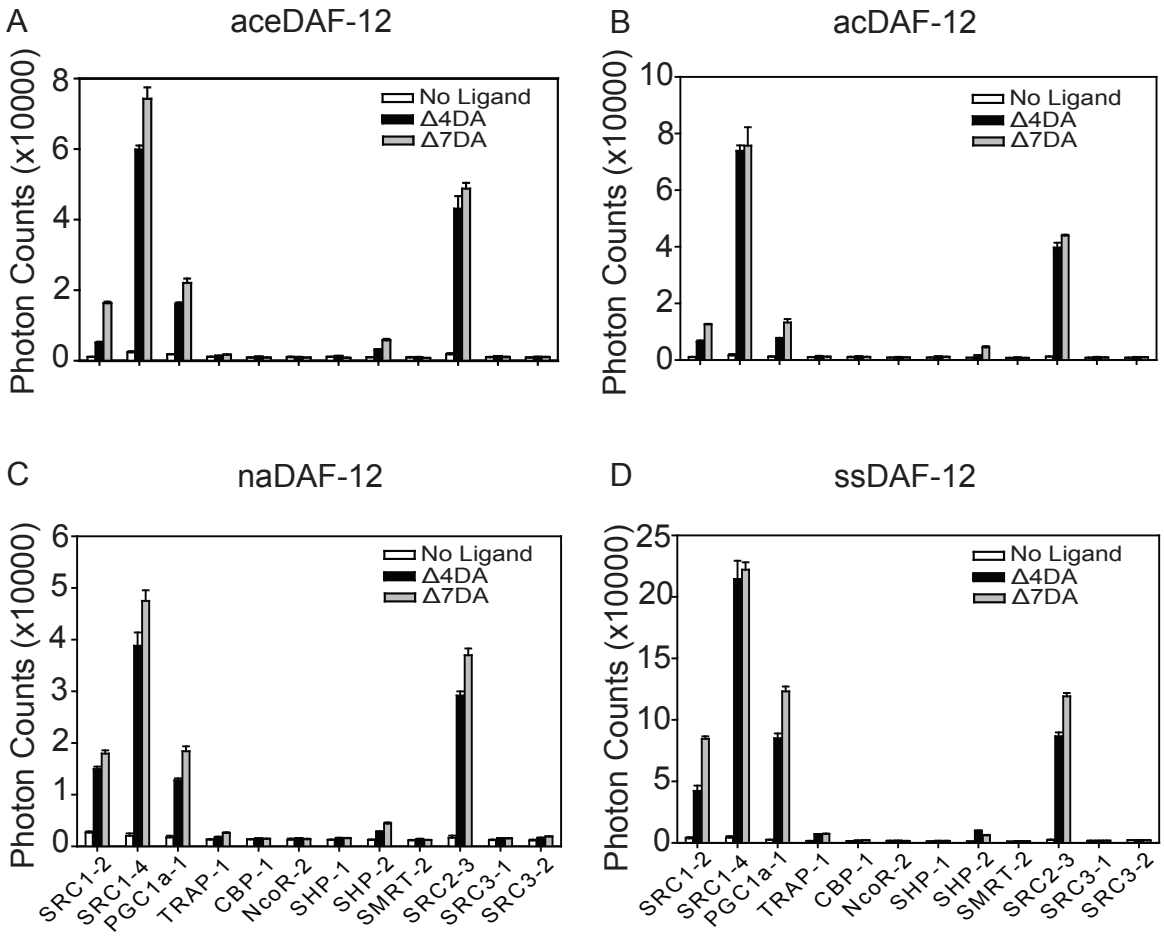

Figure 5.2 AlphaScreen Assays to Search for ace, ac, na and ss DAF-12 Interacting Peptides

(A) aceDAF-12 (B) acDAF-12 (C) naDAF-12 (D) ssDAF-12. 1μM of DA is used.

ability of aceDAF-12 to bind cofactor peptides in the presence of ligand in AlphaScreen assays (Fig. 5.1C).

5.3.2 Structure Analysis of the aceDAF-12 LBD

The aceDAF-12 LBD structure shows that every asymmetric unit contains two complexes, herein referred to as *a* and *b*, arranged with non-crystallographic asymmetry. Comparison of the two complexes by superposition indicates that they have a root mean squared deviation (RMSD) of 0.563 Å. The major difference between the two complexes is the conformation of β-turns, which causes the ligand (Δ7-DA) to take a slightly different conformation in the ligand binding pocket (see below). The overall architecture of both complexes is similar to other nuclear receptor LBDs, appearing as a well-wrapped three layer α-helical sandwich made of thirteen α-helices and three β-strands (Fig. 5.3A). The ligand is surrounded by the same sets of amino acids as seen in the ssDAF-12 LBD in both complexes, consisting of hydrophobic amino acids surrounding the steroid skeleton and polar amino acids interacting with both ends of the ligand (Fig. 5.3B). However, *a* and *b* show distinct ligand binding conformations due to the differential space arrangements of the ligand in the two complexes. The C3-keto group of Δ7-DA forms an H-bond with Q57 in *b* (3.1 Å), which is absent in *a* (compare Fig. 5.3C and D). Instead, Δ7-DA forms a single H-bond with a nearby water molecule (2.8 Å) in *a*, an interaction also witnessed in *b* (3.3 Å) (Fig. 5.3C and D). There is also a difference in the length of H-bonds formed with the C27-carboxyl group of Δ7-DA in the two complexes (Fig. 5.3E and F). This finding suggests that aceDAF-12 LBD may bind ligands in two different modes, which are interconvertible in solution.

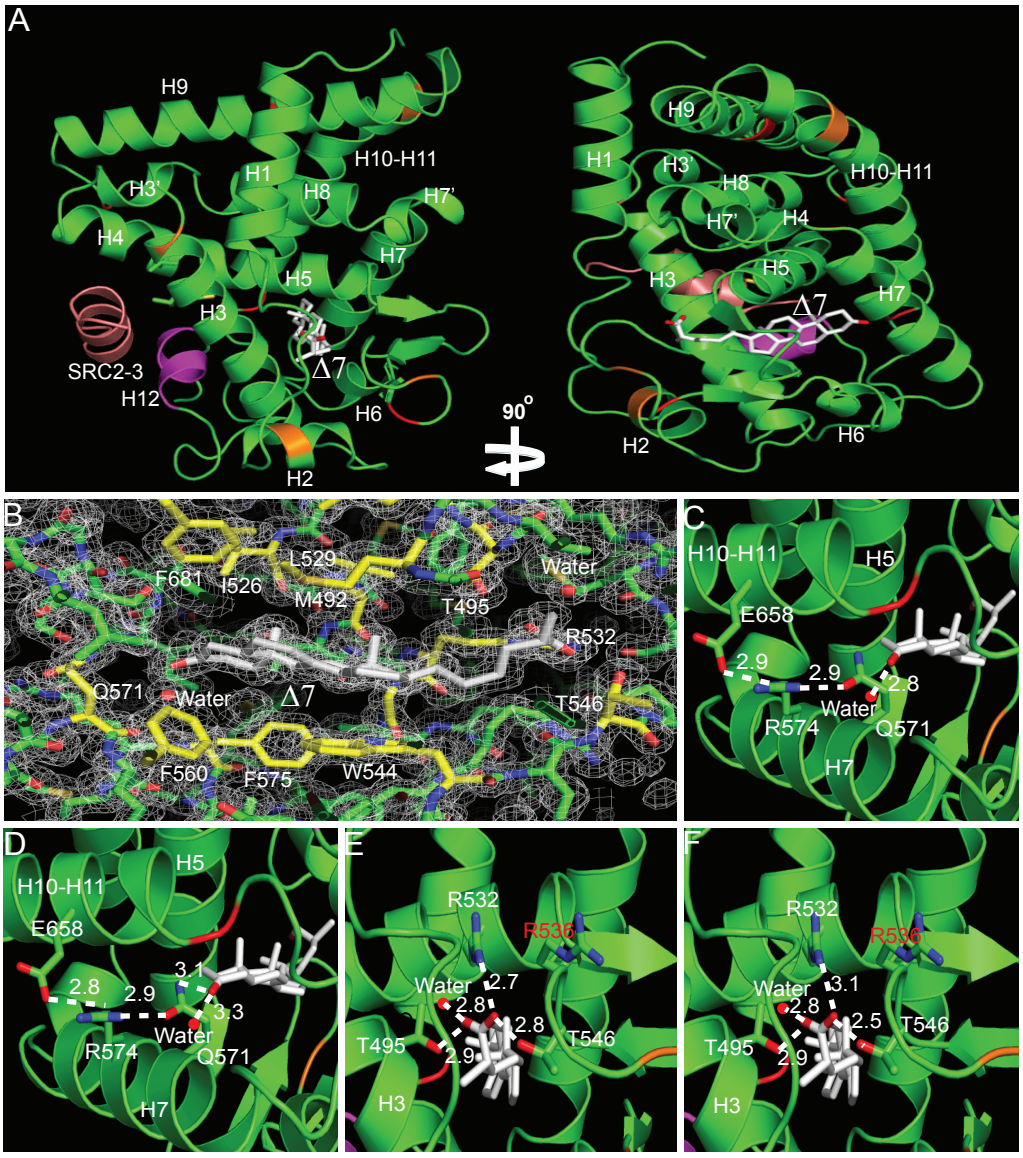

Figure 5.3 Structure Analysis of the aceDAF-12 LBD
(A) The ribbon model reveals the overall architecture of the aceDAF-12 LBD chain *a* (green) complexed with Δ7-DA (white) and the coactivator peptide SRC2-3 (salmon). The AF-2 helix is in magenta. Mutated cysteines are in red and mutated lysines in orange. (B) The electron density map of the aceDAF-12 ligand binding pocket bound to Δ7-DA. (C-D) H-bonding of aceDAF-12 amino acids and water involved in binding the C3-keto group of Δ7-DA in complex *a* (C) and *b* (D). Different H-bonding patterns are present in *a* and *b*. (E-F) H-bonding of aceDAF-12 amino acids and water to the C27-carboxyl group of Δ7-DA in complex *a* and *b* (F). R536 (marked in red) can compensate R532 for interacting with the ligand. H-bonds are illustrated by white dashed lines with bond lengths noted in Å.

aceDAF-12 binds to the coactivator peptide (SRC2-3) in a manner reminiscent of other activated nuclear receptors (Li et al., 2005b; Bledsoe et al., 2002; Gampe et al., 2000a; Krylova et al., 2005). Fig. 5.4A shows that the AF2 helix is in its active conformation and packed against helices H3-H5 to form a functional coactivator binding surface. K504 from the C-terminal end of helix H3 and E681 from the center of the AF2 helix (H12) form the charge clamp that anchors both ends of the SRC2-3 peptide by H-bonding. The locked SRC2-3 peptide adopts a two-turn α-helical conformation and sticks to the binding surface via hydrophobic interactions with V500, L521, and M525. These charge clamp and hydrophobic amino acids are conserved in ceDAF-12 and ssDAF-12, implying that they may use the same mechanism for coactivator binding. Experimental evidence shows that mutation of any of these amino acids greatly compromises the ability of aceDAF-12 or ceDAF-12 to recruit coactivator after ligand stimulation in mammalian two hybrid assays (Fig. 5.4B and C).

5.3.3 Comparison of aceDAF-12 and ssDAF-12 Structures

Respective superposition of the aceDAF-12 LBD complex *a* and *b* onto the ssDAF-12 LBD (complexed with Δ7-DA) shows a similar RMSD of 1.13 Å. By comparison of the two species-specific DAF-12 structures reveals a noticeable difference in ligand conformation in the binding pocket of each structure (Fig. 5.5A). Δ7-DA in ssDAF-12 is more stretched and its C27 end forms a single H-bond with R599 (2.8 Å) (Fig. 5.5B). In contrast, Δ7-DA in the aceDAF-12 LBD complex *a* or *b* makes a slight turn at the C27 end, allowing for it to form two H-bonds with R532, one stronger (2.7 Å in *a* and 3.1 Å in *b*) and one weaker (3.4 Å in *a* and 3.5 Å in *b*) (Fig. 5.5B). This

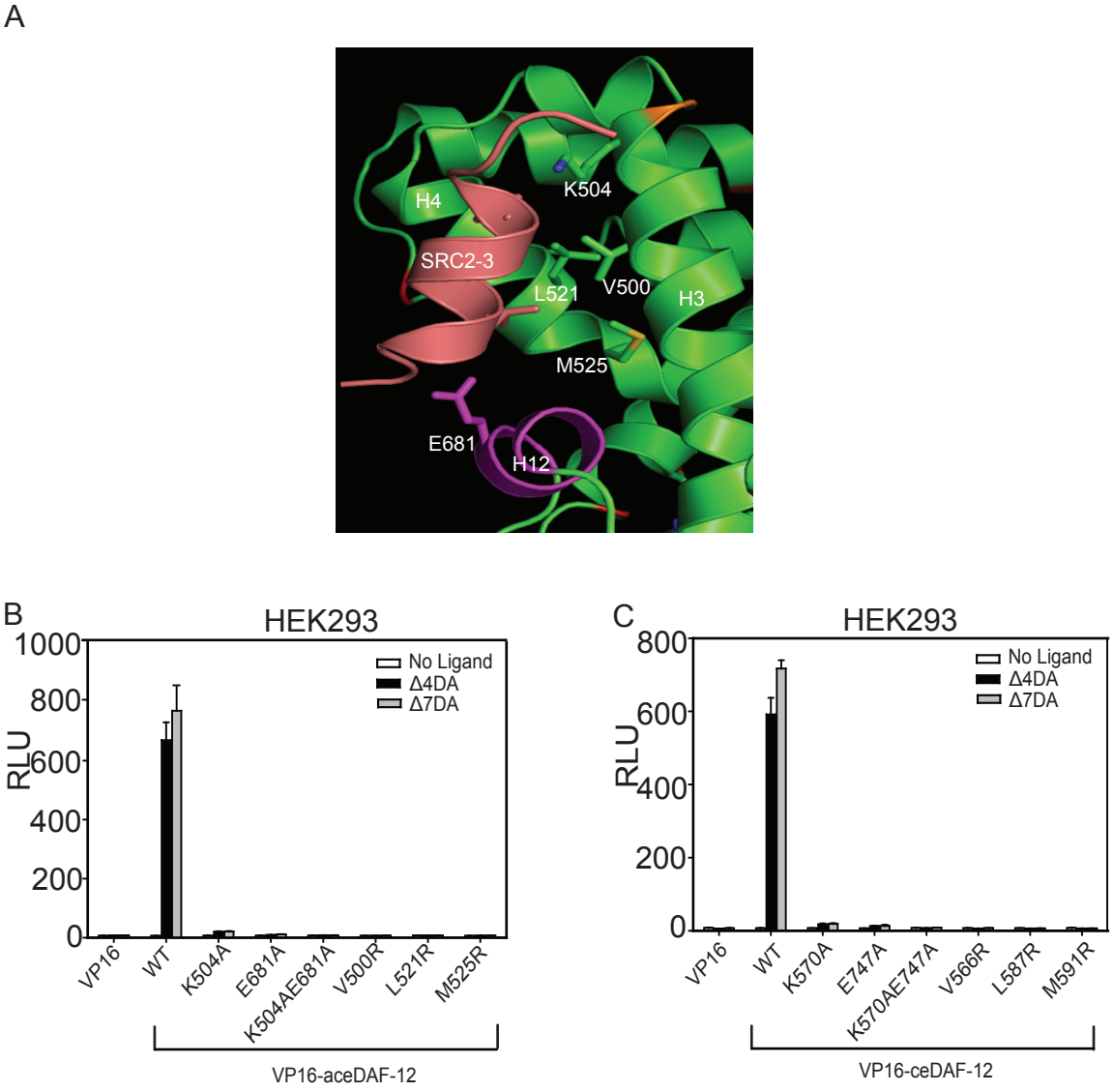

Figure 5.4 Structural Basis for DAF-12 Binding Coactivators
(A) Amino acids involved in binding the coactivator peptide SRC2-3 (salmon) are marked. (B-C) Mutation of these amino acids in aceDAF-12 (B) or corresponding amino acids in ceDAF-12 (C) disrupts the coactivator (Gal4-SRC1) binding in mammalian two hybrid assays. 1 μM of DA is used. RLU, relative light unit.

hookworm specific ligand conformation in DAF-12, together with other structure features elucidated below, is consistent with the observations that hookworm DAF-12s have stronger responses to DA treatment than ssDAF-12 (Wang et al., 2009).

Despite the same set of amino acids involved in ligand binding in both species, we found that the aceDAF-12 LBD exhibits specific molecular environments in proximity of the ligand. In both complexes, one water molecular is located nearby either end of Δ7-DA and H-bonds with the ligand, which is not seen in the ssDAF-12 LBD structure (Fig 5.3C-F). At the C27-carboxyl end of Δ7-DA, arginine 536 (R536) is pointed away from the carboxyl group due to charge repelling from R532, but it can possibly swing over for H-bonding with the ligand if R536 is replaced by a non-positively charged amino acid (Fig. 5.3E-F). The corresponding amino acid in ssDAF-12 is a valine (V603), which can not compensate if R599 is mutated. At the other end of Δ7-DA, there is an H-bonding network based on R574, which interacts with Q571 and E658 (Fig. 5.3C). This network gives hookworm DAF-12s better tolerance to the mutation of Q571, which locks the C3-keto group of the ligand by H-bonding (Fig. 5.3C and D).

These hookworm specific structural elements are responsible for the species-specific pharmacological responses revealed by our mutation studies (Wang et al., 2009). As previously described, acDAF-12R598M and ceDAF-12R532M (but not ssDAF-12R599M) are still responsive to Δ7-DA, because both of these DAF-12s have a compensating arginine (R536 in acDAF-12 and R602 in ceDAF-12). However, this compensation is missing in acDAF-12R598K and ceDAF-12R532K because the mutated lysine repels the charge of the compensating arginine, thereby preventing H-bonding to the ligand. acDAF-12Q571E could be activated by Δ7-DA, but not ceDAF-12Q638E or

ssDAF-12Q637E, because the H-bonding network hub R574 still makes the glutamic acid an effective H-bond donor for the C3-keto group of Δ7-DA. The corresponding amino acids K641 in ceDAF-12 or G640 in ssDAF-12 prevent this H-bonding interaction.

To provide further evidence for the pharmacological differences noted above, I mutated R536 and R574 in acDAF-12 to the corresponding amino acids in ceDAF-12 or ssDAF-12. As predicted, mutation of R536V in acDAF-12R532M or R602V in ceDAF-12R598M compromised receptor activity in the presence of ligands (Fig. 5.5C and E). In contrast, the reciprocal mutation of V603R in ssDAF-12R599M recovered receptor activity (Fig. 5.5D). Mutation of R574G on the basis of acDAF-12Q571E caused the receptor to fail to respond to Δ7-DA stimulation. A similar mutation, R574K, also impaired receptor activity (Fig. 5.5C). However, mutation of K641R in ceDAF-12Q638E or G640R in ssDAF-12Q637E did not rescue the receptor response to Δ7-DA (Fig. 5.5D and E), suggesting the involvement of other structural elements in the hookworm DAF-12s that assist in ligand binding.

5.3.4 Structural Comparison between DAF-12 and FXR LBDs

Sequence analysis suggested that DAF-12 is most similar to mammalian LXR, PXR, VDR, and FXR (Antebi et al., 2000; Mooijaart et al., 2005). We wanted to understand the similarity between DAF-12 and mammalian nuclear receptors on a 3-D structural basis. Therefore, we superpositioned the aceDAF-12 LBD complex *a* on a number of mammalian nuclear receptor LBD-ligand complexes. Interestingly, DAF-12 shares the closest 3-D structure appearance to FXR among nuclear receptors examined, with an RMSD of 1.611 (Table 5.3). Further inspection of the two structures revealed that

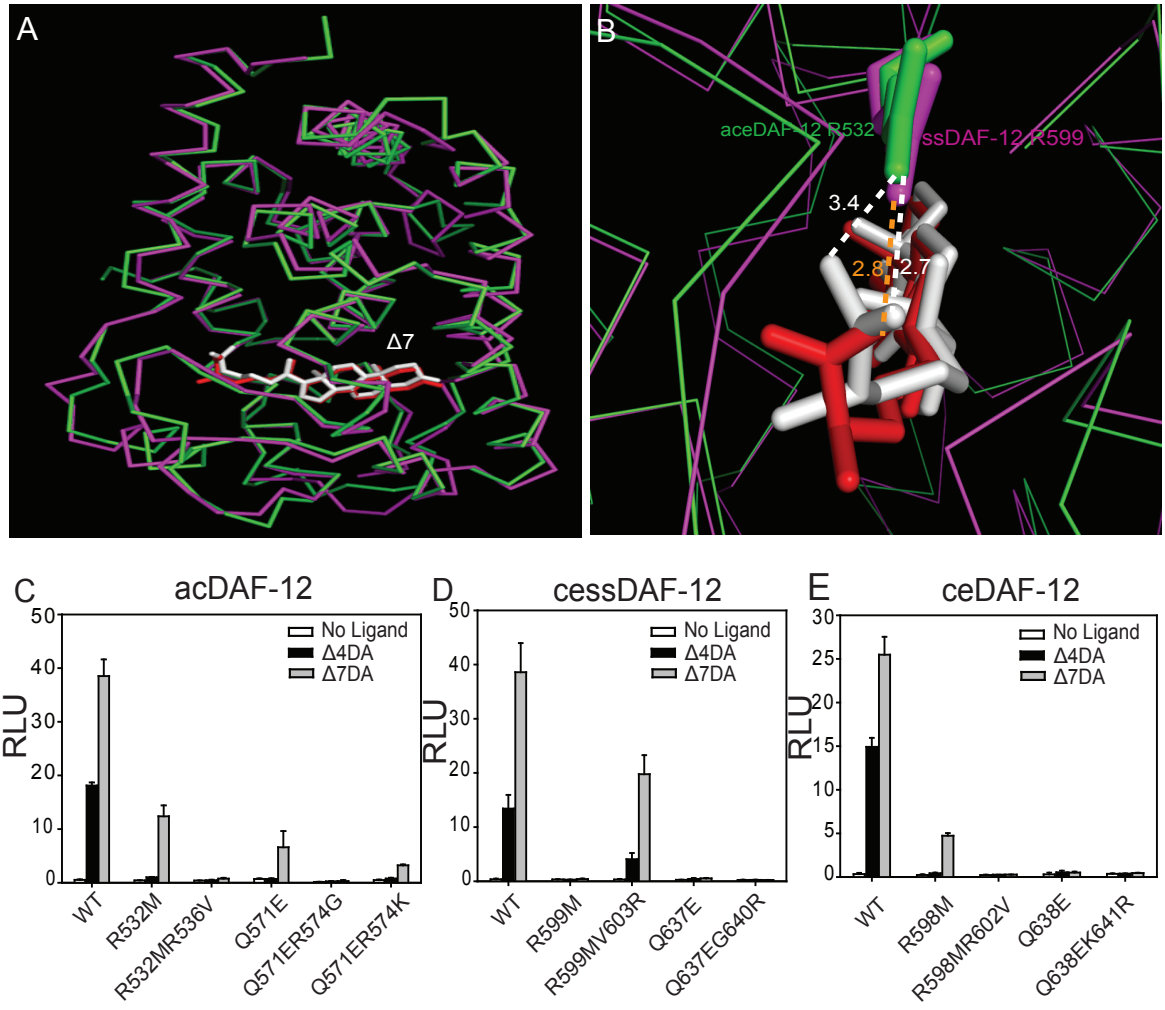

Figure 5.5 Structural Understanding of DAF-12 Species-specific Ligand Binding
(A) Superposition of aceDAF-12 and ssDAF-12 LBD. The aceDAF-12 LBD complex *a* is shown in green and ssDAF-12 in magenta. Δ7-DA is white in aceDAF-12 and red in ssDAF-12. (B) The aceDAF-12 R532 (green) forms two H-bonds (white dashed line) with the ligand, while the corresponding amino acid in ssDAF-12, R599 (magenta) forms one H-bond (orange dashed line). H-bond lengths are noted in Å. (C) Site-directed mutagenesis validates the structural elements responsible for species-specific ligand binding, as revealed by structural comparison between aceDAF-12 and ssDAF-12 LBDs. Cotransfection assays are performed in COS7 cells. 1 μM of DA is used. RLU, relative light units.

Mammalian Nuclear Receptor	PDB ID	RMSD
FXR	1OSV	1.611
LXR	1P8D	1.722
VDR	1DB1	1.742
PR	1A28	1.803
GR	1M2Z	1.821
ROR	1N83	1.844
MR	2A3I	1.849
ER	1ERE	1.85
AR	1I37	1.965

Table 5.3 Structural Comparison between aceDAF-12 and Mammalian Nuclear Receptors by Superpostion
RMSD, root mean square deviation

DAF-12 adopts the unique ligand orientation that is unique among all other nuclear receptors to FXR. The A ring of the steroid skeleton faces the back layer of the ligand binding pocket in both receptors and the D ring faces outward toward the helix H1 (Fig. 5.6A), whereas all other known nuclear receptors (e.g., LXR and VDR) arrange their cognate steroid-based ligands in the opposite direction (Williams et al., 2003; Mi et al., 2003; Rochel et al., 2000). Furthermore, DAF-12 and FXR use conserved amino acids to interact with the carboxyl group of the ligand. In correspondence with R532 binding to the carboxyl group of Δ7-DA in aceDAF-12, R328 in FXR forms an H-bond with the carboxyl group of 6α-ethyl-CDCA (6ECDCA) and mutation of this amino acid affects receptor activity (Mi et al., 2003) (Fig. 5.6B). Although amino acids are not conserved in binding the other end of the ligand, a similar H-bond interaction between Q571 and the C3-keto group of Δ7-DA in aceDAF-12, also occurs with the corresponding amino acid Y358 in FXR to form an H-bond with the C3-hydroxyl group of 6ECDCA (Fig. 5.6C). The 3-D structural similarity between DAF-12 and FXR indicates that they share the common structural features in binding bile acid-like molecules and suggests that DAF-12 and FXR are functional orthologs.

5.3.5 Crosstalk between Bile Acid Signaling Pathways

In mammals, bile acids are produced in the liver from cholesterol through two pathways that involves a number of P450 enzymes (Russell, 2003). In the classic pathway, CYP7A1 initiates the biosynthetic process (Fig. 5.7A). Other enzymes such as CYP8B1 and CYP27A1 catalyze downstream to generate bile acid precursors. Postprandial release of bile acids from the gallbladder are sensed by FXR, which regulates the lipid,

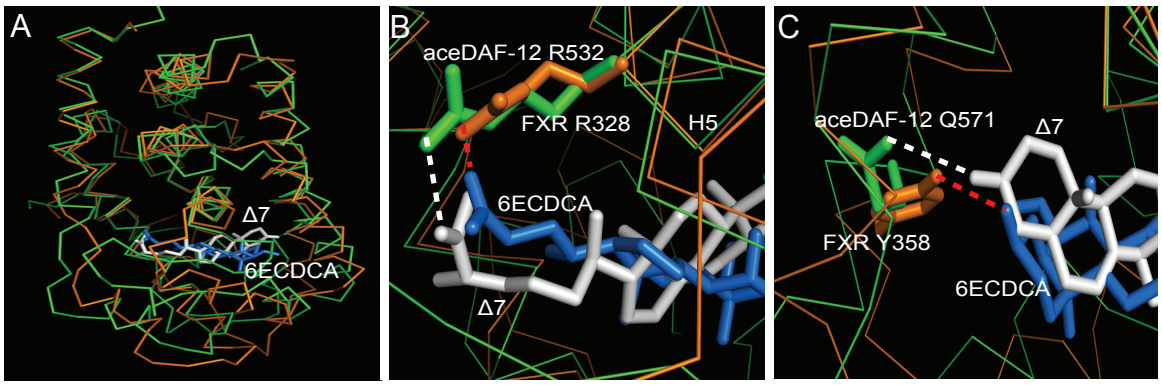

Figure 5.6 Structural Similarity between DAF-12 and FXR LBDs
(A) Superposition of the aceDAF-12 LBD (green) onto the FXR LBD (orange). Δ7–DA is in white and the FXR ligand 6ECDCA in blue. The ligand orientation is the same in FXR and DAF-12, but different from that in other nuclear receptors. (B) Conserved amino acids involved in binding the carboxyl group of the ligand. (C) Similar H-bond interactions with the C3 end of the ligand. FXR Y358 H-bonds with the C3-hydroxyl group of 6ECDCA (red dashed line), while aceDAF-12 Q571 H-bonds with the C3-keto group of Δ7-DA (white dashed line).

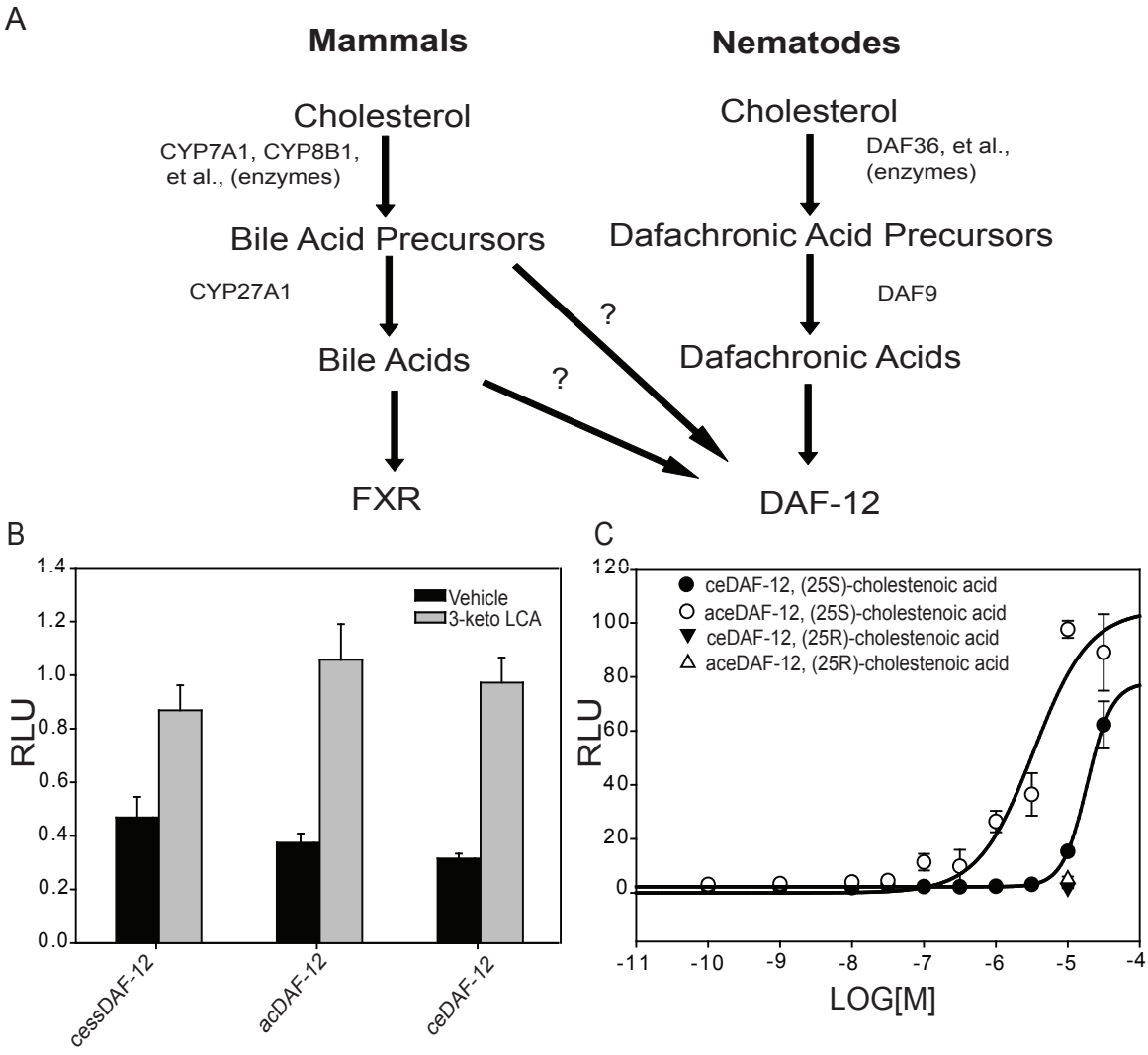

Figure 5.7 Crosstalk between Bile Acid-like Signaling Pathways
(A) Schematic comparison between the mammalian bile acid signaling pathway and the bile acid-like signaling pathway in nematodes. Studies (B-C) indicate that two pathways can crosstalk, but the physiological relevance remains a question. (B) 3-keto LCA (10 μM) activates the DAF-12s from *S.stercoralis*, *A. caninum*, and *C.elegans* in COS7 cells. (C) (25S)-cholestenoic acid activates the DAF-12s from *C.elegans* and *A. ceylanicum* in a dose-dependent manner in HEK293 cells. RLU, relative light unit.

carbohydrate, and energy metabolism, as well as feedback regulation of bile acid synthesis in the body (Pellicciari et al., 2005).

Here, we propose the existence of a parallel bile acid-like signaling pathway in nematodes. As exemplified in *C. elegans*, cholesterol is converted to DA precursors through steps involving the action of DAF-36, which is a believed to function as a Δ7-desaturase (Rottiers et al., 2006). The resultant DA precursors are further modified by DAF-9, which is a functional ortholog of CYP27A1, into DA ligands for DAF-12. As shown in this study, FXR and DAF-12 bind their bile acid-like ligands in a structurally conserved manner. Also like FXR, DAF-12 is shown to modulate events related to lipid and energy metabolism in *C. elegans* (Antebi et al., 1998; Gerisch et al., 2001). Taken together, this suggests that these two bile acid-like signaling pathways have been conserved across evolution.

Previous studies showed that some mammalian bile acids such as 3-keto LCA could activate ceDAF-12 (Motola et al., 2006). In this study, we also examined the effect of 3-keto LCA on parasitic DAF-12s from *S. stercoralis* and *A. caninum*. As shown in Fig. 5.7B, 3-keto LCA stimulated the activity of all the tested DAF-12s to a comparable level. Notably, (25S)-cholestenoic acid, a mammalian bile acid precursor that is synthesized by CYP7A1 (the DAF-9 homolog), weakly activated ceDAF-12 and rescued dauer formation in *daf-9* mutants (Held et al., 2006). We also investigated activation of the hookworm aceDAF-12 by cholestenoic acid. In a cell-based assay, aceDAF-12 was more sensitive to (25S)-cholestenoic acid (EC_{50}=4 μM), than ceDAF-12 (EC_{50} >30 μM) (Fig. 5.7C). Neither DAF-12 was stimulated by (25R)-cholestenoic acid, suggesting the importance of stereochemistry at the C25 position as previously shown (Motola et al.,

2006)

The ability of mammalian bile acids and bile acid precursors to activate DAF-12 indicates that the mammalian bile acid signaling pathway can crosstalk with the nematode bile acid-like signaling pathway. Since most parasitic nematodes constitutively enter iL3 outside their hosts, they may not possess the complete set of enzymes to generate DAF-12 ligands like free living species such as *C. elegans* (Wang et al., 2009). Thus, the parasites might depend on the host factors for DAF-12 activation. In this regard, mammalian bile acids or bile acids precursors are promising candidates for these factors (Fig 5.7A).

5.4 DISCUSSION

In *C. elegans*, the nuclear receptor superfamily is composed of 284 members. Among them, DAF-12 is one of the most extensively studied and characterized to date. It functions as a decision maker to regulate many aspects of worm life history, from growth to reproduction and aging. From an evolutionary perspective, its function is similar in many ways to more advanced animals. Previous studies suggested the closest DAF-12 relatives in mammals are LXR, PXR, VDR, and FXR, based on sequence comparison (Antebi et al., 2000; Mooijaart et al., 2005). In this study, we suggest that FXR is the mammalian ortholog to DAF-12 based on 3-D structure analysis, ligand binding specificity, and functional activity. This hypothesis is supported by a similar overall 3-D architecture that uses the same ligand binding orientation and conserved amino acids involved in ligand binding.

FXR is known as an intracellular bile acid sensor and maintains bile acid

homeostasis by regulating bile acid biosynthesis and enterohepatic circulation (Makishima et al., 1999; Houten et al., 2006; Kullak-Ublick et al., 2004). FXR null mice develop normally, but manifest unbalanced lipid profiles in the serum and liver. FXR null mice have reduced bile acid pools and are susceptible to exogenous bile acid toxicity (Sinal et al., 2000). Glucose metabolism is also impaired in FXR knockout mice (Ma et al., 2006). In light of our hypothesis, it is interesting to speculate that FXR may play a role in mammalian reproduction and longevity, similar to that of DAF-12 in nematodes. In line with this, I note FXR is also expressed in mouse ovary and adrenal gland (Bookout et al., 2006).

We compared the biosynthetic pathways for generation of bile acids and dafachronic acids. Together with the structural similarity between DAF-12 and FXR, a bile acid-like signaling pathway is now known to exist in nematodes. This pathway can crosstalk with the mammalian bile acid signaling pathway, as evidenced by the ability of the mammalian bile acid 3-keto LCA and the bile acid precursor (25S)-cholestenoic acid to stimulate the activity of DAF-12. This finding is interesting because mammalian bile acids or bile acid precursors may work as host signals to activate the parasitic DAF-12. As a consequence, the parasitic larvae are recovered from the iL3 stage and become reproductive adults. This hypothesis is supported by our current work that indicates parasitic nematodes may not possess the complete set of enzymes to generate DAF-12 ligands as seen in *C. elegans* (Wang et al., 2009).

LCA or 3-keto LCA can activate a number of mammalian nuclear receptors including FXR, PXR, and VDR (Makishima et al., 1999; Makishima et al., 2002; Staudinger et al., 2001). In our study, 3-keto LCA was shown to activate DAF-12s from *C.*

elegans or parasitic nematodes by 2- or 3-fold. 3-keto LCA is toxic at high concentrations and represents a low percentage in the bile acid pool (Martinez-Augustin and Sanchez de Medina, 2008). Therefore, 3-keto LCA is unlikely to be the host signal for iL3 recovery. In comparison, the mammalian bile acid precursor (25S)-cholestenoic acid activates DAF-12 more potently and with a preference for the parasitic DAF-12 over *C. elegans* DAF-12. However, the EC_{50} (~ 4 μM) for aceDAF-12 activation achieved from our cell reporter assays (Fig. 5.5B) is well above the reported circulating concentration of 25-cholestenoic acids and their derivatives in human blood, which ranges from 200-250 nM (Axelson et al., 1988), suggesting (25S)-cholestenoic acid may be a ligand precursor in humans. Thus, identification of the host physiological signals that control the reproductive development of parasitic nematodes is an interesting topic for future studies that should provide insights into nematode evolution and parasitism control.

The main motivation for this study was to understand the species-specific pharmacological responses of DAF-12. By comparing the LBD structures of aceDAF-12 and ssDAF-12, we found that despite the same sets of amino acids involved in ligand binding, different environments of neighboring amino acids can still influence the receptor's sensitivity to ligand stimulation or tolerance to mutations. This provides insights into the design of species-specific pharmaceuticals. In addition, it also provides some hints about nematode evolution. It reveals the possibility that some parasitic nematodes are more tolerant to mutations in order to adapt to the environment.

From our structural work, DAF-12 associates with mammalian co-activator peptides. This hints that there should be similar coactivators for DAF-12 in worms and very likely they contain LXXLL motifs for interaction. My studies point to a novel

strategy to answer this question by taking advantage of our AlphaScreen assays (Fig. 5.2) and the use of bioinformatics to scan through the worm genome for motifs similar to those of known interacting peptides. The discovery of natural coactivators would be expected to help us better understand the functions of DAF-12 or other nuclear receptors in *C. elegans*.

CHAPTER SIX

Conclusions and Perspectives

Bile acids are important signaling molecules in mammals. Our recent findings show that bile acid-like molecules are also important signaling molecules in nematodes to control dauer formation and reproduction (Motola et al., 2006). In this thesis, studies have been conducted toward understanding how bile acid homeostasis is regulated in mammals and how bile acids are sensed in nematodes. My results suggest that bile acid-like signaling pathways have been conserved across evolution and mediate the parasitic crosstalk between mammals and nematodes.

6.1 SHP BIOCHEMISTRY

SHP represents a critical element in the feedback regulation of bile acid homeostasis in mammals. Isolation of SHP interacting proteins would provide insights into the molecular basis underlying the negative control of bile acid production by SHP. Therefore, a number of biochemical strategies have been applied to identify SHP interacting proteins from cultured cells or animal tissues. In Chapter Three, several SHP interacting proteins were identified using the tandem affinity purification strategy. Although the interaction between these proteins and SHP could not be validated, the strategy is promising for future attempts, which might work by slightly modifying the current reaction system (e.g., adding FGF15). The strategy of recombinant protein pull down was also tried. MBP-SHP and GST-SHP pull down exhibited inconsistent results (data not shown). With respect to this, an *in vitro* SHP repression reconstitution system might be considered. By referring to the previously reported *in vitro* transcription system,

which contained recombinant human general transcription factors TFII A, B, E, and F together with highly purified human RNA polymerase II, immunopurified TFII D and H (Lemon et al., 2001), we can include LRH-1 response element containing chromatin templates, soluble MBP-LRH-1 full length, and SHP protein into this system. Attenuation of the LRH-1-dependent transcription mediated by SHP from chromatin templates after addition of cell nuclear extracts would suggest the existence of SHP-associated repressive activities in these extracts. These activities can be purified by successive chromatographic columns and sequenced by mass spectrometry. As an advantage to this strategy, the entire purification process can be directed by the activity assays.

6.2 SHP STRUCTURAL BIOLOGY

SHP represents one of a few structures in the nuclear receptor superfamily that remain to be solved. One rate-limiting step of solving the SHP structure is the solubilization of SHP recombinant protein. In Chapter Three, the first successful strategy to solubilize SHP protein (in bacteria) was reported. By mutating the cysteines in SHP to serines and coexpressing SHP with the LRH-1 LBD, a large quantity of SHP recombinant protein was achieved for crystallization. Importantly, mutation of cysteines did not affect the SHP functionality in all the assays examined. This cysteine to serine mutation strategy also worked for other protein solubilization such as DAX-1 and aceDAF-12. So far, SHP crystals were obtained that diffracted to 3.2 Angstroms. A number of strategies have been used for optimization, one of which, co-crystallization with the SHP AF2 helix interacting peptides, is promising since crystallization of several nuclear receptor complexes requires stabilization of the nuclear receptor AF2 helix by interaction peptides (Wang et al., 2009;

Li et al., 2005b; Bledsoe et al., 2002; Li et al., 2005a). Determination of the SHP crystal structure will be my goal in the very near future.

6.3 HOOKWORM DAF-12 STRUCTURAL BIOLOGY

Bile acid-like molecules are ligands for the nuclear receptor DAF-12 in *C. elegans*, which control dauer formation and reproduction. These molecules (DAs) also regulate the iL3 recovery in parasitic nematodes such as hookworms by a similar mechanism. Hookworms affect more than one billion people worldwide and cause iron-deficient anemia (Hotez et al., 2006). Elucidation of the hookworm DAF-12 structure would direct the design of effective pharmaceuticals to treat hookworm-caused diseases. In Chapter Five, the first hookworm DAF-12 LBD structure was reported. According to this structure, although the same set of amino acids are involved in ligand binding in comparison to the ssDAF-12 LBD structure, different environments of neighboring amino acids can still influence the receptor's sensitivity to ligand stimulation or tolerance to mutations. In addition, this structure represents a high definition 3-D structure for DAF-12, which allows for us to perform computer adaptive design to identify DAF-12 agonists or antagonists.

6.4 DAF-12 AND FXR

Primary protein sequence analysis suggests that DAF-12 is related to LXR, VDR, PXR, and FXR (Antebi et al., 2000; Mooijaart et al., 2005). In Chapter Five, comparison of the ssDAF-12 and aceDAF-12 3-D structures to the FXR structure supported the similarity between DAF-12 and FXR, as evidenced by a closer overall 3-D architecture

that uses the same ligand binding orientation and conserved amino acids involved in ligand binding. This finding, together with the similarity of the enzymatic systems in the production of bile acid-like ligands, suggests the existence of a parallel bile acid-like signaling pathway in nematodes.

In *C. elegans*, fat metabolism, reproduction, and life span are closely interrelated and regulation of these events converges onto DAF-12 (Antebi et al., 1998; Gerisch et al., 2001). Interestingly, studies show that these life traits also crosstalk with each other in mammals. For example, longevity and metabolic levels are strongly linked in mammals, and both are potently modulated by the insulin signaling pathway (Narasimhan et al., 2009). The onset of reproductive age is associated with menarche in young women, and was found to be positively correlated with the body fat and regulated by the leptin signaling pathway (Kaplowitz, 2008). Therefore, identification of the underlying molecular links, like insulin and leptin, would be an interesting topic. In consideration of the structural and functional similarity between FXR and DAF-12, FXR might be a promising candidate. As evidence, the role of FXR in reproduction and longevity should be examined.

6.5 PARASITIC DAF-12 ACTIVATION IN MAMMALS

The existence of a parallel bile acid-like signaling pathway in nematodes supports the notion that the bile acid-like signaling pathways have been conserved across evolution. In Chapter Five, it was demonstrated that the nematode DAF-12 can respond to mammalian bile acids and bile acid precursors. This finding suggests that nematodes may depend on mammalian bile acid-related lipids for recovery from the infective stage,

which links their parasitic life cycle to host metabolic status. In order to validate this hypothesis, bile acids from non-infected or infected mammals will be collected and fractionated by HPLC. Then each fraction will be examined with respect to its ability to activate the parasitic DAF-12 (e.g., aceDAF-12) in AlphaScreen assays and/or cotransfection assays. Identification of host ligands for the parasitic DAF-12 will increase our knowledge of parasitic evolution in nematodes and improve our strategies to control nematode parasitism.

REFERENCES

(1999). A unified nomenclature system for the nuclear receptor superfamily. Cell *97*, 161-163.

Antebi, A. (2006). Nuclear hormone receptors in C. elegans. WormBook, 1-13.

Antebi, A., Culotti, J.G., and Hedgecock, E.M. (1998). daf-12 regulates developmental age and the dauer alternative in Caenorhabditis elegans. Development *125*, 1191-1205.

Antebi, A., Yeh, W.H., Tait, D., Hedgecock, E.M., and Riddle, D.L. (2000). daf-12 encodes a nuclear receptor that regulates the dauer diapause and developmental age in C. elegans. Genes Dev *14*, 1512-1527.

Aranda, A., and Pascual, A. (2001). Nuclear hormone receptors and gene expression. Physiol Rev *81*, 1269-1304.

Augereau, P., Badia, E., Balaguer, P., Carascossa, S., Castet, A., Jalaguier, S., and Cavailles, V. (2006). Negative regulation of hormone signaling by RIP140. J Steroid Biochem Mol Biol *102*, 51-59.

Axelson, M., Mork, B., and Sjovall, J. (1988). Occurrence of 3 beta-hydroxy-5-cholestenoic acid, 3 beta,7 alpha-dihydroxy-5-cholestenoic acid, and 7 alpha-hydroxy-3-oxo-4-cholestenoic acid as normal constituents in human blood. J Lipid Res *29*, 629-641.

Baek, S.H., Ohgi, K.A., Nelson, C.A., Welsbie, D., Chen, C., Sawyers, C.L., Rose, D.W., and Rosenfeld, M.G. (2006). Ligand-specific allosteric regulation of coactivator functions of androgen receptor in prostate cancer cells. Proc Natl Acad Sci U S A *103*, 3100-3105.

Bavner, A., Johansson, L., Toresson, G., Gustafsson, J.A., and Treuter, E. (2002). A transcriptional inhibitor targeted by the atypical orphan nuclear receptor SHP. EMBO Rep *3*, 478-484.

Bledsoe, R.K., Montana, V.G., Stanley, T.B., Delves, C.J., Apolito, C.J., McKee, D.D., Consler, T.G., Parks, D.J., Stewart, E.L., Willson, T.M., *et al.* (2002). Crystal structure of the glucocorticoid receptor ligand binding domain reveals a novel mode of receptor dimerization and coactivator recognition. Cell *110*, 93-105.

Bookout, A.L., Jeong, Y., Downes, M., Yu, R.T., Evans, R.M., and Mangelsdorf, D.J. (2006). Anatomical profiling of nuclear receptor expression reveals a hierarchical transcriptional network. Cell *126*, 789-799.

Borgius, L.J., Steffensen, K.R., Gustafsson, J.A., and Treuter, E. (2002). Glucocorticoid signaling is perturbed by the atypical orphan receptor and corepressor SHP. J Biol Chem *277*, 49761-49766.

Boulias, K., and Talianidis, I. (2004). Functional role of G9a-induced histone methylation in small heterodimer partner-mediated transcriptional repression. Nucleic Acids Res *32*, 6096-6103.

Bourguet, W., Ruff, M., Chambon, P., Gronemeyer, H., and Moras, D. (1995). Crystal structure of the ligand-binding domain of the human nuclear receptor RXR-alpha. Nature *375*, 377-382.

Chandra, V., Huang, P., Hamuro, Y., Raghuram, S., Wang, Y., Burris, T.P., and Rastinejad, F. (2008). Structure of the intact PPAR-gamma-RXR-alpha nuclear receptor complex on DNA. Nature, 350-356.

Chawla, A., Repa, J.J., Evans, R.M., and Mangelsdorf, D.J. (2001). Nuclear receptors and lipid physiology: opening the X-files. Science *294*, 1866-1870.

Chen, D., Huang, S.M., and Stallcup, M.R. (2000). Synergistic, p160 coactivator-dependent enhancement of estrogen receptor function by CARM1 and p300. J Biol Chem *275*, 40810-40816.

Chen, D., Kon, N., Li, M., Zhang, W., Qin, J., and Gu, W. (2005). ARF-BP1/Mule is a critical mediator of the ARF tumor suppressor. Cell *121*, 1071-1083.

Chen, G., Liang, G., Ou, J., Goldstein, J.L., and Brown, M.S. (2004). Central role for liver X receptor in insulin-mediated activation of Srebp-1c transcription and stimulation of fatty acid synthesis in liver. Proc Natl Acad Sci U S A *101*, 11245-11250.

Chen, J.D., and Evans, R.M. (1995). A transcriptional co-repressor that interacts with nuclear hormone receptors. Nature *377*, 454-457.

Chitwood, D.J. (1999). Biochemistry and function of nematode steroids. Crit Rev Biochem Mol Biol *34*, 273-284.

Cress, W.D., and Seto, E. (2000). Histone deacetylases, transcriptional control, and cancer. J Cell Physiol *184*, 1-16.

Dieterich, C., and Sommer, R.J. (2009). How to become a parasite - lessons from the genomes of nematodes. Trends Genet *25*, 203-209.

Fielenbach, N., and Antebi, A. (2008). C. elegans dauer formation and the molecular basis of plasticity. Genes Dev *22*, 2149-2165.

Forman, B.M., Goode, E., Chen, J., Oro, A.E., Bradley, D.J., Perlmann, T., Noonan, D.J., Burka, L.T., McMorris, T., Lamph, W.W.*, et al.* (1995). Identification of a nuclear receptor that is activated by farnesol metabolites. Cell *81*, 687-693.

Gampe, R.T., Jr., Montana, V.G., Lambert, M.H., Miller, A.B., Bledsoe, R.K., Milburn, M.V., Kliewer, S.A., Willson, T.M., and Xu, H.E. (2000a). Asymmetry in the PPARgamma/RXRalpha crystal structure reveals the molecular basis of heterodimerization among nuclear receptors. Mol Cell *5*, 545-555.

Gampe, R.T., Jr., Montana, V.G., Lambert, M.H., Wisely, G.B., Milburn, M.V., and Xu, H.E. (2000b). Structural basis for autorepression of retinoid X receptor by tetramer formation and the AF-2 helix. Genes Dev *14*, 2229-2241.

Gerisch, B., Weitzel, C., Kober-Eisermann, C., Rottiers, V., and Antebi, A. (2001). A hormonal signaling pathway influencing C. elegans metabolism, reproductive development, and life span. Dev Cell *1*, 841-851.

Germain, P., Staels, B., Dacquet, C., Spedding, M., and Laudet, V. (2006). Overview of nomenclature of nuclear receptors. Pharmacol Rev *58*, 685-704.

Glozak, M.A., and Seto, E. (2007). Histone deacetylases and cancer. Oncogene *26*, 5420-5432.

Gobinet, J., Carascossa, S., Cavailles, V., Vignon, F., Nicolas, J.C., and Jalaguier, S. (2005). SHP represses transcriptional activity via recruitment of histone deacetylases. Biochemistry *44*, 6312-6320.

Goodwin, B., Jones, S.A., Price, R.R., Watson, M.A., McKee, D.D., Moore, L.B., Galardi, C., Wilson, J.G., Lewis, M.C., Roth, M.E., *et al.* (2000). A regulatory cascade of the nuclear receptors FXR, SHP-1, and LRH-1 represses bile acid biosynthesis. Mol Cell *6*, 517-526.

Gronemeyer, H., Gustafsson, J.A., and Laudet, V. (2004). Principles for modulation of the nuclear receptor superfamily. Nat Rev Drug Discov *3*, 950-964.

Gurevich, I., Flores, A.M., and Aneskievich, B.J. (2007). Corepressors of agonist-bound nuclear receptors. Toxicol Appl Pharmacol *223*, 288-298.

Hayhurst, G.P., Lee, Y.H., Lambert, G., Ward, J.M., and Gonzalez, F.J. (2001). Hepatocyte nuclear factor 4alpha (nuclear receptor 2A1) is essential for maintenance of hepatic gene expression and lipid homeostasis. Mol Cell Biol *21*, 1393-1403.

Held, J.M., White, M.P., Fisher, A.L., Gibson, B.W., Lithgow, G.J., and Gill, M.S. (2006). DAF-12-dependent rescue of dauer formation in Caenorhabditis elegans by (25S)-cholestenoic acid. Aging Cell *5*, 283-291.

Hofmann, A.F. (2009). The enterohepatic circulation of bile acids in mammals: form and functions. Front Biosci *14*, 2584-2598.

Hollenberg, S.M., Weinberger, C., Ong, E.S., Cerelli, G., Oro, A., Lebo, R., Thompson,

E.B., Rosenfeld, M.G., and Evans, R.M. (1985). Primary structure and expression of a functional human glucocorticoid receptor cDNA. Nature *318*, 635-641.

Horlein, A.J., Naar, A.M., Heinzel, T., Torchia, J., Gloss, B., Kurokawa, R., Ryan, A., Kamei, Y., Soderstrom, M., Glass, C.K., *et al.* (1995). Ligand-independent repression by the thyroid hormone receptor mediated by a nuclear receptor co-repressor. Nature *377*, 397-404.

Hotez, P.J., Bethony, J., Bottazzi, M.E., Brooker, S., Diemert, D., and Loukas, A. (2006). New technologies for the control of human hookworm infection. Trends Parasitol *22*, 327-331.

Houten, S.M., Watanabe, M., and Auwerx, J. (2006). Endocrine functions of bile acids. EMBO J *25*, 1419-1425.

Hu, P.J. (2007). Dauer. WormBook, 1-19.

Hylemon, P.B., Zhou, H., Pandak, W.M., Ren, S., Gil, G., and Dent, P. (2009). Bile acids as regulatory molecules. J Lipid Res.

Inagaki, T., Choi, M., Moschetta, A., Peng, L., Cummins, C.L., McDonald, J.G., Luo, G., Jones, S.A., Goodwin, B., Richardson, J.A., *et al.* (2005). Fibroblast growth factor 15 functions as an enterohepatic signal to regulate bile acid homeostasis. Cell Metab *2*, 217-225.

Jasmer, D.P., Goverse, A., and Smant, G. (2003). Parasitic nematode interactions with mammals and plants. Annu Rev Phytopathol *41*, 245-270.

Johansson, L., Bavner, A., Thomsen, J.S., Farnegardh, M., Gustafsson, J.A., and Treuter, E. (2000). The orphan nuclear receptor SHP utilizes conserved LXXLL-related motifs for interactions with ligand-activated estrogen receptors. Mol Cell Biol *20*, 1124-1133.

Jones, T.A., Zou, J.Y., Cowan, S.W., and Kjeldgaard, M. (1991). Improved methods for building protein models in electron density maps and the location of errors in these models. Acta Crystallogr A *47 (Pt 2)*, 110-119.

Kaplowitz, P.B. (2008). Link between body fat and the timing of puberty. Pediatrics *121 Suppl 3*, S208-217.

Karagianni, P., and Wong, J. (2007). HDAC3: taking the SMRT-N-CoRrect road to repression. Oncogene *26*, 5439-5449.

Kerr, T.A., Saeki, S., Schneider, M., Schaefer, K., Berdy, S., Redder, T., Shan, B., Russell, D.W., and Schwarz, M. (2002). Loss of nuclear receptor SHP impairs but does not eliminate negative feedback regulation of bile acid synthesis. Dev Cell *2*, 713-720.

Klinge, C.M., Jernigan, S.C., Mattingly, K.A., Risinger, K.E., and Zhang, J. (2004). Estrogen response element-dependent regulation of transcriptional activation of estrogen receptors alpha and beta by coactivators and corepressors. J Mol Endocrinol *33*, 387-410.

Kruse, S.W., Suino-Powell, K., Zhou, X.E., Kretschman, J.E., Reynolds, R., Vonrhein, C., Xu, Y., Wang, L., Tsai, S.Y., Tsai, M.J., *et al.* (2008). Identification of COUP-TFII orphan nuclear receptor as a retinoic acid-activated receptor. PLoS Biol *6*, e227.

Krylova, I.N., Sablin, E.P., Moore, J., Xu, R.X., Waitt, G.M., MacKay, J.A., Juzumiene, D., Bynum, J.M., Madauss, K., Montana, V., *et al.* (2005). Structural analyses reveal phosphatidyl inositols as ligands for the NR5 orphan receptors SF-1 and LRH-1. Cell *120*, 343-355.

Kullak-Ublick, G.A., Stieger, B., and Meier, P.J. (2004). Enterohepatic bile salt transporters in normal physiology and liver disease. Gastroenterology *126*, 322-342.

Kurosu, H., Choi, M., Ogawa, Y., Dickson, A.S., Goetz, R., Eliseenkova, A.V., Mohammadi, M., Rosenblatt, K.P., Kliewer, S.A., and Kuro-o, M. (2007). Tissue-specific expression of betaKlotho and fibroblast growth factor (FGF) receptor isoforms determines metabolic activity of FGF19 and FGF21. J Biol Chem *282*, 26687-26695.

Laudet, V. (1997). Evolution of the nuclear receptor superfamily: early diversification from an ancestral orphan receptor. J Mol Endocrinol *19*, 207-226.

Lee, Y.K., Dell, H., Dowhan, D.H., Hadzopoulou-Cladaras, M., and Moore, D.D. (2000). The orphan nuclear receptor SHP inhibits hepatocyte nuclear factor 4 and retinoid X receptor transactivation: two mechanisms for repression. Mol Cell Biol *20*, 187-195.

Lee, Y.K., Schmidt, D.R., Cummins, C.L., Choi, M., Peng, L., Zhang, Y., Goodwin, B., Hammer, R.E., Mangelsdorf, D.J., and Kliewer, S.A. (2008). Liver receptor homolog-1 regulates bile acid homeostasis but is not essential for feedback regulation of bile acid synthesis. Mol Endocrinol *22*, 1345-1356.

Lee, Y.S., Chanda, D., Sim, J., Park, Y.Y., and Choi, H.S. (2007). Structure and function of the atypical orphan nuclear receptor small heterodimer partner. Int Rev Cytol *261*, 117-158.

Lemon, B., Inouye, C., King, D.S., and Tjian, R. (2001). Selectivity of chromatin-remodelling cofactors for ligand-activated transcription. Nature *414*, 924-928.

Li, Y., Choi, M., Cavey, G., Daugherty, J., Suino, K., Kovach, A., Bingham, N.C., Kliewer, S.A., and Xu, H.E. (2005a). Crystallographic identification and functional characterization of phospholipids as ligands for the orphan nuclear receptor steroidogenic factor-1. Mol Cell *17*, 491-502.

Li, Y., Choi, M., Suino, K., Kovach, A., Daugherty, J., Kliewer, S.A., and Xu, H.E.

(2005b). Structural and biochemical basis for selective repression of the orphan nuclear receptor liver receptor homolog 1 by small heterodimer partner. Proc Natl Acad Sci U S A *102*, 9505-9510.

Lonard, D.M., and O'Malley, B.W. (2007). Nuclear receptor coregulators: Judges, juries, and executioners of cellular regulation. Molecular Cell *27*, 691-700.

Lu, T.T., Makishima, M., Repa, J.J., Schoonjans, K., Kerr, T.A., Auwerx, J., and Mangelsdorf, D.J. (2000). Molecular basis for feedback regulation of bile acid synthesis by nuclear receptors. Mol Cell *6*, 507-515.

Ludewig, A.H., Kober-Eisermann, C., Weitzel, C., Bethke, A., Neubert, K., Gerisch, B., Hutter, H., and Antebi, A. (2004). A novel nuclear receptor/coregulator complex controls C. elegans lipid metabolism, larval development, and aging. Genes Dev *18*, 2120-2133.

Luisi, B.F., Xu, W.X., Otwinowski, Z., Freedman, L.P., Yamamoto, K.R., and Sigler, P.B. (1991). Crystallographic analysis of the interaction of the glucocorticoid receptor with DNA. Nature *352*, 497-505.

Lunyak, V.V., Prefontaine, G.G., and Rosenfeld, M.G. (2004). REST and peace for the neuronal-specific transcriptional program. Gastroenteropancreatic Neuroendocrine Tumor Disease: Molecular and Cell Biological Aspects *1014*, 110-120.

Ma, K., Saha, P.K., Chan, L., and Moore, D.D. (2006). Farnesoid X receptor is essential for normal glucose homeostasis. J Clin Invest *116*, 1102-1109.

Macchiarulo, A., Rizzo, G., Costantino, G., Fiorucci, S., and Pellicciari, R. (2006). Unveiling hidden features of orphan nuclear receptors: the case of the small heterodimer partner (SHP). J Mol Graph Model *24*, 362-372.

Magner, D.B., and Antebi, A. (2008). Caenorhabditis elegans nuclear receptors: insights into life traits. Trends Endocrinol Metab *19*, 153-160.

Makishima, M., Lu, T.T., Xie, W., Whitfield, G.K., Domoto, H., Evans, R.M., Haussler, M.R., and Mangelsdorf, D.J. (2002). Vitamin D receptor as an intestinal bile acid sensor. Science *296*, 1313-1316.

Makishima, M., Okamoto, A.Y., Repa, J.J., Tu, H., Learned, R.M., Luk, A., Hull, M.V., Lustig, K.D., Mangelsdorf, D.J., and Shan, B. (1999). Identification of a nuclear receptor for bile acids. Science *284*, 1362-1365.

Mangelsdorf, D.J., Thummel, C., Beato, M., Herrlich, P., Schutz, G., Umesono, K., Blumberg, B., Kastner, P., Mark, M., Chambon, P.*, et al.* (1995). The nuclear receptor superfamily: the second decade. Cell *83*, 835-839.

Martinez-Augustin, O., and Sanchez de Medina, F. (2008). Intestinal bile acid physiology

and pathophysiology. World J Gastroenterol *14*, 5630-5640.

Maruyama, T., Miyamoto, Y., Nakamura, T., Tamai, Y., Okada, H., Sugiyama, E., Itadani, H., and Tanaka, K. (2002). Identification of membrane-type receptor for bile acids (M-BAR). Biochem Biophys Res Commun *298*, 714-719.

Matyash, V., Geier, C., Henske, A., Mukherjee, S., Hirsh, D., Thiele, C., Grant, B., Maxfield, F.R., and Kurzchalia, T.V. (2001). Distribution and transport of cholesterol in Caenorhabditis elegans. Mol Biol Cell *12*, 1725-1736.

Mehnert, J.M., and Kelly, W.K. (2007). Histone deacetylase inhibitors: biology and mechanism of action. Cancer J *13*, 23-29.

Merris, M., Wadsworth, W.G., Khamrai, U., Bittman, R., Chitwood, D.J., and Lenard, J. (2003). Sterol effects and sites of sterol accumulation in Caenorhabditis elegans: developmental requirement for 4alpha-methyl sterols. J Lipid Res *44*, 172-181.

Mi, L.Z., Devarakonda, S., Harp, J.M., Han, Q., Pellicciari, R., Willson, T.M., Khorasanizadeh, S., and Rastinejad, F. (2003). Structural basis for bile acid binding and activation of the nuclear receptor FXR. Mol Cell *11*, 1093-1100.

Miao, J., Xiao, Z., Kanamaluru, D., Min, G., Yau, P.M., Veenstra, T.D., Ellis, E., Strom, S., Suino-Powell, K., Xu, H.E., *et al.* (2009). Bile acid signaling pathways increase stability of Small Heterodimer Partner (SHP) by inhibiting ubiquitin-proteasomal degradation. Genes Dev *23*, 986-996.

Mitreva, M., Blaxter, M.L., Bird, D.M., and McCarter, J.P. (2005). Comparative genomics of nematodes. Trends Genet *21*, 573-581.

Modica, S., Bellafante, E., and Moschetta, A. (2009). Master regulation of bile acid and xenobiotic metabolism via the FXR, PXR and CAR trio. Front Biosci *14*, 4719-4745.

Mooijaart, S.P., Brandt, B.W., Baldal, E.A., Pijpe, J., Kuningas, M., Beekman, M., Zwaan, B.J., Slagboom, P.E., Westendorp, R.G., and van Heemst, D. (2005). C. elegans DAF-12, Nuclear Hormone Receptors and human longevity and disease at old age. Ageing Res Rev *4*, 351-371.

Motola, D.L., Cummins, C.L., Rottiers, V., Sharma, K.K., Li, T., Li, Y., Suino-Powell, K., Xu, H.E., Auchus, R.J., Antebi, A., *et al.* (2006). Identification of ligands for DAF-12 that govern dauer formation and reproduction in C. elegans. Cell *124*, 1209-1223.

Narasimhan, S.D., Yen, K., and Tissenbaum, H.A. (2009). Converging pathways in lifespan regulation. Curr Biol *19*, R657-666.

Nolte, R.T., Wisely, G.B., Westin, S., Cobb, J.E., Lambert, M.H., Kurokawa, R., Rosenfeld, M.G., Willson, T.M., Glass, C.K., and Milburn, M.V. (1998). Ligand binding

and co-activator assembly of the peroxisome proliferator-activated receptor-gamma. Nature *395*, 137-143.

Ogawa, A., Streit, A., Antebi, A., and Sommer, R.J. (2009). A conserved endocrine mechanism controls the formation of dauer and infective larvae in nematodes. Curr Biol *19*, 67-71.

Onate, S.A., Tsai, S.Y., Tsai, M.J., and O'Malley, B.W. (1995). Sequence and characterization of a coactivator for the steroid hormone receptor superfamily. Science *270*, 1354-1357.

Otte, K., Kranz, H., Kober, I., Thompson, P., Hoefer, M., Haubold, B., Remmel, B., Voss, H., Kaiser, C., Albers, M.*, et al.* (2003). Identification of farnesoid X receptor beta as a novel mammalian nuclear receptor sensing lanosterol. Mol Cell Biol *23*, 864-872.

Park, Y.Y., Kim, H.J., Kim, J.Y., Kim, M.Y., Song, K.H., Cheol Park, K., Yu, K.Y., Shong, M., Kim, K.H., and Choi, H.S. (2004). Differential role of the loop region between helices H6 and H7 within the orphan nuclear receptors small heterodimer partner and DAX-1. Mol Endocrinol *18*, 1082-1095.

Parks, D.J., Blanchard, S.G., Bledsoe, R.K., Chandra, G., Consler, T.G., Kliewer, S.A., Stimmel, J.B., Willson, T.M., Zavacki, A.M., Moore, D.D.*, et al.* (1999). Bile acids: natural ligands for an orphan nuclear receptor. Science *284*, 1365-1368.

Peet, D.J., Turley, S.D., Ma, W., Janowski, B.A., Lobaccaro, J.M., Hammer, R.E., and Mangelsdorf, D.J. (1998). Cholesterol and bile acid metabolism are impaired in mice lacking the nuclear oxysterol receptor LXR alpha. Cell *93*, 693-704.

Pellicciari, R., Costantino, G., and Fiorucci, S. (2005). Farnesoid X receptor: from structure to potential clinical applications. J Med Chem *48*, 5383-5403.

Puigserver, P., Adelmant, G., Wu, Z., Fan, M., Xu, J., O'Malley, B., and Spiegelman, B.M. (1999). Activation of PPARgamma coactivator-1 through transcription factor docking. Science *286*, 1368-1371.

Robinson-Rechavi, M., Maina, C.V., Gissendanner, C.R., Laudet, V., and Sluder, A. (2005). Explosive lineage-specific expansion of the orphan nuclear receptor HNF4 in nematodes. J Mol Evol *60*, 577-586.

Rochel, N., Wurtz, J.M., Mitschler, A., Klaholz, B., and Moras, D. (2000). The crystal structure of the nuclear receptor for vitamin D bound to its natural ligand. Mol Cell *5*, 173-179.

Rottiers, V., Motola, D.L., Gerisch, B., Cummins, C.L., Nishiwaki, K., Mangelsdorf, D.J., and Antebi, A. (2006). Hormonal control of C. elegans dauer formation and life span by a Rieske-like oxygenase. Dev Cell *10*, 473-482.

Russell, D.W. (2003). The enzymes, regulation, and genetics of bile acid synthesis. Annu Rev Biochem *72*, 137-174.

Russell, D.W. (2009). Fifty years of advances in bile acid synthesis and metabolism. J Lipid Res *50 Suppl*, S120-125.

Sablin, E.P., Woods, A., Krylova, I.N., Hwang, P., Ingraham, H.A., and Fletterick, R.J. (2008). The structure of corepressor Dax-1 bound to its target nuclear receptor LRH-1. Proc Natl Acad Sci U S A *105*, 18390-18395.

Sanyal, S., Bavner, A., Haroniti, A., Nilsson, L.M., Lundasen, T., Rehnmark, S., Witt, M.R., Einarsson, C., Talianidis, I., Gustafsson, J.A.*, et al.* (2007). Involvement of corepressor complex subunit GPS2 in transcriptional pathways governing human bile acid biosynthesis. Proc Natl Acad Sci U S A *104*, 15665-15670.

Savage-Dunn, C. (2005). TGF-beta signaling. WormBook, 1-12.

Schapira, M., Raaka, B.M., Samuels, H.H., and Abagyan, R. (2001). In silico discovery of novel retinoic acid receptor agonist structures. BMC Struct Biol *1*, 1.

Schmidt, D.R., and Mangelsdorf, D.J. (2008). Nuclear receptors of the enteric tract: guarding the frontier. Nutr Rev *66*, S88-97.

Schnitzler, G.R., Sif, S., and Kingston, R.E. (1998). A model for chromatin remodeling by the SWI/SNF family. Cold Spring Harb Symp Quant Biol *63*, 535-543.

Seol, W., Choi, H.S., and Moore, D.D. (1995). Isolation of proteins that interact specifically with the retinoid X receptor: two novel orphan receptors. Mol Endocrinol *9*, 72-85.

Seol, W., Choi, H.S., and Moore, D.D. (1996). An orphan nuclear hormone receptor that lacks a DNA binding domain and heterodimerizes with other receptors. Science *272*, 1336-1339.

Sheng, Z., Otani, H., Brown, M.S., and Goldstein, J.L. (1995). Independent regulation of sterol regulatory element-binding proteins 1 and 2 in hamster liver. Proc Natl Acad Sci U S A *92*, 935-938.

Shiau, A.K., Barstad, D., Loria, P.M., Cheng, L., Kushner, P.J., Agard, D.A., and Greene, G.L. (1998). The structural basis of estrogen receptor/coactivator recognition and the antagonism of this interaction by tamoxifen. Cell *95*, 927-937.

Shulman, A.I., Larson, C., Mangelsdorf, D.J., and Ranganathan, R. (2004). Structural determinants of allosteric ligand activation in RXR heterodimers. Cell *116*, 417-429.

Shundrovsky, A., Smith, C.L., Lis, J.T., Peterson, C.L., and Wang, M.D. (2006). Probing SWI/SNF remodeling of the nucleosome by unzipping single DNA molecules. Nat Struct Mol Biol *13*, 549-554.

Sinal, C.J., Tohkin, M., Miyata, M., Ward, J.M., Lambert, G., and Gonzalez, F.J. (2000). Targeted disruption of the nuclear receptor FXR/BAR impairs bile acid and lipid homeostasis. Cell *102*, 731-744.

Sluder, A.E., and Maina, C.V. (2001). Nuclear receptors in nematodes: themes and variations. Trends Genet *17*, 206-213.

Snow, M.I., and Larsen, P.L. (2000). Structure and expression of daf-12: a nuclear hormone receptor with three isoforms that are involved in development and aging in Caenorhabditis elegans. Biochim Biophys Acta *1494*, 104-116.

Staudinger, J.L., Goodwin, B., Jones, S.A., Hawkins-Brown, D., MacKenzie, K.I., LaTour, A., Liu, Y., Klaassen, C.D., Brown, K.K., Reinhard, J., *et al.* (2001). The nuclear receptor PXR is a lithocholic acid sensor that protects against liver toxicity. Proc Natl Acad Sci U S A *98*, 3369-3374.

Suzuki, T., Kasahara, M., Yoshioka, H., Morohashi, K., and Umesono, K. (2003). LXXLL-related motifs in Dax-1 have target specificity for the orphan nuclear receptors Ad4BP/SF-1 and LRH-1. Mol Cell Biol *23*, 238-249.

Thakur, M.K., and Paramanik, V. (2009). Role of steroid hormone coregulators in health and disease. Horm Res *71*, 194-200.

Thomas, J.H., Birnby, D.A., and Vowels, J.J. (1993). Evidence for parallel processing of sensory information controlling dauer formation in Caenorhabditis elegans. Genetics *134*, 1105-1117.

Uppenberg, J., Svensson, C., Jaki, M., Bertilsson, G., Jendeberg, L., and Berkenstam, A. (1998). Crystal structure of the ligand binding domain of the human nuclear receptor PPARgamma. J Biol Chem *273*, 31108-31112.

Viney, M.E. (2009). How did parasitic worms evolve? Bioessays *31*, 496-499.

Viney, M.E., and Lok, J.B. (2007). Strongyloides spp. WormBook, 1-15.

Viney, M.E., Thompson, F.J., and Crook, M. (2005). TGF-beta and the evolution of nematode parasitism. Int J Parasitol *35*, 1473-1475.

Wagner, R.L., Apriletti, J.W., McGrath, M.E., West, B.L., Baxter, J.D., and Fletterick, R.J. (1995). A structural role for hormone in the thyroid hormone receptor. Nature *378*, 690-697.

Walter, P., Green, S., Greene, G., Krust, A., Bornert, J.M., Jeltsch, J.M., Staub, A., Jensen, E., Scrace, G., Waterfield, M., *et al.* (1985). Cloning of the human estrogen receptor cDNA. Proc Natl Acad Sci U S A *82*, 7889-7893.

Wang, H., Chen, J., Hollister, K., Sowers, L.C., and Forman, B.M. (1999). Endogenous bile acids are ligands for the nuclear receptor FXR/BAR. Mol Cell *3*, 543-553.

Wang, L., Lee, Y.K., Bundman, D., Han, Y., Thevananther, S., Kim, C.S., Chua, S.S., Wei, P., Heyman, R.A., Karin, M., *et al.* (2002). Redundant pathways for negative feedback regulation of bile acid production. Dev Cell *2*, 721-731.

Wang, X., Briggs, M.R., Hua, X., Yokoyama, C., Goldstein, J.L., and Brown, M.S. (1993). Nuclear protein that binds sterol regulatory element of low density lipoprotein receptor promoter. II. Purification and characterization. J Biol Chem *268*, 14497-14504.

Wang, Z., Zhou, X.E., Motola, D.L., Gao, X., Suino-Powell, K., Conneely, A., Ogata, C., Sharma, K.K., Auchus, R.J., Lok, J.B., *et al.* (2009). Identification of the nuclear receptor DAF-12 as a therapeutic target in parasitic nematodes. Proc Natl Acad Sci U S A *106*, 9138-9143.

Williams, S., Bledsoe, R.K., Collins, J.L., Boggs, S., Lambert, M.H., Miller, A.B., Moore, J., McKee, D.D., Moore, L., Nichols, J., *et al.* (2003). X-ray crystal structure of the liver X receptor beta ligand binding domain: regulation by a histidine-tryptophan switch. J Biol Chem *278*, 27138-27143.

Xie, W., Radominska-Pandya, A., Shi, Y., Simon, C.M., Nelson, M.C., Ong, E.S., Waxman, D.J., and Evans, R.M. (2001). An essential role for nuclear receptors SXR/PXR in detoxification of cholestatic bile acids. Proc Natl Acad Sci U S A *98*, 3375-3380.

Xie, Y.B., Lee, O.H., Nedumaran, B., Seong, H.A., Lee, K.M., Ha, H., Lee, I.K., Yun, Y., and Choi, H.S. (2008). SMILE, a new orphan nuclear receptor SHP-interacting protein, regulates SHP-repressed estrogen receptor transactivation. Biochem J *416*, 463-473.

Xu, H.E., Lambert, M.H., Montana, V.G., Parks, D.J., Blanchard, S.G., Brown, P.J., Sternbach, D.D., Lehmann, J.M., Wisely, G.B., Willson, T.M., *et al.* (1999). Molecular recognition of fatty acids by peroxisome proliferator-activated receptors. Mol Cell *3*, 397-403.

Xu, H.E., Stanley, T.B., Montana, V.G., Lambert, M.H., Shearer, B.G., Cobb, J.E., McKee, D.D., Galardi, C.M., Plunket, K.D., Nolte, R.T., *et al.* (2002). Structural basis for antagonist-mediated recruitment of nuclear co-repressors by PPARalpha. Nature *415*, 813-817.

Yamane, K., Toumazou, C., Tsukada, Y., Erdjument-Bromage, H., Tempst, P., Wong, J., and Zhang, Y. (2006). JHDM2A, a JmjC-containing H3K9 demethylase, facilitates transcription activation by androgen receptor. Cell *125*, 483-495.

Yang, T., Espenshade, P.J., Wright, M.E., Yabe, D., Gong, Y., Aebersold, R., Goldstein, J.L., and Brown, M.S. (2002). Crucial step in cholesterol homeostasis: sterols promote binding of SCAP to INSIG-1, a membrane protein that facilitates retention of SREBPs in ER. Cell *110*, 489-500.

Yu, J., Li, Y., Ishizuka, T., Guenther, M.G., and Lazar, M.A. (2003). A SANT motif in the SMRT corepressor interprets the histone code and promotes histone deacetylation. EMBO J *22*, 3403-3410.

Zhang, J., Huang, W., Qatanani, M., Evans, R.M., and Moore, D.D. (2004). The constitutive androstane receptor and pregnane X receptor function coordinately to prevent bile acid-induced hepatotoxicity. J Biol Chem *279*, 49517-49522.

Zhang, Y., Lee, F.Y., Barrera, G., Lee, H., Vales, C., Gonzalez, F.J., Willson, T.M., and Edwards, P.A. (2006). Activation of the nuclear receptor FXR improves hyperglycemia and hyperlipidemia in diabetic mice. Proc Natl Acad Sci U S A *103*, 1006-1011.